Design of an Affordable, Precise Irrigation Controller that Lowers the Barrier to Water- and Energy-Sustainable Agriculture

by

Carolyn Sheline

B.S.
University of California, Santa Barbara, 2015

S.M.
Massachusetts Institute of Technology, 2019

Submitted to the Department of Mechanical Engineering
in Partial Fulfillment of the Requirements for the Degree of

DOCTOR OF PHILOSOPHY IN MECHANICAL ENGINEERING

at the

MASSACHUSETTS INSTITUTE OF TECHNOLOGY

February 2024

Authored by:	Carolyn Sheline Department of Mechanical Engineering January 12, 2024
Certified by:	Amos G. Winter V Associate Professor of Mechanical Engineering, Thesis Supervisor
Accepted by:	Nicolas Hadjiconstantinou Professor of Mechanical Engineering Chairman, Department Committee on Graduate Theses

Design of an Affordable, Precise Irrigation Controller that Lowers the Barrier to Water- and Energy-Sustainable Agriculture

by

Carolyn Sheline

Submitted to the Department of Mechanical Engineering
on January 12, 2024 in Partial Fulfillment of the Requirements for the Degree of
Doctor of Philosophy in Mechanical Engineering

ABSTRACT

With climate change and population growth exacerbating global food insecurity, it has become urgent to establish more water- and energy-efficient means to raise agricultural production. Available techniques to bolster crop productivity, such as solar-powered drip irrigation (SPDI) and precision irrigation, are currently cost-prohibitive for farmers in low- and middle-income countries (LMICs), where food insecurity will be most severe. This thesis demonstrates one method to reduce the barrier to these systems, by pairing them with a Predictive Optimal Water and Energy Irrigation (POWEIr) controller that optimizes irrigation schedules to make efficient use of solar and water resources for maximum crop yield. In doing so, POWEIr also decreases SPDI system costs.

First, this work confirms the hypothesis that scheduling irrigation activity to match the availability of variable solar power enables SPDI cost savings. For a fixed irrigation system, a SPDI full-season operation simulation study was conducted and the impact of adjusting the pumping load dynamically to match solar power availability was assessed. When evaluated against conventional operation, this process of profile matching enabled a power system lifetime cost decrease of >18% while delivering 100% of the required irrigation for a simulated two-hectare Kenyan tomato farm with over 50 m well depth.

To exploit these cost and reliability benefits, this work proposes the POWEIr controller. The POWEIr controller leverages machine learning and utilizes a small set of inexpensive sensors to optimize irrigation schedules based on solar energy and crop water demand predictions. The performance of the POWEIr controller was evaluated with an experimental SPDI prototype and compared to simulated typical farming practices. For the same irrigation delivered, a six-fold decrease in the required battery capacity was observed. With no batteries, the POWEIr controller still satisfied a greater fraction of the irrigation demand. Overall, compared to typical practice, the controller provided more reliable irrigation using solar power, with minimal battery usage.

High reliability at low cost necessitates that the POWEIr controller's irrigation schedules are robust to errors in agronomy inputs and weather data. Sensitivity to these errors was assessed by evaluating the impact on simulated irrigation amounts and crop yield. It was found possible to rely on weather data from an economical station, costing $190, 83% less

than a better-equipped research-quality alternative, with negligible consequences to crop yields. This conclusion held steadfast across diverse crop and soil types. The crop coefficient was the most significant factor affecting irrigation performance, thereby pointing to the need for calibration of this factor alone. This underscores the POWEIr controller's capability to accurately optimize irrigation schedules for only essential water use while relying on affordable sensors and minimal calibration.

Finally, the POWEIr controller was piloted on farms in Jordan and Morocco and performance was benchmarked against measured local, conventional drip irrigation practices on similar farms. It provided up to 44% and 43% savings in water use and pumping energy consumption, respectively, for similar crop yields. This result demonstrates theory to practice of accessible precision agriculture technology and offers tangible evidence of the POWEIr controller's potential to raise agricultural sustainability.

Thesis Supervisor: Amos G. Winter V
Title: Associate Professor of Mechanical Engineering

Acknowledgments

The achievement of this thesis would not have been possible without the work of key contributors.

I would like to thank my advisor, Professor Amos Winter, the principal investigator of the Global Engineering and Research (GEAR) lab. You've imparted invaluable insights into global design, elevating my skills as both a researcher and engineer. Your contagious enthusiasm for this field has consistently propelled our work forward, and being a member of the GEAR lab has been both an honor and a profound source of inspiration for me.

I would also like to thank my thesis committee. Thank you, Professor Maria Yang, for being part of not only my committee but also Fiona and Georgia's, you have helped provide holistic feedback on this project. Thank you, Professor Tonio Buonassisi, for providing me with resources on solar power modeling and machine learning. I also appreciated our coffee chat! Thank you, Professor Suat Irmak, for giving me guidance and feedback on agronomy modeling and being a sounding board for me on best practices.

Thank you to my GEAR lab research partners Fiona and Georgia, you both taught and helped me so much during my time at MIT. Thank you for always being available for a last-minute brainstorming session and for being great travel companions. I couldn't have asked for better colleagues to work with.

I would like to thank all of the GEAR lab past and present members, especially those who have been part of the irrigation team and who have helped me throughout my PhD. Thank you Susan, Simone, and Julia for your mentorship during this project. You gave me support and guidance during the early development of this work and helped shape me into the researcher that I am now for which I am sincerely grateful. Thank you Shane for helping to develop the controller hardware, the controller would not have run with all the capabilities that it did without your hard work. Thank you Aditya, Jeff, Z, Jacob, and Elizabeth for all your efforts in setting up the different prototypes. I would not have been able to pull off the experiments that I did without your dedication. Thank you Sam for helping me run analyses for the controller's crop parameters. I appreciated being able to bounce ideas off of you and your insights.

This work would not have been possible without the guidance from our international partner organizations, the International Center for Agricultural Research in the Dry Areas

(ICARDA) and the National Institute of Agricultural Research (INRA) in Morocco and the Methods for Irrigation and Agriculture (MIRRA) in Jordan. Thank you for helping with planning, coordinating, setting up, executing, and analyzing our user testing and field trials, as well as advising us on best local practices and agronomy resources. The international experimental work would not have been possible without you all. Furthermore, thank you to our company partners Toro and Xylem who helped to guide the system modeling and irrigation controller work.

Thank you MIT Sailing Pavilion and Gaining Ground Farm for letting me test early prototypes of the controller at your facilities. The experimental findings would not have been possible without your hospitality.

Thank you to the Julia Burke Foundation, the MIT Department of Mechanical Engineering, and USAID-MENA, for financially supporting this project.

Thank you so much to all my friends and family for your support over the years. You've been my pillars of strength, and I extend my heartfelt gratitude to you for your unwavering support throughout the years. Your encouragement has been my driving force, keeping me motivated. You inspired me to work hard while still making time for fun and to see the bigger picture. I couldn't have reached this point without each of you, and I am very thankful for you all.

Thank you Sahil for encouraging me to overcome challenges and grow. I truly appreciate your ability to bring laughter, comfort, and excitement into my life, especially during the stressful time when I was wrapping up my PhD. I can't wait for the adventures to come.

Acknowledgement of Joint Work

The development of the POWEIr controller was done jointly with Fiona Grant and Georgia Van de Zande as part of our Ph.D. theses in the Global Engineering and Research (GEAR) lab at MIT. To highlight each of our individual contributions, I developed the weather predictions and irrigation schedule optimization (Level 3), Fiona developed the battery energy management and pressure feedback control (Levels 1 and 2) and conducted stakeholder and energetic analyses in Jordan and Morocco, and Georgia spearheaded the stakeholder analysis in Kenya and the phone application development. My thesis summarizes some of Fiona's and Georgia's work for completeness and clarity, but the main focus will be my work.

Contents

List of Figures

List of Tables

Nomenclature

Abbreviations

HCWS High Cost Weather Station

LCWS Low Cost Weather Station

LMIC Low- and Middle-income Countries

LSTM Long Short-Term Memory

MENA Middle East and North Africa

MPPT Maximum Power Point Tracking

POWEIr Predictive Optimal Water and Energy Irrigation (Controller)

SDG Sustainable Development Goal

SDrOP Solar-powered Drip Irrigation Optimal Performance (Model)

SPDI Solar-powered Drip Irrigation

SPM Solar Profile Matching

SSO Single Section Operation

TMY Typical Meteorological Year

VAR Vector Autoregression

VFD Variable Frequency Drive

Variables

α Battery management weighting factor

δt Length of time step in hours

η_{batt} Battery efficiency

ρ Density

θ_g Weight soil water content

θ_v Volumetric soil water content

A_s Section area

b_{inv} Inverter linear constant

b_{MPPT} MPPT linear constant

b_{VFD} VFD linear constant

c Vector of constants

C_{inv} Inverter cost

C_{MPPT} MPPT cost

C_{VFD} VFD cost

d Binary control variable for irrigating a section

D_r Root zone depletion

e Vector of errors

ET_0 Reference evapotranspiration

ET_c Crop evapotranspiration

f_d Depletion fraction

f_{solar} Solar prediction scaling factor

f_w Soil wetted fraction

G Solar radiation

i Time step index

I_{del} Irrigation delivered

I_{dem} Irrigation demand

IR Irrigation reliability

k_b Lifetime cost weight for energy storage

k_b Unit cost weight for energy storage

K_c Crop coefficient

k_c Cost weight for the crop

k_{RO} Runoff coefficient

K_{st} Water stress coefficient

k_w Cost weight for water

K_y Crop yield response factor

L Function to minimize battery and water use

M Function to track battery reference state of charge

m Mass

m_{inv} Inverter linear coefficient

m_{MPPT} MPPT linear coefficient

m_{VFD} VFD linear coefficient

n Day index

N_{crop} Total days in the crop growing season

N_{hor} Prediction horizon length in hours

N_s Total number of field sections

p Lag order

P_{avail} Available solar power

P_{pump} Pump power

Pr Precipitation

q_s Section flow rate

R Function to maximize crop revenue

s Section index

SOC Battery state of charge

SOC_{ref} Reference battery state of charge

SOI State of irrigation

t Amount of time

TAW Total available water

u_1 Battery charging rate control variable

u_2 Battery discharging rate control variable

V Function to maximize battery stored energy

W Weight matrix

WUE Water use efficiency

x Soil water depletion state variable

y Vector of prediction variables

Y_a Adjusted crop yield

Y_{max} Maximum yield without water stress

Z_r Crop root depth

Chapter 1

Introduction

This thesis aims to reduce the costs of renewable-powered irrigation systems and improve the energy and water efficiency of agricultural irrigation practices. Specifically, this thesis presents the Predictive Optimal Water and Energy Irrigation (POWEIr) controller, an affordable, precise irrigation controller that reduces water and pumping energy use for comparable crop yield to existing solar-powered drip irrigation (SPDI) systems. The POWEIr controller uses low-cost weather sensors, physics-based models, and machine learning to predict crop water demands and available solar energy and then optimize irrigation schedules for SPDI systems based on these predicted variables.

1.1 The Need for Affordable, Precise Irrigation Control

Global efforts to achieve the second sustainable food development goal of ending hunger by 2030 are falling short, with 2.4 billion people facing food insecurity in 2022, especially in low- and middle-income countries (LMICs) [1]. To address this, sustainable crop production must increase while conserving water and reducing energy consumption [2], [3]. Agriculture currently uses a significant portion of global freshwater resources and energy, contributing

to water scarcity and greenhouse gas emissions [4]–[7].

Technological solutions like SPDI and precision agriculture can help to achieve food security sustainably [8]–[10]. SPDI systems, powered by solar panels, have significantly lower greenhouse gas emissions compared to more common diesel and electric pumps [11]. Drip irrigation efficiently delivers water directly to crop roots, reducing water consumption and increasing yields compared to traditional methods which involve flooding fields with water [12]. Precision agriculture utilizes various sensing technologies to optimize farm operations for sustainable productivity. Despite their benefits, SPDI and precision agriculture technologies are not widely adopted in LMICs due to high costs and complexity [13]–[15]. Even when these technologies are adopted, farmers may choose to over-irrigate to mitigate perceived risks to crop yield [16]–[18].

Current solutions for precise, irrigation control require many sensors and technical expertise, which are impractical in resource-constrained settings [19]. For example, sophisticated precision agriculture systems in greenhouses (e.g., PRIVA, Hotraco Horti, Agrowtek, and Munters) allow for complete control of the environment but call for automation, numerous integrating sensor suites, and remote data monitoring. These complex systems require significant capital investment and technical training that is out of reach for a majority of farmers. Lower-cost precision irrigation systems exist (e.g., Netafim GrowSphere, Toro Tempus series, Rainbird ESP series, Hunter Pro-C), but they still rely on costly sensors and automatic valves to deliver irrigation based on a user-defined schedule. Additionally, many of these solutions do not address the issue of over-irrigation. Thus, there is a pressing need for affordable irrigation control that encourages sustainable practices for SPDI systems in LMICs.

1.2 SPDI System Description

Figure 1.1 gives some background on what a SPDI system is described as in this thesis. The SPDI system consists of a pump, depicted as a surface pump but could also be subsurface, that pumps water through a network of pipes onto a field. The network of pipes is divided into sections that are irrigated by opening and closing a valve to deliver water to different portions of the field. Each section has several pipe laterals that have evenly spaced drip emitters in them which deliver water directly to the root zone of the crop. The pump is powered by a solar panel array and can also be powered by a battery. A solar pump controller converts the electricity generated by the panels to what is needed for the battery and the pump. The solar pump controller can have an inverter, maximum power point tracking, battery energy management, and a Variable Frequency Drive. The POWEIr controller interfaces with these solar pump control components and a weather station in order to deliver optimal irrigation schedules. The optimal irrigation schedules depend on inputs from the weather, crop type, and soil texture.

1.3 User Analysis

The development of the POWEIr controller was informed by extensive user analysis, which was instrumental in its design. The user analysis is not the focus of my thesis as I did not lead this work. However, I actively participated in the user testing, discovering valuable insights that influenced my design process for the controller. These findings will be emphasized in this section.

Over 200 interviews were conducted with SPDI stakeholders in Kenya, Jordan, and Morocco [20]–[24]. The findings from user testing in these areas can be summarized into the following categories; farmers face challenges of

High costs and could not afford or did not have access to all SPDI and precision

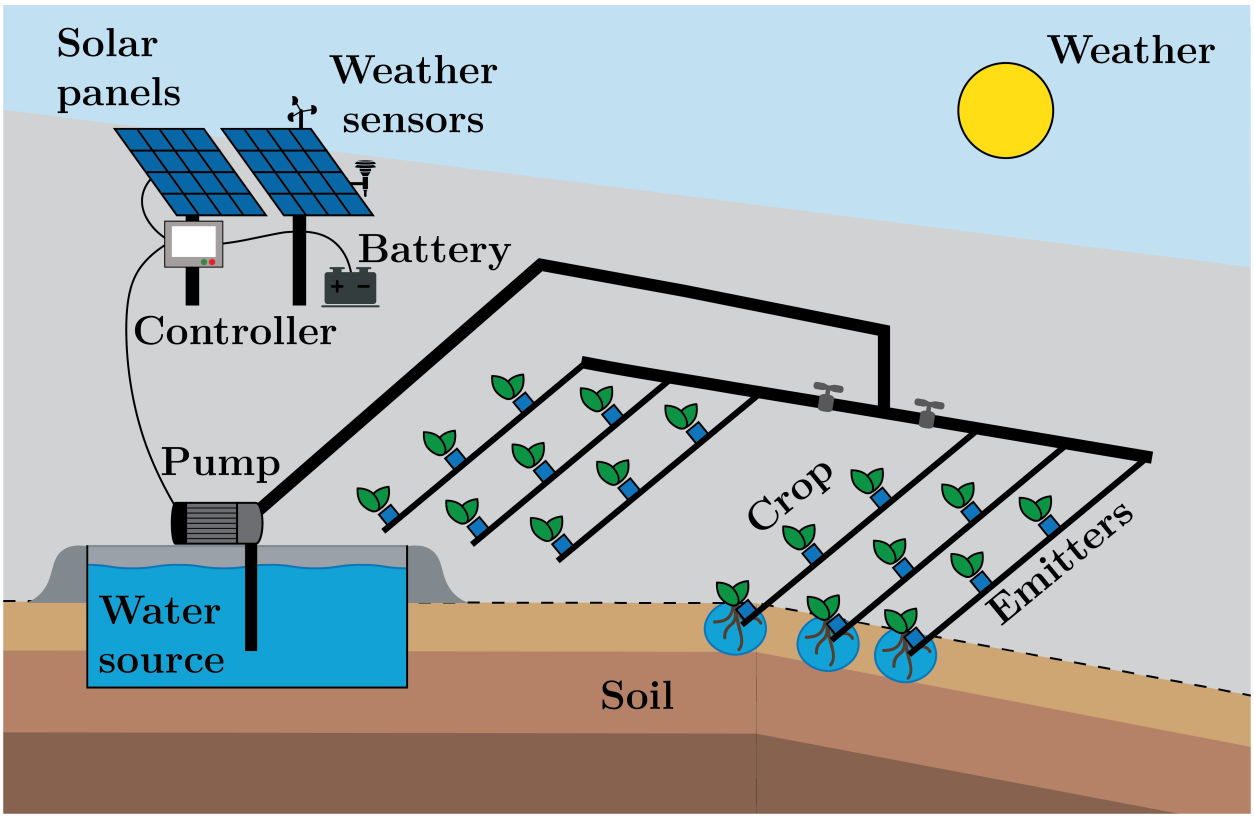

Figure 1.1: An example of a solar-powered drip irrigation (SPDI) system and its components.

agriculture technologies;

Lack of support, with no free, recurring support to manage their irrigation systems farmers will pay for agronomists' advice; and

Over-irrigation, farmers have a range of experience in irrigation but the majority will over-irrigate to reduce perceived risks to their crops.

When shown the concept of the POWEIr controller farmers wanted

Lower energy costs, farmers would like to reduce their energy bill but some did not like the uncertainty in varying solar power;

Advanced notice, farmers would like advance notice of irrigation schedules to facilitate planning other activities;

Varying degrees of automation, farmers interviewed in different countries had varying degrees of desire for automation; and

No harm to crops, farmers wanted accurate schedules so that their yields would not be negatively impacted.

These findings have been incorporated into the design of the POWEIr controller's optimal irrigation schedules. Particularly, the controller was designed to predict available solar power and exact crop water requirements and communicate energy- and water-efficient irrigation schedules to farmers through a phone application a day in advance. Automatic valves could be incorporated to carry out the schedules automatically or farmers could manually irrigate based on the schedule they were sent. The controller was designed with a feedback loop from the farmer so that changes to a schedule could be made in real time; these changes would impact future schedules.

1.4 Thesis Outline and Contributions

This thesis aims to address the need for affordable, precise irrigation control with the development of the POWEIr controller, a predictive irrigation controller that reduces the cost of SPDI systems and uses inexpensive weather sensors to reduce the barrier to sustainable agriculture technology. The following summarizes the research contributions contained in this thesis:

Section 2.2: A cost analysis is conducted and is shown to achieve over 18% less SPDI pump and power system lifetime cost while delivering irrigation 31-66% more reliably than an existing commercial sizing tool by modeling various irrigation operation schemes.

Section 2.3 and Section 2.4: The POWEIr controller theory is outlined and an initial prototype used six times less battery storage to deliver the required irrigation compared to a simulation of typical operation. If no batteries were used the prototype could have delivered up to 46% more of the required irrigation compared to the reference operation.

Chapter 3: The sensitivity of the POWEIr controller's optimized irrigation schedules to errors in agronomy inputs and weather data is explored and it is found that weather sensor cost could be reduced by 83% with negligible simulated effect on crop yield.

Chapter 4: The performance of the POWEIr controller is validated on farms in Jordan and Morocco with reductions in pumping energy up to 43% and water use by 44% for similar crop yields compared to measured local farmer drip irrigation practices.

Chapter 2

Designing a Predictive Optimal Water and Energy Irrigation (POWEIr) Controller for Solar-powered Drip Irrigation Systems in Resource-constrained Contexts

The content of this chapter was derived from work with contributors besides the author of this thesis including Fiona Grant, Simone Gelmini, Shane Pratt, and Amos G. Winter, V. A publication of the same title of this chapter is in preparation as Sheline, Grant, Gelmini, *et al.* [25].

2.1 Introduction

The increasing global population necessitates a boost in food production [14], [26]. To meet this demand sustainably, agriculture must intensify its operations using existing farmland, water, and other natural resources [14], [26], [27]. Currently, agriculture consumes 70% of global freshwater withdrawals annually [26], [28], and climate change is exacerbating global

water scarcity [29], posing challenges to agricultural intensification.

Solar-powered drip irrigation (SPDI) is a potential solution to sustainably enhance agricultural productivity [8]. Solar power is a renewable-energy solution that needs solar irradiance and is particularly feasible in arid, water-stressed regions with abundant sun [4], [30], [31]. However, the high upfront costs of solar power systems act as a barrier to adoption for many farmers [13]–[15]. Farmers may also be hesitant to adopt an intermittent power source that is not operable in all weather conditions [22]. Drip irrigation holds the potential to increase crop yields while conserving water and agricultural inputs [12], [32]. Nevertheless, the effectiveness of drip irrigation in water conservation relies on correct on-farm system operation [21], [33]. Additionally, traditional farming practices may not align with ideal irrigation volumes [33]. Farmers often rely on personal observations and experience to make irrigation decisions [22], [33], which can be unreliable in a changing climate, potentially leading to unsustainable overuse of water and fertilizer [34], [35].

Sustainable agriculture hinges on improving irrigation practices, a goal achievable through precision irrigation control [34]. Precision irrigation controllers utilize integrated sensors to monitor crop, soil, weather conditions, and hydraulic and power system performance to inform irrigation scheduling decisions [34]. Previous studies have revealed that the operation scheme of a SPDI system significantly influences its energy consumption, water use, and cost [36]–[38]. Pairing SPDI with precision irrigation control could optimize resource use while enhancing crop production [39].

The 2022 FAO State of Food and Agriculture report emphasizes the increasing prevalence of precision agriculture technologies and their potential to enhance the resilience of food systems to climate change [39]. However, these technologies remain inaccessible to many farmers due to their high costs and technical complexities [22], [39], posing a significant barrier to realizing the sustainability benefits of precision agriculture on a large scale. The report outlines key criteria for widespread adoption of precision agriculture devices, namely that they should be

Scale-neutral, meaning devices should function effectively across a variety of farm sizes;

Adaptable to local contexts, recognizing that sustainability gains depend on farm-level operations;

Accessible, including to individuals with limited access to training and a diverse range of technical knowledge; and

Low-cost.

Cutting-edge commercial precision irrigation control systems (e.g., PRIVA, Hotraco Horti, Agrowtek, and Munters) are predominantly tailored for users engaged in large-scale, high-quality crop production, such as precision agriculture in greenhouses. These sophisticated control systems come with a high price tag and technical intricacies, integrating sensor suites, automation features, and online data monitoring. They often require complex inputs and can pose challenges in adapting to existing irrigation setups [40]. Implementation of such products necessitates end users to possess the capacity for significant investments in equipment, technical know-how, and network connectivity. Consequently, these technologies remain out of reach for numerous medium-to-small scale farmers in LMICs [22].

While more economical irrigation controllers (e.g., Netafim GrowSphere, Toro Tempus series, Rainbird ESP series, Hunter Pro-C) are available, they either rely on costly sensors to recommend irrigation schedules or require users to manually determine and input schedules that automatic valves then execute. A reliance on sensors and automatic valves drives up costs while a dependence on user expertise and decision-making compromises system performance [41]. Unfortunately, such devices fail to cater to the needs of cost-sensitive farmers with limited access to technical training who struggle to make informed irrigation decisions [22].

Crafting a widely adoptable precision irrigation controller that aligns with all the criteria outlined in the 2022 FAO report [39] is non-trivial. The diversity of farm-level contexts,

especially in smaller farms [14], [42], introduces variations in crop choices, soil compositions, local weather patterns, micro-climates across the farmland, and the quality of hydraulic equipment. The controller must enhance both energy and water use efficiency to realize the sustainability advantages of precision irrigation with SPDI systems [10], [43]. To achieve scale-neutrality, adaptability, and accessibility for a diverse user base, the chosen control algorithm needs to be easily calibrated and robust in diverse environmental conditions. Moreover, while ensuring the affordability of the controller itself, it is also crucial to evaluate the economic implications of the selected control algorithm on the overall cost of the SPDI system.

Classical control methods, such as linear feedback control, and rule-based controllers, known for their simplicity in design and implementation, often prove unsuitable for agricultural processes without extensive calibration [44]. These methods necessitate on-site technical expertise for sensor installation and calibration, potentially inaccessible to end users. Similarly, fuzzy-logic controllers, although finely tuned to specific systems, struggle with adaptation to diverse contexts [45]. Recent literature reviews indicate that model predictive control (MPC), a process control technique, is better suited for irrigation systems [34], [44], [46]. The MPC algorithm utilizes a dynamic model to predict system behavior over a moving time window, optimizing performance based on an objective function, constraints, and feedback measurements of the system state [44]. Because the dynamic model is system-specific, the MPC approach inherently accommodates various scales and adapts to different contexts, making it well-suited for handling variability in weather conditions and crop behavior during SPDI operation.

Studies have implemented MPC-based irrigation controllers, showcasing reduced water use compared to other control techniques. For instance, Delgoda, Malano, Saleem, *et al.* [45] demonstrates an MPC-based irrigation controller capable of reducing water use while preventing crop water stress. Similarly, Lozoya, Mendoza, Aguilar, *et al.* [41] illustrates that MPC lowers water consumption compared to manual operation, timer-based opera-

tion, open-loop control with soil moisture sensors, and closed-loop feedback control with soil moisture sensors. In a study by Abioye, Abidin, Aman, *et al.* [46], their MPC-based controller for soil moisture levels, which ran on an embedded device in the field, resulted in a 30% reduction in water use compared to a benchmark model-based control optimization technique. While these studies enhance water use efficiency, they fall short in optimizing irrigation system energy use, limiting the potential sustainability and cost benefits at the system level. Additionally, these controller designs rely on feedback measurements from soil moisture sensors, which may not be available or affordable for certain users.

A proposed optimization strategy by Roje, Sáez, Muñoz, *et al.* [47] minimizes the cost of energy transfer and excess water in rural irrigation systems, ensuring sustainable use of a communal aquifer. However, this strategy is tailored for a communal-scale system with a microgrid power source and does not address the execution of the optimal irrigation schedule. Hence, its effectiveness for individual farmers or scalability to diverse farm contexts, encompassing different power system configurations, water sources, and access to automation, remains uncertain.

Prior studies indicate that irrigating multiple sections of a field simultaneously to harness solar power when available can save energy and reduce the cost of solar-powered systems [43]. Studies have demonstrated up to 30% energy savings through optimized irrigation sectioning and operation strategies, with some estimating a 13% increase in profits compared to traditional farming methods [48]. Further advancements, such as synchronizing the irrigation load schedule with the variable solar power source [10], herein termed solar profile matching (SPM) (Figure 2.1), present an efficient shift from the typical single section operation (SSO) approach. This transition enhances the utilization of variable power, enabling reliable operation with smaller, more cost-effective solar power systems [38], potentially fostering increased adoption of SPDI among farmers.

A predictive irrigation controller that simultaneously optimizes water use and energy efficiency has the potential to capitalize on the interplay between system operation, reliability,

and power sizing, thereby enabling more cost-effective SPDI systems. Such a controller could contribute to sustainable resource utilization and assist smaller-scale farmers in making well-informed agricultural decisions [22]. This research introduces a SPDI controller architecture designed to optimize both system energy and water use. By considering farm-level weather conditions and crop water demand, the proposed controller aims to render sustainable irrigation practices technically and economically viable for farmers in LMICs. The controller introduced in this chapter is the Predictive Optimal Water and Energy Irrigation (POWEIr) controller.

This chapter assesses the economic advantages of adopting SPM in SPDI scheduling. It achieves this by conducting simulations of a cost-optimized system utilizing SPM operation throughout an entire crop season and comparing it with a commercially sized system applying SSO. Additionally, the chapter outlines the theory of the POWEIr controller and verifies the efficacy of the proposed controller with an initial prototype that showcases its capabilities in weather prediction, irrigation scheduling, and energy management. The aims of this chapter are to:

1. Quantify the economic benefits derived from SPM operation, encompassing reductions in life cycle costs and heightened irrigation reliability.

2. Propose an irrigation controller architecture for SPDI that integrates SPM, optimizing both system energy and water use. This design accounts for case-specific weather conditions and crop water demand.

3. Validate the performance of the proposed controller through an initial prototype, highlighting its capabilities in energy management, irrigation scheduling, and weather prediction.

Achieving these aims would provide an initial assessment of the POWEIr controller's potential to enhance accessibility to sustainable and precise irrigation practices in LMICs.

2.2 SPDI Scheduling and Economic Analysis

2.2.1 SPDI Scheduling Methods

A SPDI system is comprised of solar panels, an electrical converter (DC/DC) or inverter (DC/AC), and a pump that transports water through a network of pipes. The pipes deliver water directly to the crop root zone through drip emitters. A SPDI system can include energy storage, such as a battery or water tank, as well as a variable frequency drive (VFD) to control the pump speed. The solar array may also be paired with a maximum power point tracking (MPPT) charge controller, which maximizes the current and voltage output of the panels as the available solar power varies. These additional components—energy storage, charge controllers, and VFDs—can increase the reliability and efficiency of SPDI systems, but also add cost. A field with a SPDI system is often irrigated in sections. Each section of the field, denoted as s hereafter, requires a certain pumping power ($P_{pump,s}$) to pressurize the pipe network and deliver uniform flow across the section. The farmer determines the time to irrigate each section (t_s) to provide enough water for the crops each day. This combination of pump operating power and irrigation time for each section makes up the SPDI irrigation schedule.

As previous work has shown, the irrigation scheduling method directly influences the SPDI component capacities and system cost [36]. Figure 2.1 illustrates three SPDI scheduling methods. Figure 2.1a shows an SSO schedule for a SPDI system without energy storage. Although there is a large amount of solar energy available throughout the day, without energy storage irrigation can only be delivered when the available solar power is greater than or equal to the pump power. This leads to a shorter irrigation time for each section and the SSO schedule does not meet the irrigation demand for the day. Figure 2.1b shows that the same irrigation demand can be met with an SSO schedule for a system with a smaller solar array, meaning less available solar power, if it includes energy storage. The energy storage can be discharged at times of low solar power to extend the irrigation time

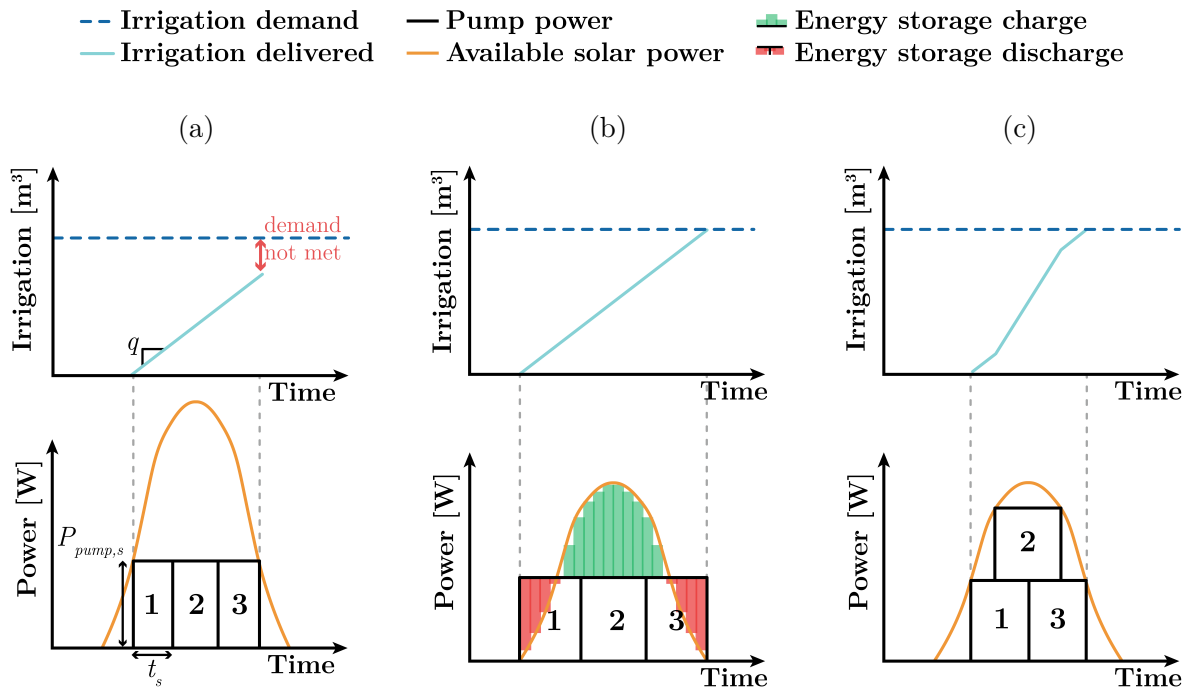

Figure 2.1: Examples of SPDI irrigation scheduling methods. The pump power ($P_{pump,s}$), irrigation time (t_s), and flow rate (q) for each of the three sections determine the pump power curve and the amount of water delivered. **a** shows single section operation (SSO) for a SPDI system without energy storage; **b** shows SSO for a system with a smaller solar array than **a** and energy storage; **c** shows solar profile matching (SPM) for the same solar array as **b**, but no energy storage. The system in **a** has the largest solar array, but the irrigation demand cannot be met with SSO without energy storage. The irrigation demand can be met with SSO and energy storage or an SPM schedule.

and meet the demand. However, this energy storage adds expense to the system design. Figure 2.1c depicts an SPM schedule that meets the same irrigation demand for a system with the same solar array size as in Figure 2.1b but with no energy storage. The SPM schedule has multiple sections opened at times of high solar power, allowing for a higher flow rate and more irrigation to be delivered in less time. The SPM schedule enables fewer solar panels compared to Figure 2.1a and less energy storage compared to Figure 2.1b. This comparison elucidates how changing the irrigation schedule can reduce the SPDI system cost while maintaining operational reliability.

2.2.2 Benefits of Pairing SPDI and SPM

An analysis was conducted to quantify the economic benefits of pairing SPDI with SPM. The cost and full-season reliability of cost-optimized SPDI designs were compared for SSO and SPM schedules. The Solar-powered Drip Irrigation Optimal Performance (SDrOP) model [36] was chosen to produce the cost-optimized designs with SSO and SPM schedules. SDrOP is a SPDI system design tool that optimizes the size of the pump, solar panels, and energy storage for the system. SDrOP simulates the system operation over a growing season with a logic loop that calculates energy and water use (Appendix A.2) and irrigation reliability [36]. However, SDrOP does not optimize the system operation scheme and does not function as an irrigation control algorithm. SDrOP minimizes the SPDI system life cycle cost using particle swarm optimization. The optimization is constrained to meet a threshold irrigation reliability (IR),

$$IR = \frac{\sum_{n=1}^{N_{crop}} I_{del}}{\sum_{n=1}^{N_{crop}} I_{dem}} \times 100, \tag{2.1}$$

where IR is the percent of the total irrigation demand (I_{dem}) that the SPDI system can deliver (I_{del}) summed over each day (n) of the total days in the crop growing season (N_{crop}). The results were benchmarked against a system that was sized using commercially available design software and simulated operation with an SSO schedule. The Grundfos solar pump sizing tool [49] was chosen as the commercial software because it takes similar inputs and, although it does not perform optimization, it conducts similar calculations to the SDrOP model. The Grundfos sizing tool selects a Grundfos pump and sizes a solar array based on inputs of the average monthly solar profile and a single, averaged water demand value. Grundfos assumes that the pump flow rate will vary to match the solar curve and deliver the required water demand. Unlike SDrOP, the Grundfos tool does not simulate a full season of SPDI operation and does not size energy storage options in the form of batteries or water tanks.

Table 2.1: Simulated baseline case for economic analysis.

Location	Nyeri, Kenya
Field area	2 ha
Section size	0.2 ha
Water source depth	2, 50, 100 m
Crop	Tomato
Emitter flow rate	1 Lph
Section pump power (for each well depth)	0.33, 2.6, 4.9 kW
Section irrigation time (daily average)	36 min.

For the analysis to simulate SPM, a farm case was split into equal sections that had a pump operating power, $P_{pump,s}$, and flow rate, q_s. At each time step, SDrOP calculated the number of field sections (N_s) that could be irrigated with the available solar power (P_{avail}),

$$N_{s,i} = \left\lfloor \frac{P_{avail,i}}{P_{pump,s}} \right\rfloor. \tag{2.2}$$

This assumed a constant pump efficiency for all section combinations. The total number of sections that could be operated at once was constrained to a maximum number of sections, $N_{s,max}$. The state of irrigation (SOI) was calculated to determine the cumulative water delivered at each time step i over the time interval Δt:

$$SOI_i = SOI_{i-1} + N_{s,i} q_s \Delta t. \tag{2.3}$$

For the economic analysis, a baseline farm case was defined using a typical medium-scale farm in Kenya (Table 2.1) [21]. A SPDI system design was produced for three different water source depths to show a broader range of section pump powers. The system's 20-year life cycle cost and season reliability were compared for the SDrOP-optimized designs using SSO and SPM and the Grundfos design using SSO. The component costs for both the SDrOP-

optimized designs and the Grundfos-sized systems were based on the market price of the SPDI system components at the time the analysis was run.

The SDrOP model was used to optimally size the pump, solar array, and energy storage for each farm case by minimizing life cycle cost and maintaining 100% IR. SSO was simulated by setting $N_{s,max}$ to one. SPM was simulated by cutting the section flow rate in half and setting $N_{s,max}$ to two. Cutting the section flow rate in half for SPM also cut $P_{pump,s}$ in half and doubled t_s. The cost parameters used in the SDrOP model for this analysis were based on the retail price of off-the-shelf components; these component prices are defined in Appendix A.1. The SDrOP model's pump unit cost was estimated based on the listed price of the Grundfos SP series pumps [50]. The SDrOP model's controller cost was based on the sum of the inverter, MPPT, and VFD costs. The cost of the inverter (C_{inv}) [$] and MPPT charge controller (C_{MPPT}) [$] were estimated based on the peak output power of the solar array (P_{peak}) [W], as

$$C_{inv} = m_{inv} P_{peak} + b_{inv}, \tag{2.4}$$

$$C_{MPPT} = m_{MPPT} P_{peak} + b_{MPPT}, \tag{2.5}$$

where m_{inv} is the inverter linear coefficient [$/W], b_{inv} is the inverter linear constant [$], m_{MPPT} is the MPPT linear coefficient [$/W], and b_{MPPT} is the MPPT linear constant [$]. The VFD cost ($C_{VFD}$) [$] was estimated based on the maximum pump power ($P_{pump,max}$) [W], as

$$C_{VFD} = m_{VFD} P_{pump,max} + b_{VFD}, \tag{2.6}$$

where m_{VFD} is the VFD linear coefficient [$/W] and b_{VFD} is the VFD linear constant [$]. The linear coefficients and constants, listed in Appendix A.1, were determined based on listed prices for inverters, MPPT charge controllers, and VFDs [51]–[53].

The Grundfos tool produced a Grundfos system made up of a pump, controller, and solar array for each farm case. Each Grundfos design was paired with an elevated tank

because the Grundfos tool assumes the pump flow rate will modulate with the solar curve. SPDI sections must operate at a constant pressure to ensure uniform flow, which produces a relatively constant section flow rate. The tank allowed the Grundfos pump to operate at higher flow rates than the section flow rate, storing excess water in the tank to avoid over-pressurizing the hydraulic network. The Grundfos tool selects inverters for its systems that include MPPT and allow for pumping to a storage tank at varying maximum power, but does not include VFDs. The Grundfos pump and panel design, and the associated tank, were input to the SDrOP operation simulation to obtain the IR over a growing season and life cycle cost for the Grundfos design.

Figure 2.2 shows the comparison of life cycle cost and IR of the Grundfos commercial tool's designs using SSO (Com. SSO), the SDrOP optimized designs using SSO (Opt. SSO), and the SDrOP optimized designs using SPM (Opt. SPM). The life cycle cost was split up by component costs—pump, solar array, controllers (inverter, MPPT, VFD), and energy storage—and by cost elements—initial, maintenance, and replacement. The SDrOP designs, which were constrained to 100% IR, had 31–66% higher IR than the Grundfos designs. For the SSO schedule, the SDrOP systems had a life cycle cost that was 75% lower, 9% higher, and 1% higher than that of the Grundfos systems for the 2, 50, and 100 m well depths, respectively. The Grundfos system was much more expensive for the 2 m case because the Grundfos sizing tool selected one of its pumps with an integrated solar inverter, which was significantly more expensive than their separate pump and inverter options. For the remaining cases, the SDrOP design was more expensive than the Grundfos design, but it was also more reliable. The SDrOP optimized systems that used SPM cost 18–74% less than Grundfos SSO systems and were 31–66% more reliable. For each well depth case, the SDrOP design using SSO had the same size pump as the SDrOP design using SPM. SDrOP designs using SPM had power systems that were 3% higher, 25% lower, and 18% lower in life cycle cost than the SDrOP designs using SSO for the 2, 50, and 100 m well depth cases, respectively. The cost comparison demonstrates that incorporating SPDI operation into the

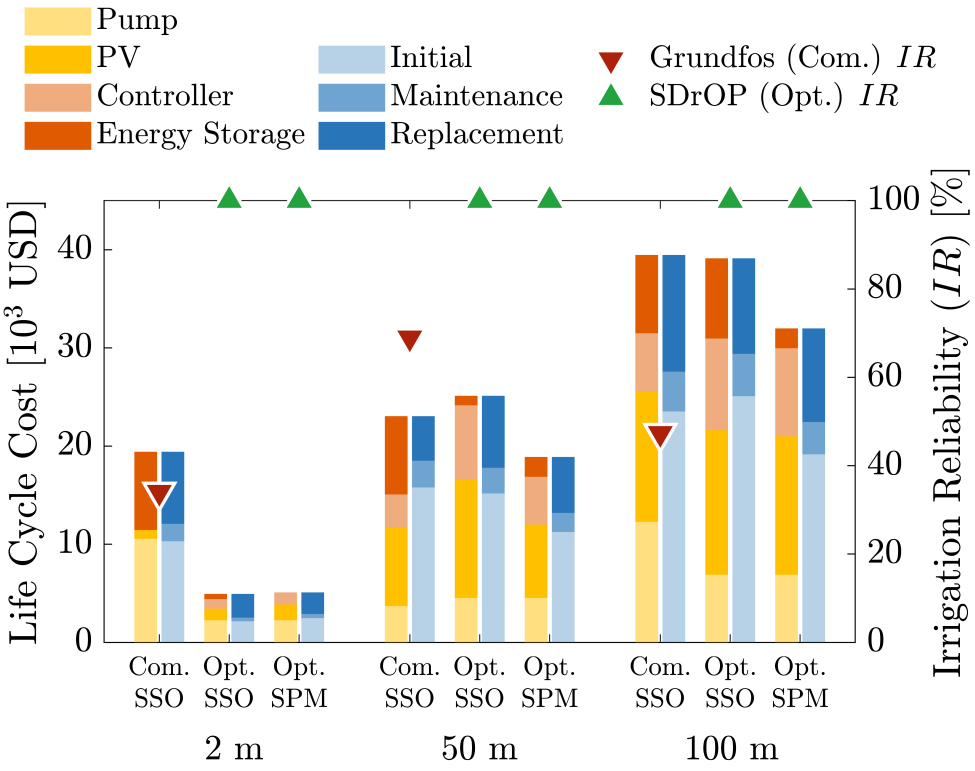

Figure 2.2: The solar pump system life cycle cost and irrigation reliability (IR) of systems designed with different software and scheduling methods for various well depths. The software and scheduling methods used are the commercially available Grundfos sizing tool operated by irrigating one section at a time (Com. SSO), the SDrOP model operated by SSO (Opt. SSO), and SDrOP operated by solar profile matching (Opt. SPM). The SDrOP optimal designs with SPM cost 18–74% less and are 31–66% more reliable at delivering the required irrigation than the Grundfos-sized systems with SSO over the 2, 50, and 100 m well depth cases.

design optimization allows for a reduction in cost without sacrificing irrigation reliability.

This analysis quantifies the system cost reduction due to SPM scheduling and shows that, for the cases of high well depth, and therefore higher pumping power, SPM is able to reduce cost compared to SSO. Although the SDrOP model can simulate irrigation operation and show the cost-saving potential of SPM, it does not model the operation in real-time and it does not optimize the irrigation schedule. This means that the SDrOP model cannot be used as an irrigation controller. There is a need for a precision irrigation controller, such as the POWEIr controller, that optimizes irrigation schedules and implements SPM in real time for a SPDI system. The POWEIr controller allows the cost and reliability benefits outlined in this economic analysis to be realized in a variety of contexts.

2.3 POWEIr Controller Theory

2.3.1 POWEIr Controller Architecture

The POWEIr controller is designed to be a widely adoptable precision irrigation tool that meets the needs of LMIC farmers in terms of scale, adaptability, accessibility, and cost [22], [39]. The controller produces an optimal SPM irrigation schedule for a SPDI system, taking into account the available solar power, the required pumping power, the irrigation demand, and the battery capacity. The aims are to maximize crop yield, manage energy efficiently, minimize water use, and reduce risk to farmers. The POWEIr controller uses a small number of sensors and can operate with manual or automatic valves. It provides farmers with the irrigation schedule one day in advance, which was found to be a preference among target users [22].

The controller employs a three-tier architecture (Fig. 2.3). Level 3 uses MPC to produce a daily optimal irrigation schedule based on its prediction of the crop water demand and available solar power. Level 2 uses MPC to manage the energy use between the panels and

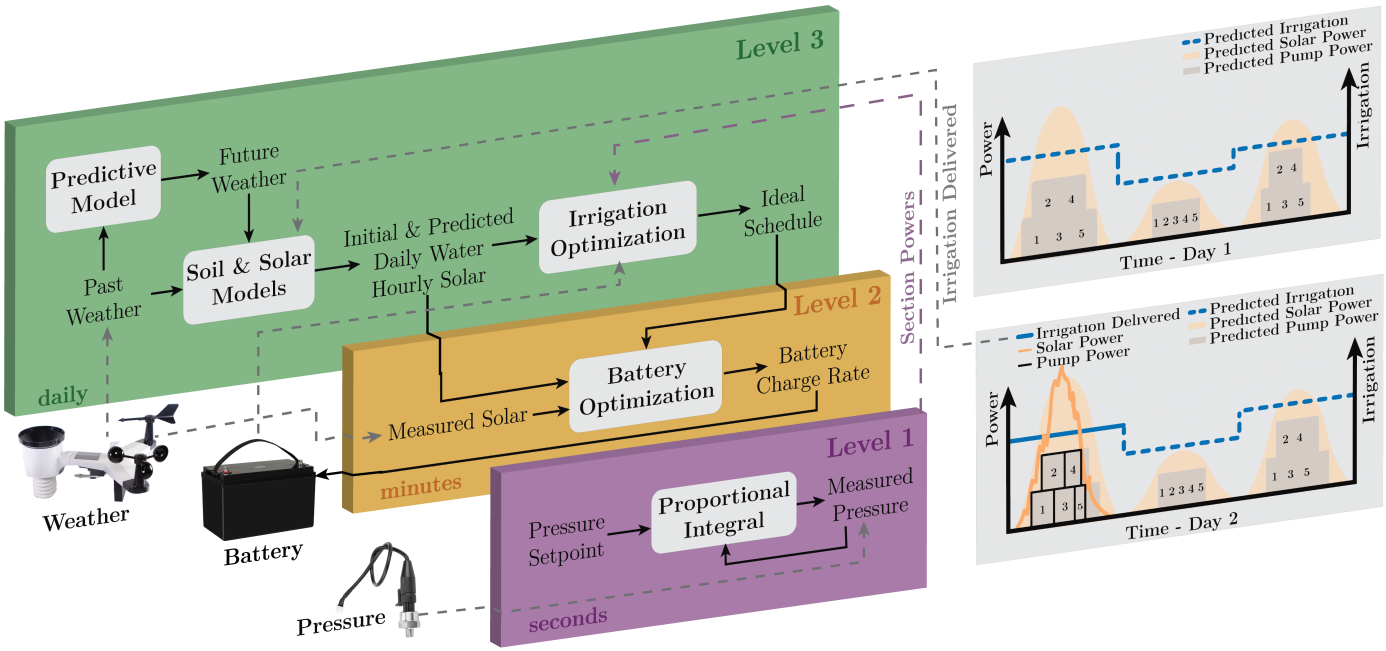

Figure 2.3: The Predictive Optimal Water and Energy Irrigation (POWEIr) controller's three-tier architecture. Level 3 (green) predicts the weather, models solar power and soil water levels, and optimizes the irrigation schedule at a daily frequency. Level 2 (yellow) re-optimizes the battery energy management at a frequency of minutes to mitigate the prediction error of Level 3 and preserve battery life. Level 1 (purple) maintains the minimum operating power of each irrigation section at a frequency of seconds to ensure uniform flow and avoid excess energy use due to over-pressurizing the system. A weather station, battery, and pressure sensor are needed on the farm to provide measurement inputs. The top right graph shows the Level 3 daily predictions, and the bottom right graph shows the sub-daily Level 2 battery and Level 1 pump power management. On the bottom right graph, the amount of irrigation delivered is fed back to Level 3.

battery on a sub-daily basis, while satisfying the Level 3 irrigation schedule, to reduce battery aging. By adjusting the system energy use in real-time, Level 2 also mitigates prediction error from Level 3. Level 1 uses proportional integral (PI) feedback control to maintain uniform flow, automatically accommodating fluctuations in the hydraulic system pressure. Level 1 facilitates the SPM schedule by adjusting the pump power based on the number of open sections and enables the pump operating points to be well characterized for the Level 3 and Level 2 calculations.

2.3.2 Level 3: Irrigation Schedule Optimization

Weather Prediction Model

Weather measurements are needed to predict the daily evapotranspiration, precipitation, and radiation. These values are used in a soil moisture model and solar power model to calculate the crop water demand and available solar power. The weather prediction methodology is a machine learning algorithm. In many LMICs, local, accurate, and reliable weather stations and forecasts are not readily available [54], [55]. Farmers in LMICs can no longer rely on historical weather patterns due to climate change, and there is a growing need for a low-cost, local method for predicting weather [56], [57]. This is especially true for rural farmers in LMICs where the nearest weather station can be thousands of kilometers away, remote sensing is not high enough resolution to discern a small farm's micro-climate, and there is not the infrastructure to support computationally expensive climate models [58], [59]. In these cases, using low-cost weather sensors paired with a computationally inexpensive machine learning algorithm to predict a farm's local weather is a viable option [60].

The machine learning algorithm chosen is vector autoregression (VAR), similar to the method chosen in [61]. VAR is a multivariate prediction algorithm that is well suited for predicting weather data as it is formulated to predict multiple time series data at once that influence each other. VAR is also an appropriate choice as it can be accurate with limited training data, making VAR an applicable method for farms with little existing local weather data. The VAR model is defined as [62]

$$y_t = c + W_1 y_{t-1} + W_2 y_{t-2} + \cdots + W_p y_{t-p} + e_t, \tag{2.7}$$

where y is a vector of variables being predicted, t is the time, c is a vector of constants, W is a weight matrix, p is the lag order, and e is an error vector. y is comprised of local historical and measured weather parameters. The weather parameters are daily average, minimum, and maximum air temperature and relative humidity; daily average wind speed; total daily

solar radiation (G) [MJ/m^2]; reference evapotranspiration (ET_0) [mm] calculated from the previous weather parameters using the Penman-Monteith equation [63]; sun hours calculated as the number of hours the hourly radiation was greater than 0.1 MJ/m^2; and precipitation (Pr) [mm].

An augmented Dickey-Fuller test is used to check the stationarity of each variable of the weather data [62]. If the p-value of the augmented Dickey-Fuller test is less than 0.05 for each variable, the null hypothesis can be rejected and it is inferred that the time series data are stationary. If the p-value of the augmented Dickey-Fuller test is greater than 0.05 for any variable of the weather data, the null hypothesis can not be rejected and up to two differences in the data are taken to re-check stationarity. The augmented Dickey-Fuller test is checked for each of the differenced data and the full data are considered stationary when the null hypothesis can be rejected for each variable.

The stationary data are split into training and testing data sets based on the number of prediction days chosen. The lag order of the VAR model is chosen by finding the optimal VAR order selection. A VAR model is built using the time series analysis function in the statsmodels package in Python [64] and fit using the selected lag order. The model is then used to predict the y vector, and the predicted weather parameters are used to calculate the solar power and crop water demand for the upcoming day. Every time an irrigation schedule is calculated the time series VAR model is re-trained and re-built using one year of historical weather and the most recent measured weather data.

Solar Power Model

The solar power model calculates the available solar power, which is used in the irrigation schedule optimization. A modified single diode model, proposed in Villalva, Gazoli, and Filho [65], is used to calculate the maximum power point given the local historical solar irradiance and temperature at each hour of the day. Then, the historic hourly solar power is calculated for the year. This solar power is used for the daily prediction and is scaled by

a factor, f_{solar}, calculated as

$$f_{solar} = \frac{G_{predict}}{G_{historic}}, \tag{2.8}$$

where $G_{predict}$ is the predicted total daily solar radiation [MJ/m^2] and $G_{historic}$ is the historic total daily solar radiation [MJ/m^2] for the prediction day.

Soil Moisture Model

The soil moisture model calculates the irrigation demand parameters used to optimize the irrigation schedule. A soil water balance calculates the depth of water depleted from the soil root zone (D_r). The D_r is related to the water stress on the crop which affects crop yield. The water stress coefficient, K_{st}, is defined as

$$K_{st} = \frac{TAW - D_r}{TAW(1 - f_d)}, \tag{2.9}$$

where TAW is the total available water that the crop can extract from the soil [mm] which depends on crop and soil properties and f_d is the depletion fraction.

D_r is calculated by substituting the equation for K_{st} into the soil water balance defined in Allen, Pereira, Raes, *et al.* [63] and solving for D_r. For each day n, D_r is calculated as

$$D_{r,n} = \frac{D_{r,n-1} - Pr_n + RO_n - \frac{1000 I_{del,n}}{A_s f_w} + \frac{ET_{c,n}}{1 - f_{d,n}}}{1 + \frac{ET_{c,n}}{TAW(1 - f_{d,n})}}, \tag{2.10}$$

where RO is the runoff [mm], estimated as a fraction of Pr based on the soil type, A_s, is the section area that D_r is being calculated for [m^2], and f_w is the soil wetted fraction. The crop evapotranspiration (ET_c) [mm] is calculated on day n as

$$ET_{c,n} = K_{c,n} ET_{0,n}, \tag{2.11}$$

where K_c is a crop coefficient. The f_d is calculated on day n as

$$f_{d,n} = f_{d,const} + 0.04\,(5 - ET_{c,n}), \tag{2.12}$$

where $f_{d,const}$ is a crop dependant constant defined in [63]. D_r is constrained every day to be between zero and TAW. The readily available water, RAW, is defined as

$$RAW_n = f_{d,n} TAW. \tag{2.13}$$

If D_r is less than or equal to the RAW then there is no water stress on the crop and K_{st} is one. If the D_r is greater than RAW, then there is water stress and K_{st} varies between zero and one. The water stress affects the amount of crop evapotranspiration:

$$ET_{c,adj} = K_{st} ET_c. \tag{2.14}$$

If there is water stress on the crop, then the reduction in evapotranspiration relates to a reduction in yield:

$$1 - \frac{Y_a}{Y_{max}} = K_y \left(1 - \frac{ET_{c,adj}}{ET_c}\right). \tag{2.15}$$

The Y_a is the adjusted yield [kg/m^2], Y_{max} is the maximum yield [kg/m^2] calculated using the agro-ecological zone method defined in [66], and K_y is the crop yield response factor [67].

Irrigation Optimization

The irrigation optimization algorithm's objective is structured to incorporate the trade-offs identified using stakeholder feedback. The trade-offs are to achieve high crop productivity and reduce SPDI costs without sacrificing irrigation reliability or introducing risk to the crops. Based on the stakeholder analysis and design requirements defined in Van de Zande, Sheline, Amrose, *et al.* [22] and Grant, Amrose, Talozi, *et al.* [24], the POWEIr controller

architecture was designed to be

Predictive, so that it provides advance notice of the irrigation schedule to the user to allow for planning,

Efficient by lowering water-use and energy storage capacity without introducing risk to the crop yields, and

Low-cost by reducing the on-field hardware to decrease complexity and cost without sacrificing irrigation accuracy.

To satisfy these design targets, Level 3 outputs a predicted daily optimal irrigation schedule. Additionally, the optimization objective is formulated to minimize the operational cost from battery use and water consumption (L), maximize revenue through crop yield (R), and minimize future risk by fully charging the battery at the end of the prediction horizon (V). The objective function is defined over a prediction horizon as

$$\min\left[\sum_{i=\delta t}^{N_{hor}} L(d_{s,i}, u_{1,i}, u_{2,i}) - \sum_{n=1}^{N_{day}} R(x_{s,n}) + V(SOC_{N_{hor}})\right], \tag{2.16}$$

where N_{hor} is the prediction horizon in hours and N_{day} is the prediction horizon in days. The prediction horizon is defined in two different time units because the system water and energy use are calculated at every time step, but the agronomy factors—including the soil moisture and yield—are calculated daily. The function L is used to minimize the battery and water use with an hourly time step, δt, and the function R is used to maximize the crop revenue with a daily time step. The function V is used to fill the battery by the end of the prediction horizon. In function L, d_s is the binary control variable for irrigating section s of the field; u is a dimensionless control variable for the rate that the battery is charged (u_1) and discharged (u_2), normalized by u_{max} [kW], the maximum dispatch rate of the battery specified by the manufacturer. In function R, x_s is the dimensionless state variable for the D_r (Eq. 2.10) of each section s normalized by TAW. In function V, $SOC_{N_{hor}}$ is the dimensionless battery

state of charge, calculated as the energy stored in the battery normalized by the battery capacity, C_{batt} [kWh], at the end of the prediction horizon. These functions are all defined in terms of cost as

$$L(d_{s,i}, u_i) = \frac{1}{N_{hor}} \left(k_b u_{max}(u_{1,i} - u_{2,i}) + \sum_{s=1}^{N_{s,tot}} k_w q_s d_{s,i} \right), \tag{2.17}$$

$$R(x_{s,n}) = \sum_{s=1}^{N_{s,tot}} \frac{1}{N_{day}} \left(k_c A_s \frac{dY_{a,s,n}}{dt} \right), \tag{2.18}$$

$$V(SOC_{N_{hor}}) = k_d(1 - SOC_{N_{hor}}), \tag{2.19}$$

where k_b [\$/kWh] is the cost weight of the battery defined by the unit battery cost and its lifetime storage; $N_{s,tot}$ is the total number of sections s the field is split into; k_w [\$/m^3] is the cost weight for water; k_c [\$/kg] is the price weight on the crop; $\frac{dY_{a,s,n}}{dt}$ is the daily yield [kg/m^2/day], which is estimated by dividing Y_a in Equation 2.15 by the number of days in the crop growing season; and k_d is the cost weight on the energy storage [\$] based on the total cost of the system over its lifetime divided by the number of prediction horizons in the lifetime.

The optimization is subject to the following boundary constraints at each time step, i or

n:

$$0 \leq u_{1,i} \leq 1, \tag{2.20}$$

$$-1 \leq u_{2,i} \leq 0, \tag{2.21}$$

$$d_{s,i} \in \{1, 0\}, \tag{2.22}$$

$$0 \leq x_{s,n} \leq 1, \tag{2.23}$$

$$SOC_{min} \leq SOC_i \leq SOC_{max}, \tag{2.24}$$

$$x_{s,0} = x_{s,ini}, \tag{2.25}$$

$$SOC_0 = SOC_{ini}, \tag{2.26}$$

where SOC_{min} is the minimum state of charge, set by the manufacturer recommended depth of discharge, SOC_{max} is the maximum state of charge, and $x_{s,ini}$ and SOC_{ini} are the initial state of the soil water depletion and battery state of charge. These initial conditions can be measured. SOC_{ini} is measured from the battery at the start of the day, and $x_{s,ini}$ is calculated based on Equation 2.10 and the previous day's agronomy parameters, measured weather, and delivered irrigation. The $x_{s,ini}$ for the start of a crop season can be estimated from measured soil moisture.

The optimization is also subject to constraints on the system dynamics. These dynamics include changes in the amount of water stored in the soil and the amount of energy stored in the battery. The model for the water stored in the soil is the daily soil water balance. The soil water balance is calculated by solving for x as the fraction of D_r over TAW in Equation 2.10:

$$x_{s,n} = \frac{TAW x_{s,n-1} - Pr_n + RO_n - \frac{1000 I_{del,s,n}}{A_s f_w} + \frac{ET_{c,s,n}}{1 - f_{d,s,n}}}{TAW + \frac{ET_{c,s,n}}{1 - f_{d,s,n}}}. \tag{2.27}$$

The irrigation delivered in Equation is calculated as

$$I_{del,s,n} = \sum_{i=\delta t}^{i=N_{hor}} d_{s,i} q_s \delta t. \tag{2.28}$$

The battery storage dynamic model is

$$SOC_i = SOC_{i-1} + \frac{u_{max}}{C_{batt}}(u_{1,i} + u_{2,i})\delta t. \tag{2.29}$$

The battery charging and discharging rates are functions of ΔP_i, the difference between available solar power and the pump power demand at time step i:

$$\Delta P_i = P_{avail,i} - P_{pump,i}, \tag{2.30}$$

$$u_{1,i} \leq \frac{\eta_{batt}}{2u_{max}}\big(|\Delta P_i| + \Delta P_i\big), \tag{2.31}$$

$$u_{2,i} = \frac{1}{2u_{max}\eta_{batt}}\big(\Delta P_i - |\Delta P_i|\big). \tag{2.32}$$

Equation 2.31 states that the battery can only charge if there is excess solar power available (P_{avail}). Equation 2.32 states that the battery must discharge to meet the pump power demand, P_{pump} [kW], if there is insufficient solar power available, P_{avail} [kW]. The battery efficiency, η_{batt}, is assumed to be the same for charging and discharging. P_{pump} is an empirical linear equation fit as a function of the number of sections opened at a given time; these values are calibrated when a system is installed.

There are also constraints on how the sections can be opened, which are

$$\sum_{s} d_{s,i} \leq d_{max}, \tag{2.33}$$

$$\sum_{i}^{N_{day}} (d_{s,i} - d_{s,i-1})^2 \leq 2, \tag{2.34}$$

where d_{max} is the maximum number of sections that can be opened at one time. Equation 2.34 requires each section to be opened and closed only once per day at most.

2.3.3 Level 2: Energy Storage Optimization

Level 2 takes in the Level 3 predictions for the upcoming day and optimizes the battery use throughout the day. The primary aims of Level 2 are to ensure the system can reliably irrigate according to the Level 3 schedule and reduce battery aging over time. Given that farmers prefer daily schedule updates [22], Level 2 is constrained to meet the optimal irrigation schedule produced by Level 3 at the beginning of the day. It was also found through stakeholder interviews that farmers would prefer smaller, less expensive energy storage components and are wary of the maintenance and replacement costs associated with batteries [24]. However, using a small battery relative to the solar panel capacity can lead to high dispatch rates, which in turn can impact battery performance and aging [68]. The Level 2 objective function aims to balance system reliability and battery longevity by storing enough energy in the battery over the day to ensure schedule adherence while also minimizing the battery charging rate to reduce energy throughput of the battery (Eqs. 2.35 and 2.36). Level 2 takes in the predicted solar power, pump load schedule, and expected battery SOC from Level 3 as shown in Fig. 2.3, and optimizes the battery charging rate at each time step. Level 2 incorporates real-time measurements of the available solar power, which allows for adjustments to the system energy use despite errors in the Level 3 solar power prediction. The objective function is defined over the same prediction horizon as Level 3, N_{hor}:

$$min \sum_{i=\delta t}^{N_{hor}} \alpha M(SOC_i) - (1-\alpha)u_{1,i}, \tag{2.35}$$

$$M(SOC_i) = \frac{1}{2}\big[(SOC_{ref,i} - SOC_i) + |SOC_{ref,i} - SOC_i|)\big], \tag{2.36}$$

where, at each time step, $SOC_{ref,i}$ is the reference SOC predicted by Level 3, SOC_i is the measured SOC, and $u_{1,i}$ is battery charging rate, which is the Level 2 control variable. The weighting factor, α, can be used to set the relative priority of the two terms in the objective function. The first term, M, in the objective function is formulated to track the predicted

SOC from Level 3, but does not penalize exceeding the reference to store more energy in the battery. This term aims to store adequate energy in the battery to ensure reliable irrigation despite prediction errors from Level 3 and disturbances in the available solar power or pump load profile during operation. The second term in the objective function aims to minimize the battery charging rate, which affects battery cyclic aging [68]. At each time step, the optimization is subject to the constraints defined in Equations 2.31 and 2.32, and the boundary conditions defined in Equations 2.20, 2.21, 2.24 and 2.26. The Level 2 optimization is effectively constrained to meet the Level 3 irrigation schedule by Equation 2.32, which requires the battery to discharge whenever the pump demand exceeds the available solar power.

2.3.4 Level 1: Pump Operating Point Control

Level 1 maintains the pump operating point using proportional integral (PI) feedback control on the pump pressure. Drip emitters have a minimum pressure at which the emitter uniformly produces its rated flow [69]. Pressure feedback control can be used to maintain the minimum operating pressure necessary to provide uniform flow without wasting power to over-pressurizing the pipe network. The pressure setpoint for a section can be determined by increasing the pump power until the last emitter in the section is operating at its rated flow. This is the calibration method to determine the section setpoints for the Level 1 control loop. The PI gains can then be tuned for the hydraulic network using standard system identification and PID tuning techniques [70]–[72].

The Level 1 feedback pressure sensor is placed downstream of the filters and fertigation unit in the mainline to enable static setpoints that only require one calibration for a given hydraulic network configuration. The primary dynamic pressure losses in the hydraulic network are the filters and fertigation unit, which are typically downstream of the pump. It was observed in previous experimental work that the pump operating power varies over time due to filters clogging and the use of the fertigation unit [36], [73]. The POWEIr controller

is programmed with the calibrated pump operating power for single and multiple sections, and these operating points are passed into the Level 3 and Level 2 optimizations. Although the pump power will vary over time, Level 1 ensures that the pump operating points are relatively consistent over time, barring any significant changes that would require hydraulic maintenance. This means Level 1 enables the Level 3 and Level 2 predictive modeling to remain accurate over the course of the irrigation season.

2.4 Experimental Prototype

2.4.1 Methods

A prototype of the POWEIr controller was built for a scaled-down SPDI system, which was representative of a small field, and tested in Cambridge, Massachusetts, USA over seven days. The experiment was designed to demonstrate the water and energy management capabilities of the controller, specifically its ability to predict weather, schedule irrigation, and manage battery storage. No crops were grown, but the daily crop water demand was simulated to produce an optimal daily irrigation schedule with Level 3. The daily test conditions were defined by the solar energy predicted by the POWEIr controller, the predicted irrigation demand, and the actual solar energy measured over the day. The experimental case, defined in Table 2.2, was used to generate the Level 3 irrigation schedule for each day by varying $x_{s,ini}$ to get a range of crop water demand test conditions. This case is a scaled-down version of the case presented in Table 2.1. The controller prototype software was implemented in MATLAB using a Gurobi solver on a laptop, interfacing with a programmable logic controller or PLC (CLICK PLUS PLC) via Ethernet, and communicating with the hardware components via MODBUS.

The SPDI prototype layout and instrumentation are shown in Figure 2.4. Two hydraulic sections were operated with manual ball valves and were used to mimic the five-section field

Table 2.2: Experiment case for POWEIr controller prototype.

Location	Cambridge, MA
Field area	0.25 ha
Section size	0.05 ha
Water source depth	2 m
Simulated Crop	Tomato
Emitter flow rate	0.5 Lph
Section pump power (for one and two sections)	0.24, 0.32 kW
Section irrigation time (daily average)	89 min.

defined in the experimental case (Table 2.2). The schedule was constrained to operate a maximum of two sections at a time. A submersible pump (Goulds 8GSZ05R) was located in the Charles River at a depth of about two meters. The hydraulic behavior of the system was recorded with a flow meter (Omega FTB4607), located downstream of the filter, and pressure sensors (ProSense SPT25-20-0060D) located at the outlet of the pump, before and after the disk filter (Irritec T-Filter 155 mesh), at the entrance of each section, and at the end of the last lateral of each section. These sensor measurements were used to compute hydraulic power and calibrate the pump operating points. The PI feedback loop in Level 1 was tuned by running the hydraulic system in open-loop and using the MATLAB system identification toolbox to determine the system dynamic response, which was found to be first-order with a response time on the order of one minute. The CLICK AutoTune feature [70] was used to identify the proportional and integral gains, which were then adjusted manually to obtain the desired system behavior. A VFD (Danfoss VACON0010-1L-0002-1) was used to modulate the pump speed and record the input and output power of the motor.

The power system consisted of a 1.3 kW solar array (CS3W-445MS) and a 3.84 kWh custom lithium iron phosphate (LFP) battery (Topbrand 16S-3P cell). Current and voltage

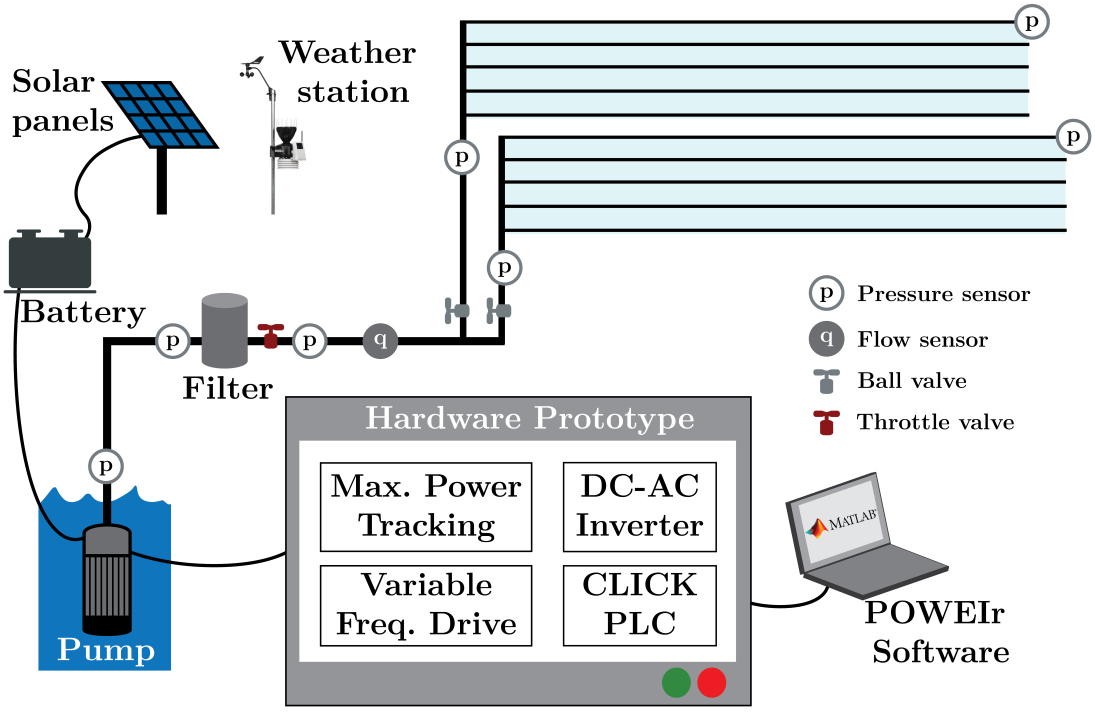

Figure 2.4: Controller prototype system layout and instrumentation.

measurements were recorded at the panels, battery, and pump motor; these data were used to compute system energy use. A pyranometer (Davis Solar Radiation Sensor #6450) and temperature sensor were located next to the panel array, which were used to calculate the available solar power using the single-diode model [65]. The on-site Davis Vantage Pro weather station measured temperature, relative humidity, rainfall, and wind velocity. The machine learning algorithm for the Level 3 daily weather predictions was built and trained for each day tested using 30 days of weather data downloaded from the Davis Vantage Pro weather station combined with one year of historical weather data [74]. The prediction horizons for Level 3 and Level 2 were set to 24 hours.

The controller was compared to several simulated benchmarks to quantify its performance. The optimal irrigation scheduling and energy use were compared to a simulated SSO reference for the same field that represents typical farmer practice, hereafter referred to as SSO reference. The SSO reference was simulated to open the first section as soon as the

solar power available was greater than or equal to the pump power for one section. Once the first section was opened it was assumed that the entire farm was irrigated, one section at a time, until the irrigation demand was reached. The amount of simulated water that was delivered by the SSO reference was constrained to be the same amount of water delivered by the POWEIr controller during the experiment.

The Level 2 optimized battery use was compared to simulated battery operation with no control to quantify the effectiveness of real-time control on cyclic battery aging. In the no-control case, the battery was simulated to charge as soon as solar power was available, at a charging rate equal to the available solar power, and discharge according to the pump load. The pump energy use with Level 1 control was compared to the pump energy use for a simulated constant operating point. The simulated constant operating point was set to the maximum pump power, or the power required to operate two sections, which would be necessary to ensure uniform flow for any section combination without Level 1 feedback control.

2.4.2 Results

The POWEIr controller experimental prototype was evaluated for a range of test conditions—predicted solar energy, measured solar energy, and predicted irrigation demand. A summary of the daily test conditions compared to the seven-day average conditions is provided in Table 2.3. Over the seven days, Level 3 over and under predicted the measured solar energy and the irrigation demand spanned a range of 82% below to 64% above the observed average. Table 2.3 shows that for the three conditions, six out of the eight possible above- and below-average combinations are tested. This indicates that the experimental prototype was tested over a comprehensive set of conditions.

Figure 2.5 shows the full power profiles of the POWEIr controller on two days where the irrigation demand was above average. On October 20$^{\text{th}}$, Level 3 underpredicted the available solar energy, and on October 11$^{\text{th}}$, Level 3 overpredicted the available solar energy. For both

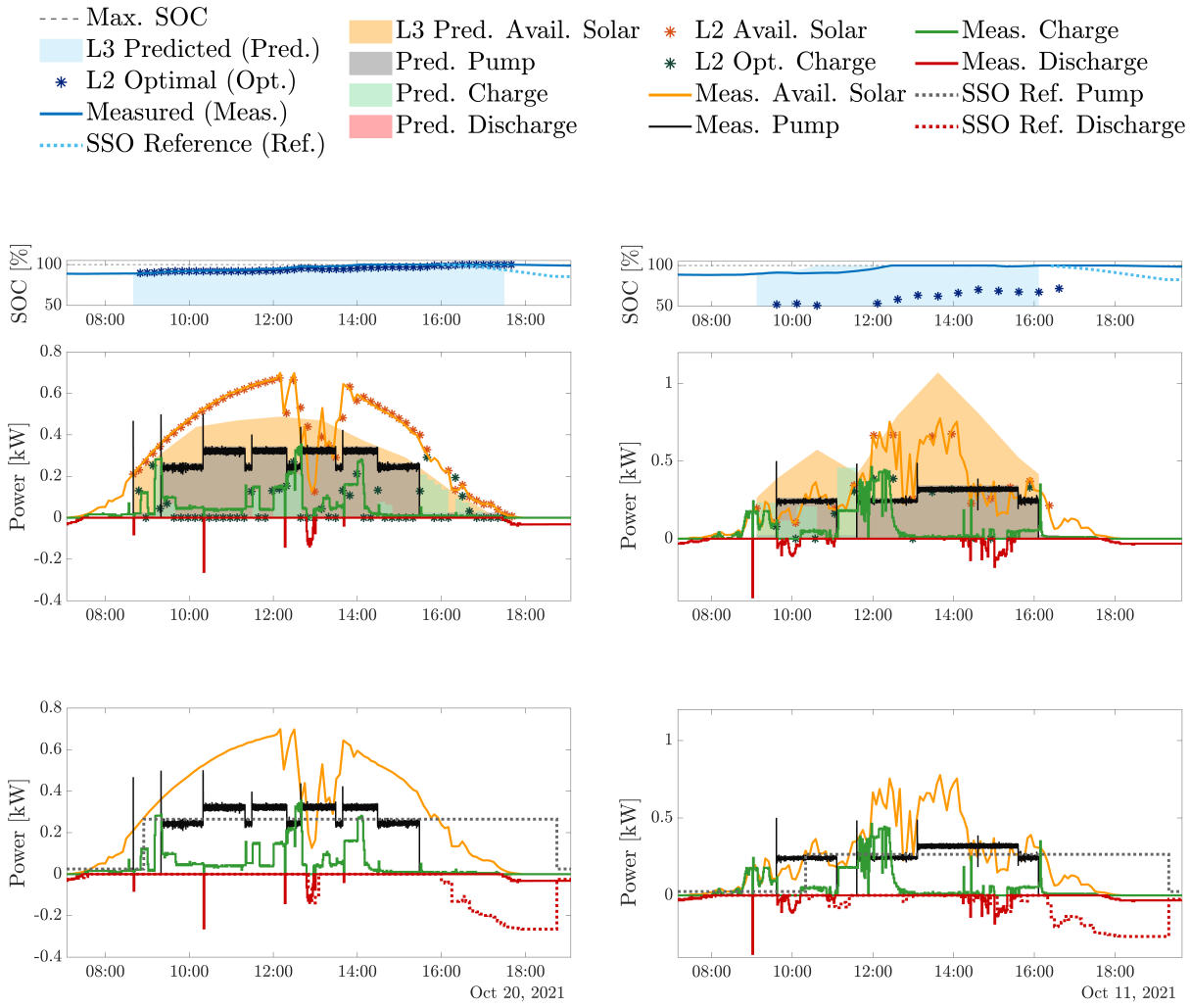

Figure 2.5: The power profiles over a day where there was higher measured solar power than predicted, October 20, 2021, and a day when there was lower measured solar power than predicted, October 11, 2021. For both of these days, the state of charge (SOC) of the battery (blue) is plotted on top and the power used by other system components: solar (orange), pump (grey), battery charge (green), battery discharge (red), are shown on the middle and bottom plots. The middle plots show the Level 3 (L3) predictions (shaded), Level 2 (L2) optimal points (asterisks), and measured data from the POWEIr controller (solid lines). The bottom plots compare the measured POWEIr controller data to single section operation (SSO) reference data (dashed line). The SSO reference data was simulated to represent how a farm with SPDI but without the POWEIr controller would have traditionally been operated, irrigating a single section at a time.

Table 2.3: Summary of the solar and irrigation daily test conditions. The percent differences are the predicted solar energy (Pred. Solar) and the measured solar energy (Meas. Solar) compared to the seven-day average measured solar energy and the irrigation demand (Irri. Demand) compared to the seven-day average irrigation demand. Above-average, at-average, and below-average conditions are highlighted in green, yellow, and red, respectively.

Date	**Pred. Solar**	**Meas. Solar**	**Irri. Demand**
1st	+11%	0%	+58%
6th	+19%	+6%	+64%
7th	+36%	+16%	-30%
11th	+27%	-28%	+12%
13th	-25%	+14%	-50%
19th	-38%	-11%	-82%
20th	-17%	+3%	+28%

days, the Level 3 solar prediction (filled orange) did not match the measured solar power (orange line) and the battery had to be discharged (red line), to meet the optimal irrigation schedule. The POWEIr controller discharged the battery less and delivered irrigation (pump power shown in black) in a shorter amount of time compared to the SSO reference (dotted lines) for both days. The POWEIr controller was able to deliver the same amount of water in a shorter amount of time by implementing SPM. The pump efficiency was 14% and 21% when one and two sections were operated, respectively. The pump efficiencies were low due to the miniature size of the prototype, which led to low pump operating points. Higher pump efficiencies are expected in practice when a pump is used for a full-scale farm. The power profile results for the remaining test days are provided in Appendix A.3.

Figure 2.6 compares the daily solar (orange), pump (grey), and battery charge (green) and discharge (red) energy for the Level 3 predicted optimal (left), measured (middle), and the simulated SSO reference (right) values. It was assumed that the SSO reference had the same solar and battery charge energy as that measured during the experiment. The volume of water delivered is the same between the POWEIr controller and the SSO reference, but the pumping energy is different because it was energetically favorable to irrigate two sections over one.

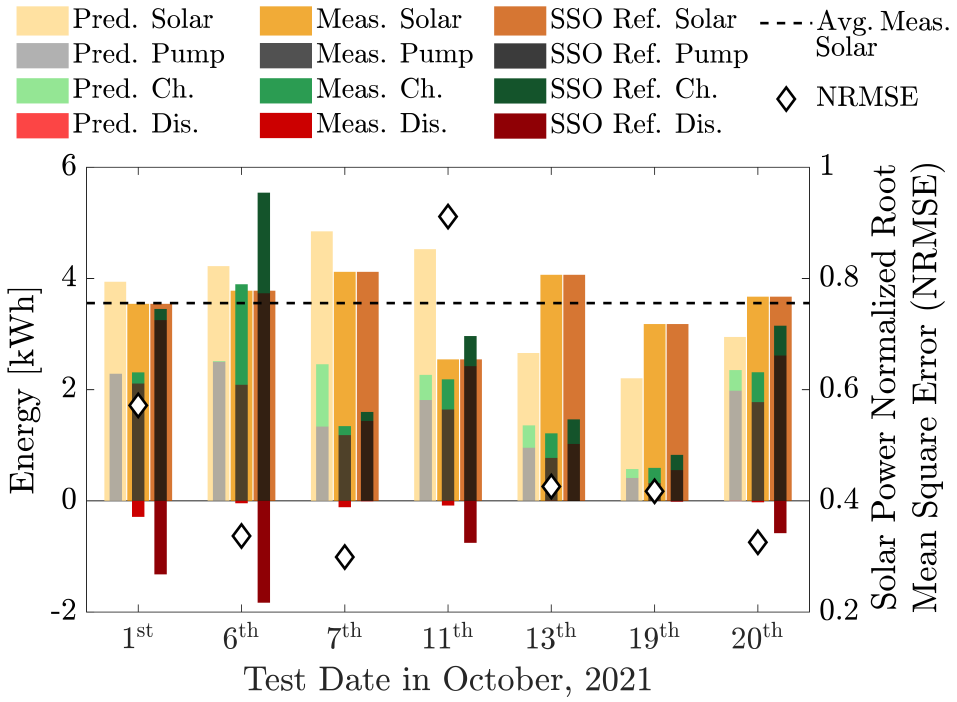

Figure 2.6: The energy breakdown and solar prediction error of each day of the POWEIr controller experiment.

Figure 2.6 shows that on days with below-average irrigation demand (October 7th, 13th, and 19th), the energy consumption that was measured is similar to that of the SSO reference because the controller implemented an irrigation schedule similar to SSO on these days. On days with above-average irrigation demand (October 1st, 6th, 11th, and 20th), the controller implemented SPM and used 78-98% less battery energy compared to the SSO reference. For all of the days, Level 3 produced an optimal schedule that did not use the battery because the predicted available solar power was sufficient for the pump load and to fill the battery by the end of the day (Fig. 2.5, solid blue line). In reality, due to Level 3 prediction errors, the battery was used as a buffer when unforeseen dips in the measured available solar power occurred.

The normalized root mean square error (NRMSE) between the predicted and measured solar power, normalized by the mean measured solar power, was 0.3–0.9, with a root mean square error (RMSE) of 0.132–0.328 kW (Fig. 2.6). NRMSE penalizes large variations be-

tween the predicted and measured values; reducing this variation improves system reliability. The solar power prediction error is comparable to the pump operating points for one and two sections, 0.24 kW and 0.32 kW, respectively. If the Level 3 prediction alone were used to determine the power system operation, the system may fail to irrigate due to the mismatch between the pump power demand and the actual available solar power. Despite the solar prediction error, the controller was able to meet the irrigation demand over all tested days because it had energy storage to draw from. The maximum amount that the battery was discharged for the POWEIr controller was 0.3 kWh, representing the battery capacity needed as a buffer during this experiment. By contrast, the SSO reference needed a battery capacity of 1.8 kWh, six times that of the POWEIr controller.

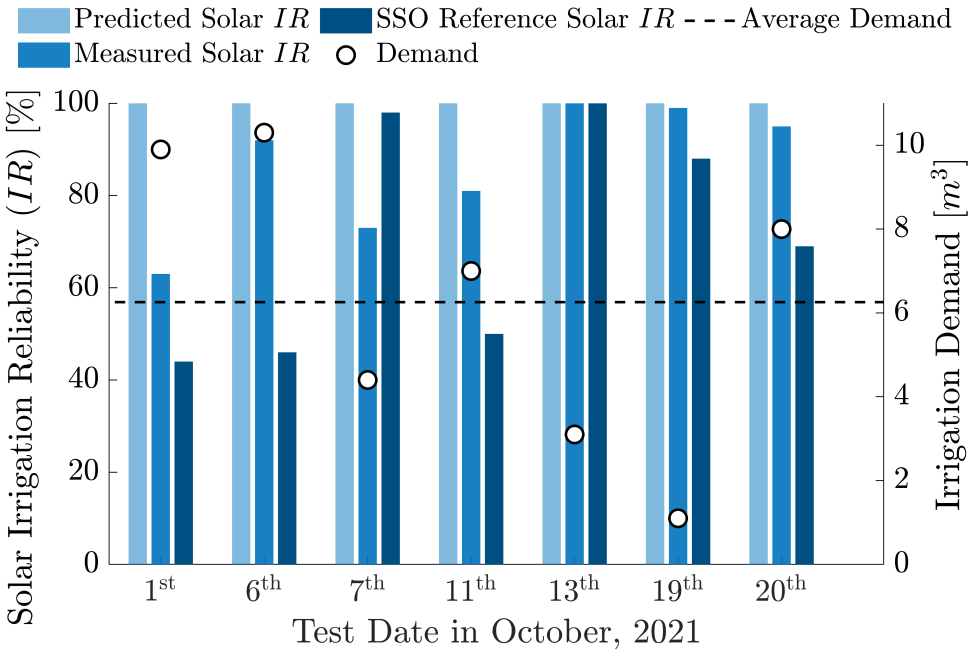

Figure 2.7: The solar irrigation reliability (solar IR) and irrigation demand of each day of the POWEIr controller experiment.

Figure 2.7 shows the solar irrigation reliability (solar IR) on each day comparing the Level 3 prediction (light blue), the measured data (blue), and the simulated SSO reference (dark blue) to demonstrate how much water could be delivered directly by solar (i.e., without relying on the battery) in each case. The solar IR was computed as the ratio of the irrigation

amount delivered using direct drive solar power to the total irrigation demand. The predicted IR was 100% for every test day. Due to Level 3 prediction errors, the measured solar IR varied from 63–100%. The daily irrigation demands (white circles) are shown along with the average irrigation demand (dashed line) over all days. On days with above-average irrigation demand, the measured solar IR was 19–46% higher than the SSO reference solar IR, meaning that more battery energy had to be used to meet the irrigation demand for the SSO reference. On low-demand days, the predicted, measured, and SSO reference solar IR were above 80%, indicating that the pump was primarily powered by the solar panels for all three cases. The solar IR is an indicator of what the IR would be without any battery buffer. Fig. 2.6 shows that the POWEIr controller needed a 0.3 kWh battery buffer to deliver all of the irrigation demand (100% IR). Therefore, a battery capacity of only 0.3 kWh enabled up to a 37% increase in the measured IR, from 63% with direct drive to 100%. This demonstrates that it is possible to use a relatively small battery capacity to mitigate weather prediction errors and ensure reliable irrigation.

2.5 Discussion

The economic analysis presented in this chapter demonstrates the benefit of using SPM irrigation scheduling and optimizing the design of SPDI systems. Combining SPM with SPDI component optimization can lead to 18–74% life cycle cost savings while increasing irrigation reliability by 31–66% compared to a commercial system sizing tool using SSO. This indicates that pairing SPDI with precision irrigation control could enable smaller, lower-cost systems that are still able to meet crop water demand in a variety of contexts. This economic analysis can be conducted for other cases to determine the benefits SPM could provide in any context. It was found that SPM provides the most benefits for farms with high pumping power and irrigation requirements. These farms require large solar power systems, which are cost prohibitive in LMICs, when designed and operated using traditional

methods. Implementing SPM in these contexts could increase the accessibility of solar-powered irrigation.

The proposed POWEIr controller implements SPM and optimizes SPDI energy and water use. The POWEIr controller software was developed to be scale-neutral and adaptable to a variety of local contexts, which means it can provide case-specific irrigation scheduling. The proposed architecture facilitates a low-cost device that would be accessible to the target user groups. The controller uses minimal on-field sensors, including a low-cost weather station and a single pressure sensor, and manual valves. In the proposed architecture, the complexity is primarily in software, and the predictive modeling computations can be conducted in the cloud rather than on-site specialized hardware. It does not require a fully instrumented hydraulic system or an array of soil moisture sensors, which are costly and require technical expertise to maintain. The integration of this controller with SPDI systems could make precision irrigation technology easier to adopt and help farmers sustainably increase crop productivity. The performance of the controller and its potential to be implemented at low cost indicate that it could meet the needs of small- and medium-scale farmers in LMICs, allowing farmers to realize the economic and sustainability benefits of SPDI.

The performance of the POWEIr controller was validated with an experimental prototype. The experimental results show that the Level 3 irrigation schedule optimization and weather prediction was able to meet the simulated crop water demand without a priori knowledge of the weather. The experiment demonstrated that the proposed three-tiered architecture was able to reliably operate an irrigation system while being robust to errors in the prediction. Although the daily solar power prediction error was on the same order as the pump power requirement, the controller was able to reliably meet the simulated crop water demand under varying weather conditions using a small battery buffer. This means that the POWEIr controller would be able to provide a daily optimal irrigation schedule to the end user while adapting to changes in real-time with an energy management strategy. The machine learning algorithm that produced the weather prediction took the majority of

the Level 3 run time. However, the results of the experiment indicate a daily prediction is sufficient for the controller to reliably meet the irrigation demand, so it is not necessary to run this computationally expensive algorithm more frequently.

The POWIEr controller had an advantage over typical farmer practices on high irrigation demand days. On the tested above-average demand days, the controller was shown to have up to 46% higher solar irrigation reliability. Even with solar prediction errors of up to 0.9 NRMSE, the controller was able to deliver irrigation more reliably while using less energy storage buffer compared to the SSO reference. These high demand conditions ultimately drive the SPDI system component capacities. The ability of the POWEIr controller to improve the solar energy use efficiency enables a smaller, less expensive power system compared to the reference case.

The presented controller prototype was not intended to validate the agronomy models. Instead, the data collected in this study represents the expected operation range of the POWEIr controller and serves as a validation of its energy management, irrigation scheduling, and weather prediction capabilities. Further work should be conducted to determine the accuracy of the irrigation scheduling calculations in terms of their effect on relevant agronomy parameters. The controller should be tested on a farm over a full growing season to measure the performance of the Level 3 soil moisture calculations. It was assumed that the SSO reference would match the irrigation demand of the POWEIr controller in the experimental prototype. In practice, farmers irrigate based on their experience and can over-irrigate, so future experiments should explore the water-saving capabilities of the controller.

For this small-scale experiment, the hydraulic system operated outside of the preferred pump operating range, leading to unrealistically low pump efficiencies. However, there are cases in which the number of sections can lead to large pump operating ranges. This has implications for the system energy use, power system capacity, and system efficiencies, which should be explored further when testing the controller prototype on a full-size field.

The energy storage selected for this experiment was an LFP battery, which is well-suited

to solar-battery systems. However, these batteries are expensive, especially compared to more common battery chemistries, like lead acid. LFP batteries are becoming more available but can be difficult to source in some countries. Furthermore, in some countries, farmers may prefer water tanks as a way to store energy. Therefore, a more detailed economic and technical analysis should be conducted on energy storage options in future iterations of the controller theory.

2.6 Conclusions

Solar-powered drip irrigation could enable sustainable agricultural intensification in low- and middle-income countries, but the investment cost and technical knowledge gaps make these systems inaccessible to small and medium-scale farmers. This study proposes a precision irrigation controller architecture for SPDI that optimizes energy and water use efficiency and could be used in a wide variety of contexts in LMICs. The controller employs a process control technique, model predictive control (MPC), which is a promising method for controlling complex agricultural systems. The economic benefits of the controller are quantified, and its performance is validated with an initial, small-scale prototype.

The three-tier controller can aid in the creation of low-cost, high-performance irrigation controllers for precision agriculture applications in resource-constrained markets. Existing precision irrigation systems are complex, expensive, and primarily designed for a market segment focused on crop quality. The POWEIr controller incorporates predictive model and process control techniques to expand some of the benefits of precision irrigation to a wider range of users at a lower cost. Integrating system design with the controller capabilities could reduce power component capacities while maintaining reliable operation and make renewable power systems with energy storage more feasible in certain markets. In particular, pairing the controller with SPDI could make SPDI more accessible to smaller-scale farmers in LMICs. This controller theory could apply to other irrigation systems with variable power inputs or

demands (e.g., wind power, cost-fluctuating grid electricity, sprinkler irrigation), especially in arid climates.

By integrating precision agriculture control with a low-cost, easy-to-use hardware platform, the POWEIr controller could make sustainable irrigation practices more accessible to farmers in LMICs, mitigating over-watering, reducing wasted agricultural inputs (e.g., fertilizer in runoff), and efficiently using power from intermittent, renewable sources. Effectively introducing precision agriculture and sustainable irrigation practices to resource-constrained markets can impact sustainable agricultural intensification globally.

Chapter 3

Sensitivity Study of the POWEIr Controller's Irrigation Schedules for SPDI Systems in Resource-constrained Contexts

The content of this chapter was derived from work with contributors besides the author of this thesis including Samuel Ingersoll, Suat Irmak, and Amos G. Winter, V. A publication of the same title of this chapter is in preparation as Sheline, Ingersoll, Irmak, *et al.* [75].

3.1 Introduction

There is a need to sustainably increase crop production to meet the growing global food and fiber demand, especially in low- and middle-income countries (LMICs) [76]. The global food demand is expected to increase by up to 62% by 2050 [77]–[79]. The growing food demand is hardest felt in LMICs with food insecurity shown to be prevalent in countries in Africa [80], [81]. Food insecurity and agricultural issues are expected to only get worse as the climate becomes more unpredictable [56], [82]. Natural resources required to grow more food, such as land and water, are now stressed to critical points [83].

In addition to implementing advanced soil and crop management practices, adopting advanced irrigation technologies can aid in enhancing the sustainability of agricultural productivity. Technologies that aim to sustainably increase crop production include photovoltaic-powered drip irrigation (SPDI) and precision agriculture [8]–[10]. SPDI has to potential to reduce emissions, reduce water use, and increase crop yield compared to traditional irrigation practices, such as surface (gravity) and sprinkler irrigation [12]. Precision agriculture involves using sensors to measure agronomic factors and respond to crop needs to improve production sustainably. SPDI and precision agriculture technologies are often not adopted in LMICs due to their high cost and complexity to operate and maintain [13]–[15]. Even when SPDI is adopted, many farmers continue to over-irrigate their crops to minimize risks, negating some of the positive effects [16]–[18]. Existing precision agriculture technologies tend to incorporate many expensive sensors and are cost-prohibitive for wide adoption in LMICs [21].

The Predictive Optimal Water and Energy Irrigation (POWEIr) controller has been proposed as one solution to increase access of SPDI and precision agriculture to low-income farmers [22], [25]. Prior work has demonstrated the potential of the POWEIr controller to reduce the cost of SPDI systems and promote sustainable, precise irrigation practices in an easy-to-use package. The POWEIr controller reduces SPDI cost by changing the order and timing of irrigation events to use available solar power more efficiently without sacrificing irrigation reliability. The controller uses machine learning to make near-term predictions of local weather, allowing for water and energy use to be predicted one day in advance. The POWEIr controller calculates daily irrigation demands to minimize risk to the crop without over-watering, thus allowing for a reduction in water use without sacrificing yield. The POWEIr controller is also designed to use minimal, local data inputs from the farmer and minimal sensors to predict tailored irrigation schedules.

The POWEIr controller leverages simple agronomy and solar power models to decrease computational and calibration complexity while still providing value to farmers. However,

the models' simplicity introduces the potential for errors if important nuances are overlooked. In the case that the errors are too large, they limit the ability of the POWEIr controller to mitigate risk to the crop, which could lead to losses in yield and limited adoption. Previous demonstrations of the POWEIr controller have not explored how changes to the inputs affect the optimal irrigation schedule and the irrigation schedule's impact on crop yield. Also, prior prototypes of the POWEIr controller have relied on highly accurate weather variables using expensive and high-resolution research-grade weather sensors. A low-cost and widespread implementation of the POWEIr controller would have to use less accurate, lower-cost sensors. The implications of moving from highly accurate weather sensors to lower accuracy sensors have not been explored.

This chapter aims to assess the POWEIr controller through a simulated sensitivity study. The objectives of this chapter are to:

1. Quantify the sensitivity of the POWEIr controller's optimal irrigation output to changes to and errors in farmer agronomy inputs related to crop types and soil textures prevalent in LMICs in Africa and similar regions.

2. Characterize the impact of the aforementioned input changes on the POWEIr controller's irrigation schedules using a simulation tool to calculate crop yield.

3. Evaluate the trade-off in cost to accuracy in generated irrigation schedules for changing weather stations from a research quality station to a lower grade station.

If these objectives are met, they will provide further assessment of the POWEIr controller's ability to provide optimal irrigation schedules that maximize yield and minimize water use with minimal sensors and hardware in the field, making it affordable. This means the POWEIr controller could provide a cost-effective solution for precision irrigation which could help to make sustainable agriculture more accessible in LMICs.

3.2 POWEIr Controller Irrigation Schedule Theory and Inputs

To understand how error can become introduced in the POWEIr controller optimization, this section summarizes the POWEIr controller theory. A full description of the theory is reported in Chapter 2. The inputs and the necessary sensors for the irrigation optimization are also summarized.

Figure 3.1 depicts the POWEIr controller architecture that generates an optimal irrigation schedule. The POWEIr controller uses historical weather in addition to a weather station to collect past weather data. The past weather data are used to calculate past solar power, grass-reference evapotranspiration (ET_0), and rain using solar and ET_0 models. Prediction models are used to forecast future solar power profiles and weather data. Past and future weather data as well as the previous day's irrigation volumes are fed into a soil moisture model to calculate crop water demand parameters. The POWEIr controller uses the predicted solar power profiles and crop water demand parameters to optimize an irrigation schedule. The predicted irrigation schedule is optimized to use energy efficiently and reduce water use without impacting crop yield. The POWEIr controller was specifically designed to use a small number of essential sensors and models that require minimal input from farmers, irrigation engineers, and practitioners. For this chapter, only the portion of the controller involved with creating optimal irrigation schedules is explored, as additional portions deal with responses to system dynamics that were not considered in the simulated study.

3.2.1 Reference Evapotranspiration (ET_0) Model

The soil moisture model and crop water demand prediction are based on an estimate of crop evapotranspiration (ET_c). ET_c is calculated as $ET_c = K_c ET_0$, where K_c is a crop coefficient and ET_0 is the reference evapotranspiration [mm]. ET_0 is calculated using the Penman-Monteith equation as described in Allen, Pereira, Raes, *et al.* [63]:

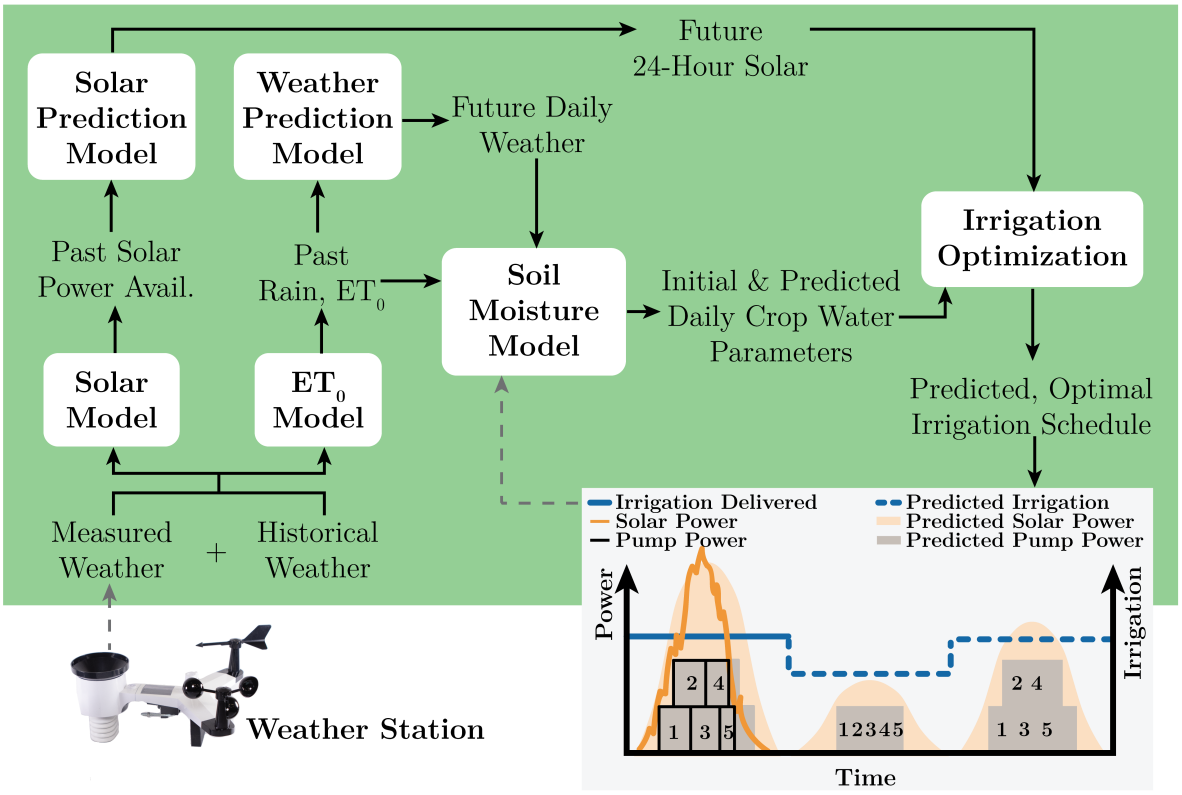

Figure 3.1: The Predictive Optimal Water and Energy Irrigation (POWEIr) controller architecture for generating an optimal irrigation schedule. Measured and historical weather data is used to calculate past solar power available, reference evapotranspiration (ET_0), and rain. This past data is used to train the solar and weather prediction models and initialize the soil moisture model. Measured delivered irrigation is also used to initialize the soil moisture model. The prediction models forecast future 24-hour solar power profiles and future daily weather parameters. The soil moisture model calculates initial and predicted daily crop water parameters. The predicted irrigation schedule is optimized based on the predicted solar power and crop water parameters.

$$ET_0 = \frac{0.408\delta(G_{net} - HF_s) + \gamma \frac{900}{T+273} u_2(e_s - e_a)}{\delta + \gamma(1 + 0.34u_2)}, \tag{3.1}$$

where G_{net} is the net irradiance at the crop surface [MJ/m^{2}day], HF_s is the soil heat flux density [MJ/m^{2}day], T is the daily or hourly average air temperature at 2 m height [°C], u_2 is the wind speed at 2 m height [m/s], e_s is the saturation vapor pressure [kPa] at air temperature T, e_a is the actual vapor pressure [kPa], δ is the slope of vapor pressure curve [kPa/°C] at air temperature T, and $\gamma = 0.665 \times 10^{-3} p_{atm}$ is the psychrometric constant [kPa/°C]. The atmospheric pressure [kPa], p_{atm}, can be determined from altitude using a simplification of the ideal gas law and assuming an atmosphere at 20 °C. ET_0 is calculated for a grass reference crop of 0.12 m height assuming complete shading of the ground and sufficient water. The weather data needed to calculate ET_0, temperature, relative humidity, solar irradiance, and wind speed, are available through weather station measurements and, in some locations, from weather databases.

3.2.2 Solar Model

The solar power model calculates the solar power available needed to optimize the irrigation schedule. Weather data averaged on an hourly basis are used to calculate the available solar power assuming a single-diode model for the solar panels. A single diode model was chosen as it has been demonstrated to simply and accurately represent maximum power output for changing weather conditions [84]–[89]. The single diode model is implemented following Bishop [90]. To calculate the maximum power output, the single-diode model requires solar panel information commonly found on the manufacturer's technical specifications in addition to solar irradiance and temperature data. Additional parameters needed for the single diode model are calculated using the method provided in De Soto, Klein, and Beckman [91].

3.2.3 Weather Prediction Model

Weather data are used to predict the daily ET_0 and rain that are inputs to the soil moisture model and used to optimize the irrigation schedule. The POWEIr controller uses historical data and weather sensors paired with machine learning to predict local weather in resource-constrained settings where reliable weather forecasts are not readily available. As described in Sheline and Grant (2023) et al., a vector autoregression algorithm (VAR) is used to predict daily weather and solar power parameters [25]. In this study, VAR is the chosen algorithm for predicting daily weather parameters.

The daily weather prediction model has requirements to be computationally inexpensive, have the ability to predict multiple variables at once that are interrelated, and not require substantial amounts of training data. VAR is well-suited for the daily weather prediction model as it predicts averages of time-series data for multiple variables that affect each other. VAR is not computationally expensive and does not require large amounts of training data [61]. The input data for the VAR model are daily average, minimum, and maximum air temperature and relative humidity, average wind speed, total solar radiation, total sun hours (calculated as the number of hours the hourly radiation was greater than 0.1 MJ/m^2), the reference evapotranspiration, ET_0 (calculated using Penman-Monteith equation), and total rain (Pr). VAR takes in a specified time period of past input data and predicts a vector of the same data over the next prediction horizon. For the POWEIr controller's daily weather predictions, a year of typical meteorological year (TMY) data from the closest weather station and measured past data from the locally connected weather station were used to train the VAR algorithm. The VAR algorithm is retrained and rebuilt with historical and incoming weather data at the start of each prediction to ensure all current trends are captured in the algorithm.

3.2.4 Solar Prediction Model

Past solar power available data are used to predict the hourly solar power available, which is used to optimize the irrigation schedule. In Sheline, Grant, Gelmini, *et al.* [25], VAR is used to predict a daily solar radiation value, then historical hourly solar power available curves are scaled based on the daily prediction [25]. However, with climate change, future weather is expected to become less similar to historical trends. Therefore weather predictions that depend on historical averages could become less accurate with time [54]–[56]. For this chapter, the POWEIr controller theory was updated to use a Long Short-Term Memory network (LSTM) for predicting the 24-hour solar power available curve. An LSTM network is a recurrent neural network that is able to store past information, noise-resistant, and designed to predict sequence data. An LSTM network was selected because it is well-suited to do single variable time series prediction for a full day's solar profile [92], [93].

The LSTM model takes in the past calculated hourly solar available data and outputs a 24-hour prediction of solar power available. The LSTM model's algorithm used the Keras deep learning package [94]. The LSTM model was comprised of a 100-cell LSTM layer with ReLU activation, a 50-cell LSTM layer with ReLU activation, and a dense layer [95]. The loss function was a mean square error and the optimizer was Adam [96]. The LSTM algorithm is typically trained on a year of TMY data from the nearest weather station and measured past data from the locally connected weather station. The LSTM is retrained and rebuilt with historical and incoming weather data at the start of each prediction to ensure all current trends are captured in the algorithm.

3.2.5 Soil Moisture Model

A soil moisture model is used to predict the daily crop water demand, which is used to determine the optimal irrigation schedule. The model employs a soil water balance that tracks the incoming, outgoing, and stored water in the soil. These calculations are done for

each day of the crop season, defined by the planting and harvest date of the crop. The soil water balance, defined in Allen, Pereira, Raes, *et al.* [63], is

$$D_{r,n} + (1 - k_{RO})Pr_n + \frac{1000 I_{del,n}}{A_s f_w} = D_{r,n-1} + K_{st} ET_{c,n}, \tag{3.2}$$

where $D_{r,n}$ and $D_{r,n-1}$ are the root zone depletion [mm] on day n and on the previous day, respectively, k_{RO} is the runoff coefficient estimated based on the soil texture, I_{del} is the delivered irrigation [m^3], A_s is the field's area [m^2], f_w is the soil wetted fraction, K_{st} is the water stress coefficient, and ET_c is the crop evapotranspiration [mm]. K_{st} is calculated as $K_{st} = \frac{TAW - D_r}{TAW(1-f_d)}$ where f_d is depletion fraction calculated as $f_{d,n} = f_{d,const} + 0.04\,(5 - ET_{c,n})$. $f_{d,const}$ is a crop-dependent constant defined in [63] and TAW is the total available water that the crop can extract from the soil [mm] which depends on the depth of the crop roots (Z_r) and soil texture.

D_r is constrained such that $0 \leq D_{r,n} \leq TAW$. If D_r is less than or equal to the readily available water ($RAW_n = f_{d,n} TAW$), then there is no water stress on the crop, $K_{st} = 1$. If the D_r is greater than RAW, then there is water stress and $0 < K_{st} < 1$. The water stress affects the amount of crop evapotranspiration as $ET_{adj} = K_{st} ET_c$. If there is water stress on the crop, then the reduction in evapotranspiration relates to a reduction in yield,

$$1 - \frac{Y_a}{Y_{max}} = K_y \left(1 - \frac{ET_{c,adj}}{ET_c}\right), \tag{3.3}$$

where Y_{max} is the maximum yield [kg/m^2] calculated using the agro-ecological zone method defined in Doorenbos and Kassam [66] and K_y is the crop yield response factor [67].

3.2.6 Irrigation Optimization

The irrigation schedule is optimized with the aim of using energy and water resources efficiently without negatively impacting the crop yield. The irrigation schedule is optimized using the predicted solar power available and crop water demand parameters. The objective

of the optimization is to maximize revenue through crop yield, minimize the operational cost from energy use and water consumption, and maximize irrigation reliability by fully charging any energy storage by the end of the prediction. The objective function is calculated in terms of cost determined by the unit capital costs of the system components. The objective function is defined over a single prediction horizon as

$$\begin{aligned} min \Bigg[& \sum_{i=\delta t}^{N_{hor}} \frac{1}{N_{hor}} \Bigg(k_b u_{max}(u_{1,i} - u_{2,i}) + \sum_{s=1}^{N_{s,tot}} k_w q_s d_{s,i} \Bigg) \\ & - \sum_{n=1}^{N_{day}} \sum_{s=1}^{N_{s,tot}} \frac{1}{N_{day}} \big(k_c A_s \frac{dY_{a,s,n}}{dt} \big) \\ & + k_d (1 - SOC_{N_{hor}}) \Bigg], \end{aligned} \tag{3.4}$$

where N_{hor} and N_{day} are the prediction horizon in hours and days; i is the time step count; δt is the hourly time step; $N_{s,tot}$ is the total number of sections s the field is split into; k_b [\$/kWh] is the unit cost of the battery defined by the unit battery cost and its lifetime storage; u_1 and u_2 are the charging and discharging rate of the energy storage, normalized by u_{max} [kW], the maximum charging or discharging rate; k_w [\$/m^3] is the unit cost for water; q_s is the flow rate for section s [m^3/hr]; d_s is the binary variable for irrigating section s of the field; k_c [\$/kg] is the price weight on the crop; $\frac{dY_{a,s,n}}{dt}$ is the daily yield [kg/m^2/day], which is estimated by dividing Y_a in Equation 3.3 by the number of days in the crop growing season; k_d is the unit cost on the energy storage [\$/day] based on the cost of the system over its lifetime; and SOC is the state of charge of the energy storage.

The optimization's control variables are d_s, u_1, and u_2. These variables determine the daily irrigation volume as well as how much the battery is charged and discharged at any moment. The control variables affect the system components' state variables, including D_r and SOC. The state variables are subject to constraints on the system dynamics, including the system energy and water flow dynamics. The state of the soil moisture is constrained

Table 3.1: POWEIr controller inputs.

Input Group	Input Variables
Field	Pump power, flow rate, field area
Agronomy	Initial root zone depletion condition, crop with specific crop parameters ($f_{d,const}$, K_c, K_y, Z_r), planting and harvest dates, soil texture, soil wetted fraction
Weather	Local historical and current hourly data for temperature, relative humidity, wind speed, solar radiation, and rain

by Equation 3.2. The state of the energy storage is constrained such that it is charged only if there is unused solar power and drained if the pump power is more than the solar power available. The pump power is a function of the flow rate of the system and is calibrated when a system is installed. The optimization is also subject to boundary constraints on its control and state variables, as described fully in [25].

3.2.7 Required Inputs

Table 3.1 enumerates the complete set of inputs required by the optimization. The inputs are categorized into groups. All of the field inputs can be measured or specified when the system is installed. The agronomy inputs are specified by the farmer. The initial root zone depletion condition can normally be assumed to be zero as it is typical practice to bring the soil moisture to field capacity for seed planting and germination. The crop is specified by the farmer and the crop parameters ($f_{d,const}$, K_c, K_y, Z_r) can either be specified by the farmer or set to default values for the crop. The default crop parameters are based on

FAO values that were calibrated for crops in specific climates and locations. Therefore, the default crop parameters may have errors associated with them when used on different crop cultivars or locations. The planting and harvest dates are specified by the farmer. The soil texture is input by the farmer and a one-time measurement of the soil texture can be taken if needed. The soil texture lab analysis typically costs on the order of $20. Large farms with varying soil conditions may need multiple soil texture measurements. The soil wetted fraction is the portion of the field area that is covered by irrigation, which can be measured when the system is set up. The weather inputs can be obtained from weather data infrastructure. Often, weather stations are sparse in LMICs, and therefore accurate estimates of local weather may not be readily accessible. The POWEIr controller allows for the use of a locally installed weather station, which is a collection of weather sensors, that collects the needed weather data in locations where weather data are not readily available.

The local weather stations have a combination of weather sensors that allow for all the measurements needed by the POWEIr controller. The required weather sensors for the POWEIr controller are rain gauges (most commonly tipping bucket), radiation sensors such as pyranometers, light sensors, or UV sensors, anemometers for measuring wind speed, and hygrometers and temperature sensors for measuring relative humidity and temperature. Many classes of weather stations exist with varying cost and sensor accuracy. This study focuses on two types of weather stations, ones that are higher cost, use more accurate sensors, and are typically used in research, and lower cost weather stations that use less accurate sensors and are typically for home use.

3.3 POWEIr Controller Irrigation Schedule Sensitivity Analysis

A simulation-based study of the POWEIr controller was conducted to understand the sensitivity of the optimal irrigation schedules to discrepancies in the inputs and the impact on crop

yield. One objective of the sensitivity study was to analyze how changes or errors in users' agronomy inputs affect the POWEIr controller's optimal irrigation amounts and the simulated crop yield. The inputs chosen for the sensitivity study focused on those that are either less easily measured or based on uncalibrated default values; these inputs are most likely to be subject to miscalibration and error in practice. The other objective was to see the effects of weather measurement error and weather prediction error on the POWEIr controller's cumulative irrigation amount. This information was used to evaluate whether low-cost sensors have sufficient performance to be recommended to resource-constrained farmers with minimal risk of crop loss. Two weather stations were examined in this study, a research-quality, higher-cost weather station (HCWS) and a home-use, lower-cost weather station (LCWS). This thesis focused on LMICs in Africa, as countries in Africa have some of the largest food insecurity issues.

3.3.1 Weather and Agronomy Context

To achieve the objectives of this chapter data were collected from a HCWS and LCWS at a farm in Concord, Massachusetts, USA. The HCWS used for this study was the Davis Vantage Pro2 weather station (Davis Instruments 6152C) with the solar radiation sensor (Davis Instruments 6450) and the LCWS was the Ambient weather station (Ambient Weather WS-2902C). The Davis Vantage Pro2 was chosen as the HCWS as it is a well-proven weather station in irrigation and agricultural studies [97]–[100]. For the HCWS, the reported sensor accuracy and resolution are 2-5% and 2.5-60 seconds. For the LCWS, the reported sensor accuracy and resolution are 10% and 12-24 seconds. The cost of the HCWS and LCWS were $1,125 and $190, respectively, at the time this thesis was written.

The farm where the data were collected was chosen as its location is close to the university where the researchers who conducted the experiment worked. Additionally, this location was found to have similar weather to agricultural areas in two LMICs in Africa with different climates, Kenya and Morocco. The data collected are shown to be similar to TMY data in the

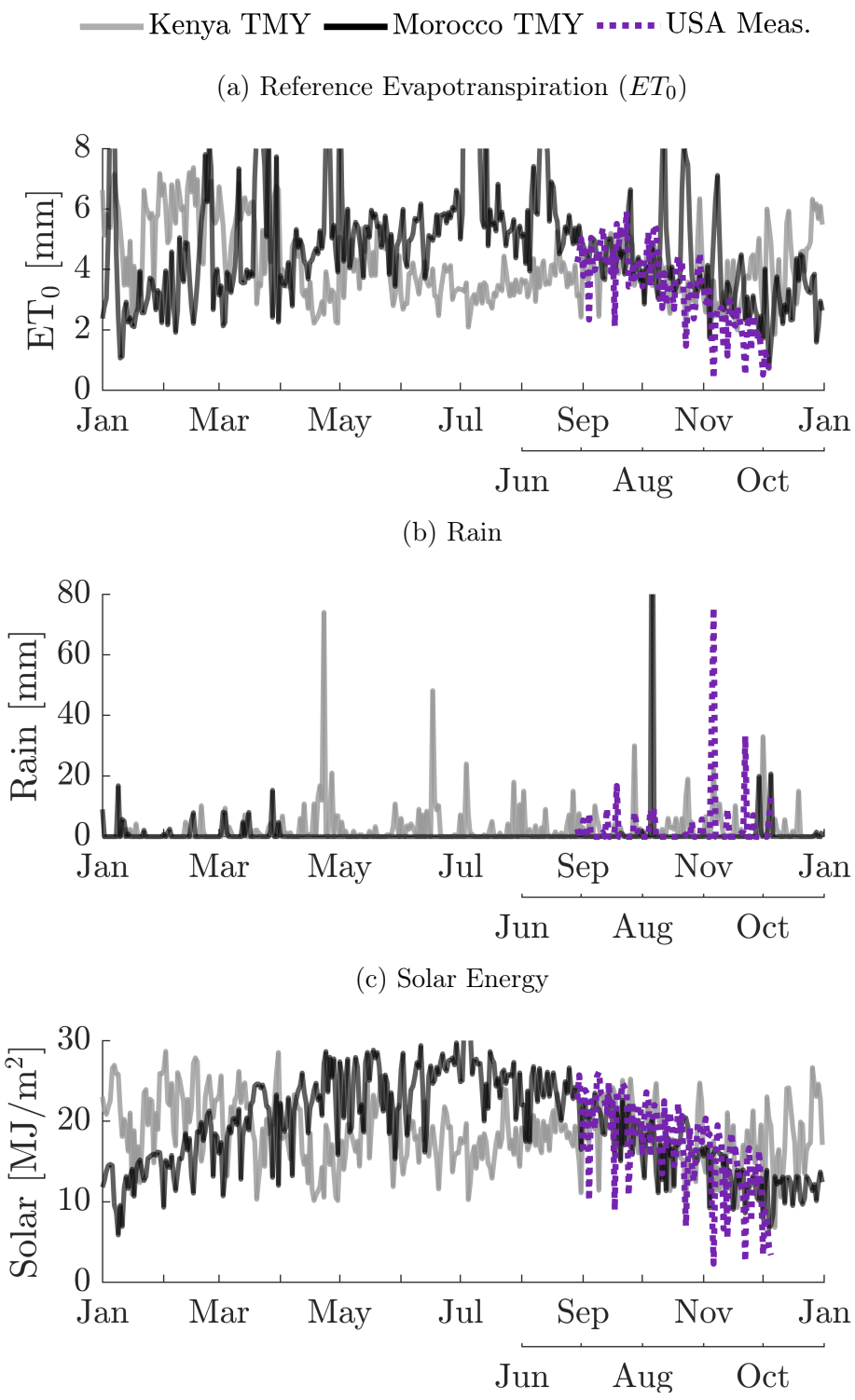

Figure 3.2: Daily weather parameters measured in Concord, MA, USA (USA Meas.) compared to typical meteorological year (TMY) data in Kenya and Morocco. The weather parameters totaled over each day are **a**, the reference evapotranspiration (ET_0), **b**, the rain, and **c**, the solar energy. The USA measured data taken from July to October 2022 aligns well with the Kenya and Morocco TMY data from September to December.

Table 3.2: Typical low-and-middle-income country (LMIC) farm case and baseline case for sensitivity study.

	LMIC Case: Medium-scale Kenya, Jordan, Morocco	**Baseline Case:** Medium-scale Massachusetts
Months	Sept-Dec	July-Oct
Crop	Maize, Potato, Tomato	Tomato
Soil	Clay Loam, Sandy Loam, Sandy Clay	Sandy Loam

dry season for Nakuru, Kenya and in the fall for Agadir, Morocco [74]. Figure 3.2 compares the Kenya and Morocco TMY data for daily rain, ET_0, and total radiation to the same values measured on the USA farm. The USA farm data measured from July to October, 2022 is comparable to the Kenya and Morocco TMY data from September to December. Comparing the USA measured data to the Kenya and Morocco TMY data, respectively, the total ET_0 during this period is 11% and 22% lower; the total rain is 0% and 37% higher; and the total radiation is 3% lower and 2% higher. Given the similarity in key weather outcomes, the results of this sensitivity study are expected to be comparable to results that would be obtained using weather data collected in Morocco or Kenya.

Soil textures and crops used in the simulation study were selected to represent conditions on typical farms in Morocco and Kenya. The most typical soil textures in the agricultural areas of Kenya and Morocco are shown in Appendix B.1. Three soil textures were chosen that are common in Kenya and Morocco and also have significantly different TAW coefficients. Three crops were chosen that have growth periods close to the length of collected weather data, are water-stress intolerant, are commonly grown in Kenya and Morocco from September to December, and have different crop parameters of interest ($f_{d,const}$, K_c, K_y, Z_r) [63]. A summary of these cases is shown in Table 3.2, along with the baseline case for the sensitivity analysis. The baseline case was chosen to have the measured weather data from the HCWS and LCWS, a crop with parameters in the middle of the other crops, and a soil texture with high sand content as a worst case.

3.3.2 Measured and Predicted Weather Data and Error in ET_0, Rain, and Solar Power

The data collected from the HCWS and the LCWS were used to calculate and predict the solar power available and crop water demand parameters needed to optimize the POWEIr controller's irrigation schedule. From these data the measurement and prediction error in the ET_0, rain, and solar power used in the POWEIr controller's irrigation schedule optimization was quantified. The weather data from the HCWS and the LCWS were used to calculate the reference evapotranspiration, following Section 3.2.1, as well as the hourly solar power available, following Section 3.2.2. Philadelphia Solar PS-M144(HC)-550W panels were assumed to predict the solar power available each day. The machine learning algorithms were trained on TMY weather data close to where the weather data was collected [74]. The machine learning models were updated with the past measured weather data from the weather station every day of the simulation, meaning they were re-trained and rebuilt with the new data each day. Once the daily rain, evapotranspiration, and solar power available were predicted, the POWEIr controller optimized an irrigation schedule for the predicted day. Default FAO 56 crop parameters were used by the POWEIr controller for all the agronomy input variables [63]. The default growth stages were all proportionally scaled from their default values to values that would make the total crop season length 92 days. It was assumed that all of the predicted irrigation demand was delivered each day. The daily ET_0 and rain calculated from the previous day's weather station data were used to calculate the $D_{r,n-1}$ in the soil water balance; this was hypothesized to stop the aggregation of prediction error in the cumulative soil water balance calculation and is referred to as re-initializing the soil water balance. The daily prediction and irrigation optimization process was repeated for the 92 days of measured weather data for both the HCWS and LCWS. The difference in the ET_0, rain, and solar power calculated from the measured weather data from the LCWS and the HCWS, as well as the difference from the predicted and measured parameters for both the LCWS and the HCWS, were characterized as a root mean square error normalized by the mean over the

simulation period (NRMSE).

3.3.3 Simulation of Cumulative Irrigation Volume

The theory of Section 3.2 was applied to optimize the irrigation schedule over the 92-day simulation using the HCWS and LCWS data with two configurations – with predicted data and with measured data – and the respective cumulative irrigation volumes were calculated. First, the baseline case (Table 3.2) was simulated using both weather stations to predict the weather and optimize the irrigation schedule, as would normally happen in the POWEIr controller. These cases are referred to as the 'HCWS with prediction error' case and the 'LCWS with prediction error' case. Then, to understand how much prediction and measurement error individually contributed to the accumulation of errors in the total irrigation over time, cases were run that removed the weather prediction component. To simulate outcomes without any prediction error, the measured weather data was used in the controller optimization instead of the predicted weather. These cases are referred to as the 'HCWS without prediction error' case and the 'LCWS without prediction error' case, and they represent the best case of perfect prediction.

3.3.4 Simulation of Crop Yield

AquaCrop 7.1 was used to calculate the crop yield from the POWEIr controller's optimal irrigation schedule [67]. AquaCrop was developed by FAO and is an open-source crop growth model that allows for assessments of the effect of weather, environment, and irrigation management on crop production. AquaCrop simulates crop yield response to water stress and is equipped to address conditions where water is the limiting factor in crop production. For the sensitivity study, the default inputs provided in the AquaCrop database were used for the tomato, potato, and maize crop files and for the sandy loam, clay loam, and sandy clay soil files. The growth stages in the default crop files were all proportionally scaled from their

default values to values that would make the total crop season length 92 days, otherwise, the simulation would stop short of capturing the total crop growth and yield. AquaCrop used the HCWS data without prediction error to do the simulated yield calculations. The HCWS measured data was chosen as the "true weather" to calculate yield as the HCWS is reported to have the higher accuracy out of the two weather stations. The daily total irrigation per hectare generated by the POWEIr controller was used in AquaCrop to estimate the yield. AcraCrop calculates the actual crop yield based on the input irrigation schedule and also calculates a maximum theoretical yield that assumes an irrigation schedule that causes no crop water stress. A comparison between the maximum theoretical yield and actual crop yield can be used to assess how much water stress an input irrigation schedule causes. Where relevant, the revenue from the crop yield was calculated by multiplying the yield by the local producer prices [$\$/10^3$ kg] from FAOSTAT [101].

3.3.5 Sensitivity Study

The total irrigation generated by the POWEIr controller and the simulated AquaCrop yield were evaluated for the HCWS and LCWS and each crop and soil texture in Table 3.2 to understand if the POWEIr controller's irrigation schedules were robust to varying the weather, crop, and soil inputs. The process outlined in Sections 3.3.2 and 3.3.3 were used to get the POWERIr controller's irrigation schedule, but only cases with prediction errors were run. The process outlined in Section 3.3.4 was used to get the simulated yield.

The effect of errors in the agronomy variables that are inputs for the POWEIr controller's irrigation optimization on total irrigation volume and simulated yield was explored. A sensitivity study was conducted to understand the sensitivity of the controller's optimal irrigation schedule to the agronomy parameters most susceptible to error. The crop parameters that are hard to measure and are most likely to have errors if default values are used are f_d, K_c, K_y, and Z_r. f_d is a scalar while K_c, K_y, and Z_r are curves described by multiple linear or constant segments. These curves represent the variation of a single number over the growing

season. Figure B.10 illustrates the different crop coefficient curves. In each of these three cases, the parameter varied is a curve with a standard characteristic shape found in [63], [66], [67]. Forty variations of each parameter were created with the characteristic curve shape uniformly scaled using a scale factor from the maximum value found in FAO 56 for common vegetable crops down to nearly zero [63]. f_d is a single number instead of a curve and was varied linearly from the maximum value for common vegetables reported in FAO 56 down to zero [63]. The scale factor for K_c was varied between 0 and 1.75, the scale factor of K_y was varied between 0 and 1.2, and the scale factor of Z_r was varied between 0 and 1.5. For these three values, the default value is one. Finally, f_d was varied from 0 to 0.73. A total of 160 cases were run. For each case, the processes outlined in Sections 3.3.2 and 3.3.3 were used to get the POWERIr controller's optimal irrigation schedule using the LCWS data. The FAO 56 default crop parameters for the baseline case, defined in Table 3.2, were used and each of the crop parameters was changed one at a time to generate an irrigation schedule for each case. The process outlined in Section 3.3.4 was used to get the simulated yield for each case.

3.4 Results

Figures 3.3a–3.3c compare the measured and predicted ET_0, rain, and solar power available calculated using the HCWS and LCWS. The LCWS has consistently lower values for evapotranspiration, rain, and solar power available calculated using measured data, 'LCWS Measured', compared to 'HCWS Measured'. This suggests that the LCWS has bias error compared to the HCWS. The ET_0 and rain data generated using the machine learning model, 'LCWS Predicted' and 'HCWS Predicted', lags behind the corresponding data calculated directly from the weather station data, 'LCWS Measured' and 'HCWS Measured'. This indicates that the ET_0 and rain predictions are highly influenced by the previous day's measured value. The solar power available predictions have some days with predicted values that track the measured values more closely than others. The predicted values for ET_0, rain, and

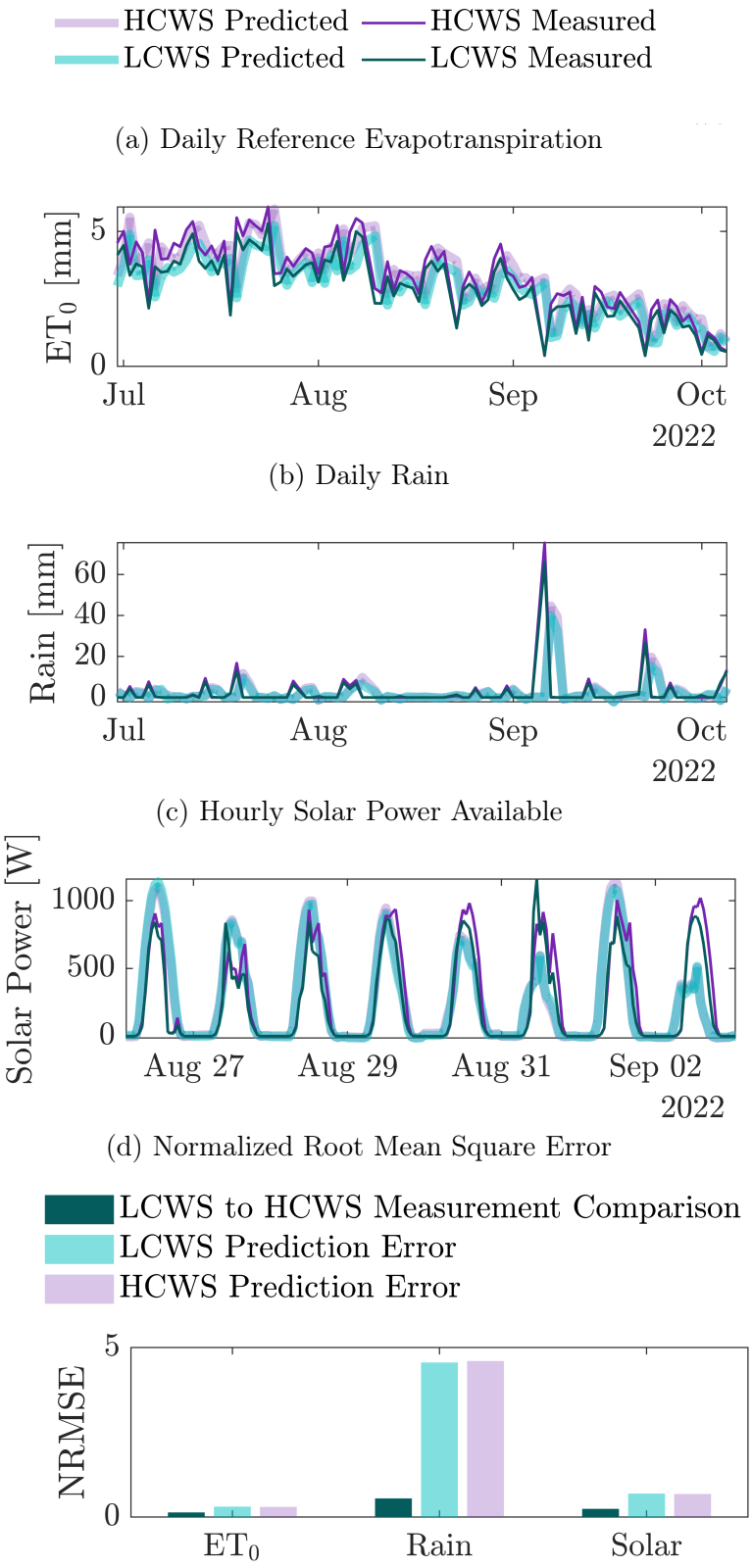

Figure 3.3: Measured and predicted weather-based parameters used in the soil moisture and solar models. The parameters are **a**, the total daily reference evapotranspiration (ET_0), **b**, the total daily rain, and **c**, the hourly solar power available. **c** is shown for a few days but it was calculated for the entire 92 days. The 'Measured' parameters were calculated using weather data from the high-cost weather station (HCWS) and low-cost weather station (LCWS). The 'Predicted' parameters came from the machine learning models trained using the HCWS or LCWS data. The normalized root mean square error (NRMSE) for the full simulation for **a**, **b**, and **c** are shown in **d**.

solar power available are similar between the LCWS and HCWS. Figure 3.3d summarizes the differences between the curves in Figures 3.3a–3.3c as NRMSE. The LCWS and HCWS prediction error is the difference between the HWS or RWS predicted case and HWS or RWS measured case, respectively. The NRMSE of the LCWS measured data to the HCWS measured data is lower than the prediction errors for both weather stations. Rain has the largest measurement error and prediction error for each weather station. ET_0 and solar power are calculated from weather parameters measured by the weather station besides rain. Rain has been shown to be hard to predict due to its highly nonlinear fluctuations [102]. The VAR algorithm used is good at predicting averages of the weather data vector over a multiple-day prediction window and is highly influenced by previous days' weather data. The VAR method works well for most weather parameters but can result in large prediction errors for rain, which tends to vary significantly between days.

Data for all of the measured and predicted weather parameters used in the weather prediction model, similar to the data shown in Figures 3.3a–3.3c, are shown in the Appendix in Figures B.3–B.5. These data include the average, minimum, and maximum air temperatures, average wind speed, average, minimum, and maximum relative humidity, total rain, total solar radiation, number of sunlight hours, and total reference evapotranspiration. Additionally, the NRMSEs for all of the weather parameters are shown in the Appendix in Figure B.6.

Figure 3.4 shows the cumulative irrigation volume based on the simulated POWEIr controller irrigation schedule for the HCWS and LCWS, each with and without prediction error cases. The total irrigation volume is the amount delivered at the end of the season. For each weather station, the case with prediction error and without prediction error differ only slightly in the total irrigation volume; the prediction error case has 1% and 0% higher total irrigation volume for the LCWS and HCWS, respectively. This suggests that the prediction error has minimal impact on the total irrigation volume. In contrast, there is a more significant difference between the HCWS and LCWS cases without prediction error; the total

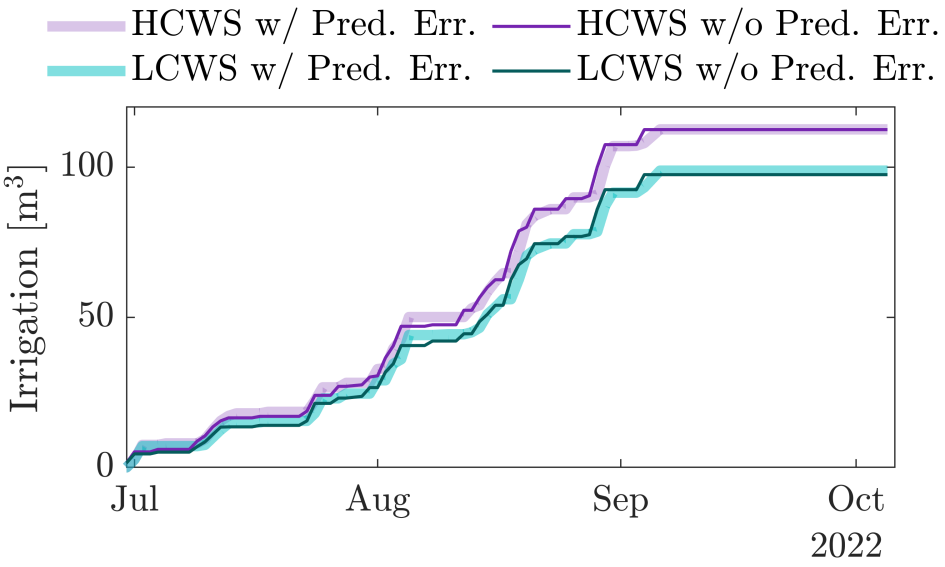

Figure 3.4: Cumulative irrigation volume for a system following the schedule recommended by the POWEIr controller fed with data from two distinct weather stations. The high-cost weather station (HCWS) and the low-cost weather station (LCWS) were used to compute optimal irrigation schedules with (w/) and without (w/o) weather prediction error (Pred. Err.). The w/o weather prediction error cases use measured weather data.

irrigation volume without prediction error is 13% lower for the LCWS case compared to the HCWS case. This suggests that the measurement error between weather stations has a greater cumulative effect on the total irrigation than the prediction error. Yet, the prediction error of each weather station is shown to have higher prediction NRMSE compared to the weather station measurement comparison NRMSE seen in Figure 3.3d. The prediction error is diminished by re-initializing the soil water balance with the previous day's measured weather at the start of each day (Figure 3.1). There is no adjustment for the weather measurement error, which is due to the inherent sensor accuracy. The increasing divergence in irrigation volume over time is likely due to the accumulation of the LCWS's bias errors demonstrated in Figure 3.4.

Figure 3.5 demonstrates the variation of the POWEIr controller's optimized total irrigation volume and simulated crop yield to changes in farm conditions, namely the crop and soil texture, for the two weather stations. Across all cases, the total irrigation volume is 10-15% lower with the LCWS data used compared to the HCWS data. The LCWS yield

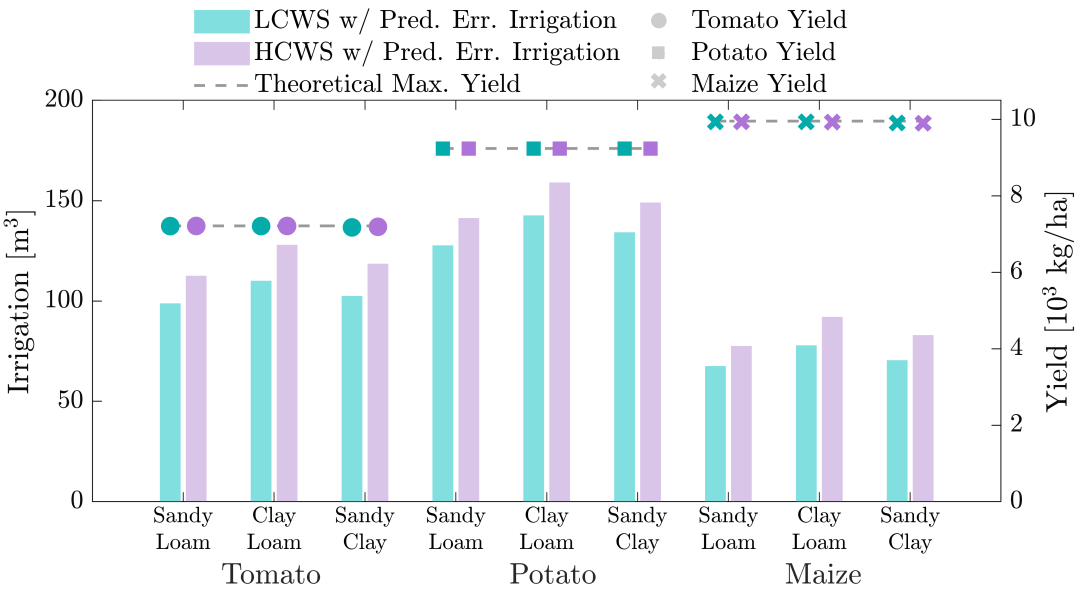

Figure 3.5: Sensitivity of total irrigation and yield to crop, soil texture, and weather stations. Data from the low-cost weather station (LCWS) and high-cost weather station (HCWS), both with prediction error (w/ Pred. Err.), were fed into the POWEIr controller to create the optimal irrigation schedules for tomato, potato, and maize crops in sandy loam, clay loam, and sandy clay soil textures.

is -0.05–0.06% (-5–15 $/ha) compared to the HCWS across all crop and soil texture cases. This suggests that even though the accuracy of the LCWS leads to lower total irrigation volume, there is minimal impact on crop yields. The difference in the tomato, potato, and maize yields calculated from the irrigation schedules generated across all soil textures and both weather stations' data compared to the theoretical maximum yield (assuming no water stress) is up to 0.5, 0.03, and 0.5% less for each crop, respectively; corresponding to a 39, 0.6, and 10.8 $/ha loss in revenue. This implies that the irrigation schedules generated by the POWEIr controller will not negatively impact yield across the tested crops, soil textures, and weather stations. The relatively low loss in revenue associated with the different total irrigation volumes suggests that the additional errors introduced by the LCWS will have minimal impact on key outcomes in spite of significant savings in cost. The weather station cost savings can thus be directly applied to increase the farmer's profit.

Figure 3.6 shows the sensitivity of the POWEIr controller irrigation amount and AquaCrop

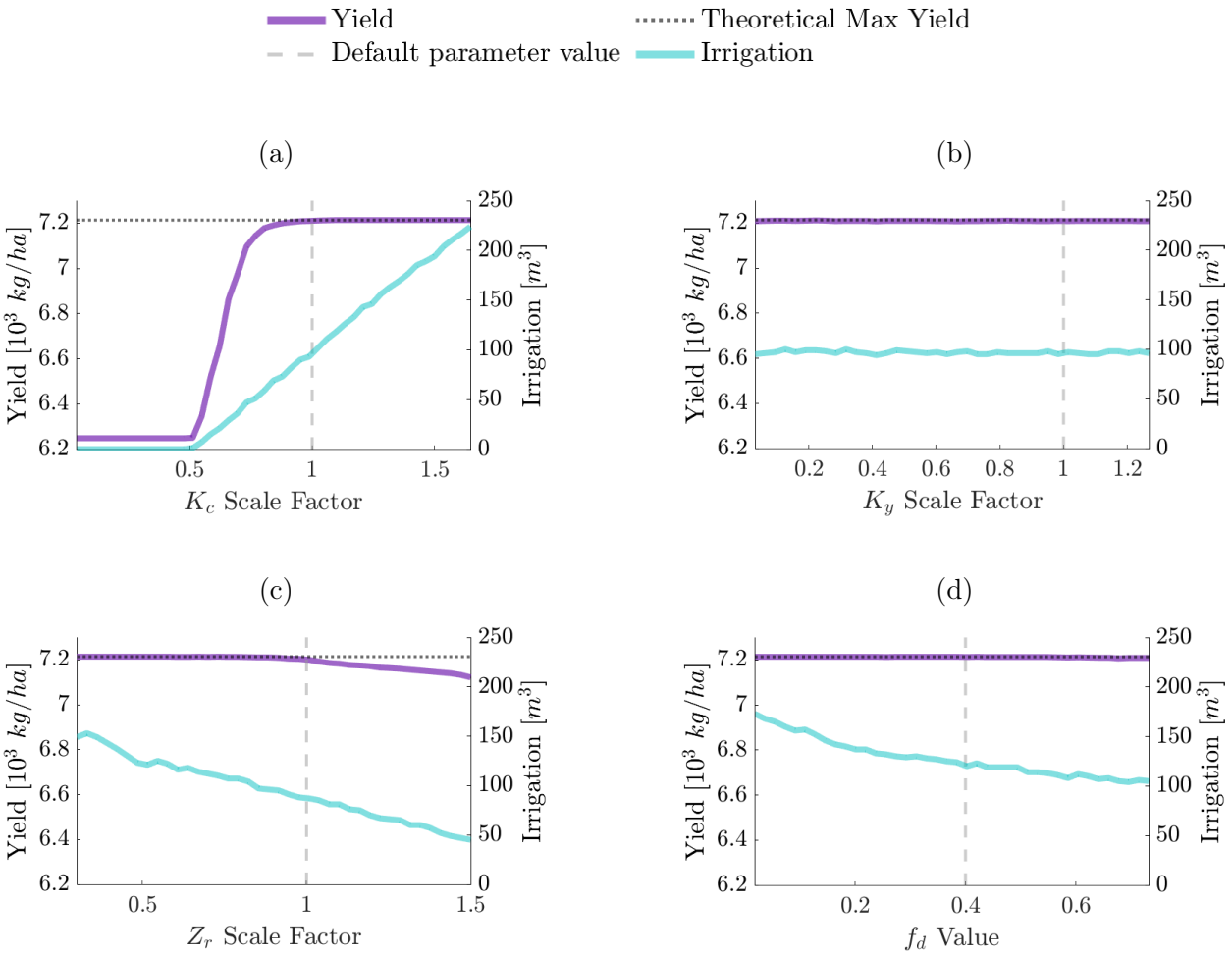

Figure 3.6: Change in yield and irrigation associated with miscalibration or error in each crop parameter in the POWEIr controller's internal model. The yield numbers were generated from an AquaCrop simulation using ground truth weather data and system parameters. The gray dashed vertical lines show the default values of each parameter according to the literature [63], [66], [67]. The horizontal lines show the theoretical maximum yield from AquaCrop.

simulated yield to changes in the default crop parameters (f_d, K_c, K_y, Z_r). Across the range tested, the K_c parameter produced the most variation in yield and irrigation with yield increasing by 15% tons/ha and irrigation increasing from 0 to 224 m^3. Varying Z_r resulted in the second largest change in yield and irrigation with yield decreasing by 1.3% and irrigation decreasing by 70% over the range tested. Over the range of parameters tested, f_d produced very little change in yield (only 0.07%) but an appreciable change in irrigation which decreased by 39%. Varying K_y produced 0.06% change in yield from the maximum to minimum values achieved and no change at all between the maximum and minimum K_y values tested (farthest left and farthest right data points). Varying K_y also resulted in very little change in irrigation with a change of 6% between the maximum and minimum irrigation values achieved and only 0.01 between the maximum and minimum K_y values tested (farthest left and farthest right data points).

If K_c is calibrated too low compared to the "true value" for the crop, the yield is reduced due to under-irrigation. If K_c is calibrated too high compared to the "true value" for the crop, irrigation increases approximately linearly, but yield does not increase because the crop cannot use the extra water. In the over-irrigation regime, irrigation scales linearly with K_c, so there is potential for significant wasted water following from an over-estimated K_c value. This result indicates that of the four parameters, the calibration of K_c is most important for preventing wasted water and lost yield in this controller. However, it also indicates that water can effectively be "traded" to minimize the risk of yield loss if parameter error is expected by purposefully increasing K_c. This may be a useful strategy if water is cheap. In many cases, water is a resource that must be used sparingly and in these cases, agricultural parameters must be calibrated to maximize yield while preventing waste.

3.5 Discussion

This chapter aimed to assess the POWEIr controller's irrigation outputs' sensitivity to agronomy inputs, the impact on crop yield, and the cost-benefit of using different weather stations. There were some limitations to the study that should be addressed in future work, yet the findings should provide value to practitioners and the academic community.

3.5.1 Sensitivity of POWEIr Controller's Irrigation Output to Changes in Agronomy Inputs

Figures 3.5 and 3.6 quantify the net impact of different uncertainties in farmer agronomy inputs on key performance outcomes of the POWEIr controller. Although the weather data used for this study were collected in Massachusetts, USA, the data were shown to be similar to typical conditions in Kenya and Morocco. Figure 3.4 confirms that the weather prediction errors could be corrected over time by the controller's method of re-initializing the soil water balance using the previous day's measured weather data. The design of the controller to continually re-initialize the soil water balance with measured data could mitigate the risk of high prediction errors. Of the four crop parameters, varying the crop coefficient was shown to have the greatest effect on the total irrigation in the case of a tomato crop in sandy loam soil. This means that when using the POWEIr controller to optimize irrigation schedules, calibrating the crop coefficient, depletion fraction, and rooting depth is important to avoid over- or under-irrigation. However, it is also potentially useful that K_y had almost no effect on irrigation, meaning that time and money need not be spent calibrating this parameter if the controller is to be used under the simulated conditions. The controller displayed an approximately linear sensitivity to its parameters with respect to irrigation in the region around the default values. This approximate linearity means that miscalibration of a given percent can be mapped reliably to corresponding changes in irrigation, allowing for a relatively objective comparison between the cost of calibrating crop parameters and

the cost of the potential extra irrigation used. This comparison between water wasted and calibration cost could be useful for making systematic recommendations about the types of calibration methods that should be used when setting up the controller.

3.5.2 Yield Impact due to Changes in POWEIr Controller's Irrigation Output

This chapter validated the accuracy of optimal POWEIr controller's irrigation schedules using a detailed agronomy model, AquaCrop, to calculate yield. Figure 3.5 depicts that for the nine different crop and soil texture cases, the POWEIr controller's irrigation schedules were shown to have minimal adverse effects on yield, with a maximum yield reduction of 2% compared to the theoretical maximum yield. The yield is expected to be minimally impacted by changes to the agronomy inputs within the tested range of crops and soil textures, as long as there are not errors in the input crop parameters. Varying the crop parameters of the POWEIr controller led to significant changes in the simulated yield and irrigation amount for K_c, as depicted in Figure 3.6. This result indicates that calibration of K_c is important for preventing over-irrigation or yield loss while error in Z_r and f_d is relevant for irrigation but they have little effect on yield for the tested case in this controller. Varying K_y did not produce significant variation in the yield or irrigation. Calibrated crop coefficients for crops grown in different locations exist in the literature [103]–[107]. Having a centralized database of crop coefficients, especially K_c values beyond the FAO defaults, would be worthwhile for the POWEIr controller. If no prior study for the calibration of K_c values exists for a particular crop in a particular location, default K_c values can be used. Unless the K_c value is significantly different from the true value, yield loss should be minimal as seen from the yield curve flattening out in the region surrounding the default K_c value in Figure 3.6a. By artificially increasing K_c and moving further into the region where yield asymptotically approaches the theoretical maximum yield, the yield will not be increased, but the risk of yield loss will be reduced. If desired, K_c values can be increased in this way -– effectively

overestimating the parameter — to reduce the risk of yield loss at the cost of additional water use. The amount of water used for any given increase in K_c can be easily understood from 3.6a which shows an approximately linear relationship between water used and K_c in the region of the true value. Therefore, a farmer could have a good idea of how much a given increase in the K_c parameter will cost. The sensitivity results show that yield under the POWEIr controller is robust to error in three out of the four crop parameters and yield is only lost when K_c is underestimated. Therefore, calibrating the controller should be relatively cheap, requiring only an estimate of the K_c value and default values for the other parameters.

3.5.3 Cost-benefit of LCWS and HCWS

Results from Figure 3.5 found that using the LCWS weather station data over the HCWS weather station data as inputs for the POWEIr controller had a negligible effect on projected revenue. The measurement errors between the home-use, low-cost weather station (LCWS) and research-quality, high-cost weather station (HCWS) had a cumulative effect on the soil moisture calculation and led to 10–15% less total irrigation over the range of simulated crops and soil textures. The minimal 0.5 $/ha reduction in yield for using the LCWS compared to the HCWS demonstrated that there was a minimal loss in revenue risk for using a lower accuracy weather station. Switching from the HCWS to the LCWS would save farmers approximately $935 per weather station at the time the thesis was written. Quantifying this change in irrigation and yield for the low-cost weather station allows farmers to make educated decisions on whether they want to use the lower-cost and more accessible home-use weather stations over research-quality ones. Currently, many farmers rely on experience and observations to irrigate which can lead to over irrigation. Having an easy-to-use, low-cost, custom option for calculating a farm's exact water needs could facilitate sustainable irrigation practices for resource-constrained farmers. The methodology used to analyze the weather stations can be used to assess the performance of other low-cost weather stations

for use in agriculture.

3.5.4 Limitations

The sensitivity study conducted was based on simulation and 92 days of data, limiting the data to a specific season. To understand how the POWEIr controller's irrigation schedules perform over a range of farm and seasonal weather conditions, it should be tested in settings with real soil and crops over different seasons. All of the irrigation schedules in this chapter were calculated under the assumption that the optimal schedule would be able to be fully carried out each day, and there would be no operational or user error that caused a change in the irrigation delivered. Future work should quantify the operational and user error of the POWEIr controller to verify its usability in terms of how much of the predicted irrigation schedule is able to be delivered and how this affects the crops.

3.5.5 Value to Practitioners and Academic Community

This chapter shows that the POWEIr controller's use of agronomy models that are not complex and rely on few inputs as well as a small amount of sensors for predicting irrigation needs can calculate the minimal crop water needs without negatively impacting yields for farmers. The POWEIr controller's design does not rely on soil moisture sensors and instead uses soil moisture calculations based on farm details and weather data. This could be a viable option for resource-constrained farmers who tend to over-irrigate as a means to reduce risk to their crops and do not have the disposable income to invest in existing high-cost precision agriculture technologies that rely on many sensors to inform on crop water needs. The POWEIr controller's optimized predictive irrigation schedules combined with a low-cost weather station is an economical, sustainable, precise irrigation solution with minimal user inputs required. Applying these findings to future work can allow sustainable, precise irrigation to be more affordable and easy to use, increasing its accessibility to cost-

constrained farmers.

3.6 Conclusions

To meet the world's growing food demand there is a need to sustainably increase crop production, especially in LMICs. The findings presented herein suggest that the POWEIr controller could help reduce the barriers to the adoption of SPDI and precision agriculture technologies in LMICs. The POWEIr controller provides a solution to reduce the cost and complexity of SPDI and water- and energy-optimized irrigation scheduling.

This chapter conducted a sensitivity study of the POWEIr controller's irrigation schedules and simulated analysis of the schedules' and LCWS' effect on yield to understand the viability of low-cost hardware and how errors in agronomy inputs affect farmers' bottom line. The matching of the cumulative change in irrigation with and without prediction error suggested that although the ET_0, rain, and solar prediction errors were large, these errors were mitigated by incorporating measured data into the POWEIr controller to re-calibrate the models with real data. Measurement error between the LCWS and the HCWS led to a 10–15% reduction in total irrigation, but only up to 0.008% change in yield, or up to 0.5 \$/ha loss in revenue. This low loss in revenue indicates that the LCWS is accurate enough to produce optimal schedules in combination with the POWEIr controller. It was found that the yield was significantly affected when there were errors in crop parameters, especially the crop coefficients used to calculate crop evapotranspiration. Calibrated crop coefficients for crops grown in specific regions exist in literature and can be incorporated into the POWEIr controller to mitigate these errors.

The POWEIr controller irrigation schedules have been validated in simulation for a range of crop and soil types. This validation, in addition to future work testing the controller on farms, will legitimize the POWEIr controller's predictive schedules. Disseminating the results of the POWEIr controller could help increase adoption by farmers in LMICs. Increasing the

accessibility of this low-cost, sustainable, precise irrigation technology could allow farmers in LMICs to grow more food using less water and energy resources.

Chapter 4

Technical Validation of the POWEIr Controller for SPDI Systems in the Middle East and North Africa

The content of this chapter was derived from work with contributors besides the author of this thesis including Fiona Grant, Georgia Van de Zande, Shane Pratt, Anas Mansouri, Ahmed Wifaya, Ammar Namarneh, Susan Amrose, Vinay Nangia, Samer Talozi, and Amos G. Winter, V. A publication of the same title of this chapter is in preparation as Sheline, Grant, Van de Zande, *et al.* [108].

4.1 Introduction

An estimated 2.4 billion people faced moderate to severe food insecurity in 2022, signifying a substantial *increase* in comparison to 2015 when the Sustainable Development Goals (SDGs) were first introduced [1]. This highlights a deviation from the trajectory required to attain the second SDG, achieving zero hunger by 2030. In UN [1] a comprehensive overview of the most recent data on the SDGs are reported along with the compelling call to action to end hunger globally. Further, the reported severe food insecurity disproportionately affects

low- and middle-income countries (LMICs), emphasizing the need for targeted interventions in these regions. Addressing this challenge requires a concerted effort to augment crop production, particularly in LMICs, in order to improve food security.

Another aim of the second SDG is to sustainably attain food security in LMICs to not further diminish the world's natural resources [2], [3]. Currently, agricultural practices use 70% of global freshwater resources, and agri-food systems account for 30% of the world's total greenhouse gas emissions [6], [7], [101], [109]. Most farms rely on fossil fuels and electricity for energy sources, which contributed to over one billion tonnes of carbon dioxide equivalent in 2019 [5]. Reducing water usage in agriculture is especially important in the Middle East and North Africa (MENA), the most water-scarce region of the world, where the total water productivity is half of the world's average [4].

Solar-powered drip irrigation (SPDI) and precision agriculture technologies can help sustainably achieve food security by increasing crop production, minimizing water use, and reducing greenhouse gas emissions [8]–[10]. Solar-powered water pumps are estimated to have 95–98% lower total lifetime greenhouse gas emissions than pumps powered by grid electricity or diesel fuel [11]. Drip irrigation delivers water to the crop root zone through a network of pipes and emitters. When properly used, drip irrigation is projected to decrease water use by 40% and increase crop yields by 20% compared to the prevailing methods, flood and furrow irrigation, where fields are flooded with water fully or through dug trenches [12], [32]. Precision agriculture directly aims to increase productivity sustainably through the management of farm operations to optimize returns while conserving resources.

However, due to the high system cost and complexity of operating and maintaining these technologies, LMICs have been slow to adopt SPDI and precision agriculture [13]–[15]. Even when drip irrigation and sustainable agriculture technologies are adopted, farmers can still choose to use the technologies unsustainably and over-irrigate to mitigate perceived risks to the crops [16]–[18]. One proposed means of reducing these negative impacts of human decision-making in irrigation is to automate SPDI precision irrigation control; however, these

solutions fall short both due to their technical difficulty – the need for many sensors and detailed calibration – but also because the automation doesn't account for local farming contexts and preferences on part of the user [19]. There is a need for low-cost, precision irrigation control of SPDI systems specifically designed for the LMIC context.

The Predictive Optimal Water and Energy Irrigation (POWEIr) controller is an affordable SPDI and precision agriculture solution for low-income farmers [22], [25]. The merits of the POWEIr controller are its potential to increase the accessibility of SPDI in LMICs by reducing system cost as well as its ability to enable predictive, precise, sustainable irrigation practices with minimal sensors and reliable irrigation delivery. The POWEIr controller has three levels of control that offer a multifaceted approach to optimizing water and energy usage in SPDI systems [22], [25].

Our prior work has established the potential of this controller to enable affordable, precise irrigation. Sheline, Grant, Gelmini, *et al.* [25] simulated a full season of SPDI operation and optimized designs that used solar profile matching (SPM), an irrigation technique that aligns the irrigation pumping power with the fluctuating solar energy supply. The simulated operation with SPM demonstrated significant reductions in life cycle costs (18-74%) and substantial enhancements in irrigation reliability (31-66%) when compared to commercial counterparts. The study also built a small-scale prototype of the POWEIr controller and verified, particularly during periods of heightened irrigation demand, the ability to increase the amount of irrigation delivered using direct-drive solar power by 19-46% and reduce battery capacity by 78-98% compared to traditional methods. Notably, the inclusion of battery use optimization has succeeded in reducing cycling and charging rates by an average of 42%, while upholding 100% irrigation reliability. The integration of feedback pressure control within the POWEIr controller yields an additional 10% energy savings when compared to constant, maximum power operation, which is typical drip irrigation practice. The study found that incorporating operational control can enable cost-effective yet reliable SPDI systems, marked by reduced panel sizes and buffer battery capacity. However, a caveat of this

finding is that smaller batteries can age more rapidly, necessitating power system management encompassing factors such as battery cycle counts, C-rates, and ambient temperatures.

Sheline, Ingersoll, Irmak, *et al.* [75] evaluated the impact of varying inputs on optimal irrigation schedules and simulated crop yields. It was found that changing to a low-cost weather station caused up to a 15% reduction in total irrigation for the simulated cases, but this change in irrigation had negligible effect on crop yield. In addition, it was shown that errors in crop parameter inputs to the POWEIr controller, especially errors in the crop coefficients, significantly affected the irrigation volume and crop yield. Therefore, it was suggested that calibrated crop coefficients should be used with the POWEIr controller for the best results.

Although the studies on the POWEIr controller show promising initial results on its ability to reliably and precisely irrigate at a low cost, the performance validation has thus far remained confined to the realm of simulation and small-scale research prototypes, over relatively brief timeframes, and not in LMIC contexts. Real-world validation of the POWEIr controller is necessary, especially given farmers' reservations regarding adoption unless practical efficacy is demonstrated. Additionally, for a precision agriculture technology to achieve widespread adoption it must be adaptable to the local context [83]. To this end, the validation of the POWEIr controller must encompass complete crop seasons within pertinent LMIC contexts.

This chapter explores the modification and deployment of the POWEIr controller in two distinct countries: Jordan and Morocco. Both countries are well positioned for the adoption of the POWEIr controller as both governments have plans to invest in more efficient use of water in agriculture and the use of renewable energy [110], [111]. Van de Zande, Sheline, Amrose, *et al.* [22] noted that more farmers in Morocco desired automated irrigation compared to Jordan. This finding led to the need for context-dependant customization of the POWEIr controller. The chapter's approach involves a combination of comprehensive experimental validation and simulation to assess the practical implementation and effectiveness

of the POWEIr controller in these diverse contexts. The aims of this chapter are to:

1. Describe customization and implementation strategies for the POWEIr controller in multiple usage contexts;

2. Validate the POWEIr controller software and hardware in relevant environments showing that Level 3 performed as expected;

3. Quantify the controller's performance in terms of water and energy savings without adversely affecting crop yields compared to typical farmer drip irrigation practice.

These aims uncover the full potential of the POWEIr controller in conserving water and energy while maintaining crop production. The POWEIr controller is proven herein to be a technology capable of sustainably increasing food production by demonstrating that it can substantially save resources without compromising agricultural output across multiple contexts. Upon implementation, the POWEIr controller holds the potential to counteract food insecurity by prompting a departure from current unsustainable agricultural practices.

4.2 POWEIr Controller Theory and Design

This section is a summary of the POWEIr controller theory and it provides a fundamental understanding of the levels of control and models within the POWEIr controller. A full description of the theory is reported in Chapter 2, with updates to the solar prediction model reported in Chapter 3.

4.2.1 POWEIr Controller Architecture

Figure 4.1 depicts the POWEIr controller architecture, the models and optimization algorithms for each of the levels, and the interactions between the system components, models, and levels. The three levels of the POWEIr controller are:

Level 3: Predicts, optimizes, and communicates the irrigation schedule a day in advance, tailored to farmers' preferences.

Level 2: Adjusts energy management throughout the day to accommodate prediction uncertainties and ensure schedule adherence.

Level 1: Maintains ideal pump operating pressure, thereby minimizing power wastage.

The POWEIr controller has been purposefully crafted to rely on a limited set of essential sensors and models, meaning minimal input and calibration are needed from farmers and irrigation engineers. This means the controller is scale-neutral and easily adapted to a variety of contexts.

Level 3

Level 3 uses physics-based models, machine learning, and Model Predictive Control (MPC) to produce daily predicted, water- and energy-optimal irrigation schedules. MPC, a process control technique that uses a dynamic model of the controlled system to predict its behavior over a moving time horizon and produce an optimal control action, is useful in precise agricultural practices [34], [44], [46]. Level 3 combines measured data from a weather station with historical weather to create a local past weather data set. Past solar power, reference evapotranspiration (ET_0), and rain are calculated using the past weather data and solar and ET_0 models. Prediction models use machine learning to forecast future solar power profiles and weather data. The soil moisture model uses past weather data, future weather data, and the previous day's irrigation volumes to calculate the parameters needed to estimate the crop water demand. The predicted solar power profiles and crop water demand parameters are fed into the irrigation optimization algorithm. The predicted irrigation schedule is optimized to enhance energy efficiency and minimize water consumption while preserving crop yield. The objective of the optimization algorithm is to maximize crop revenue, minimize operational energy and water costs, and minimize future risks by ensuring adequate energy is stored.

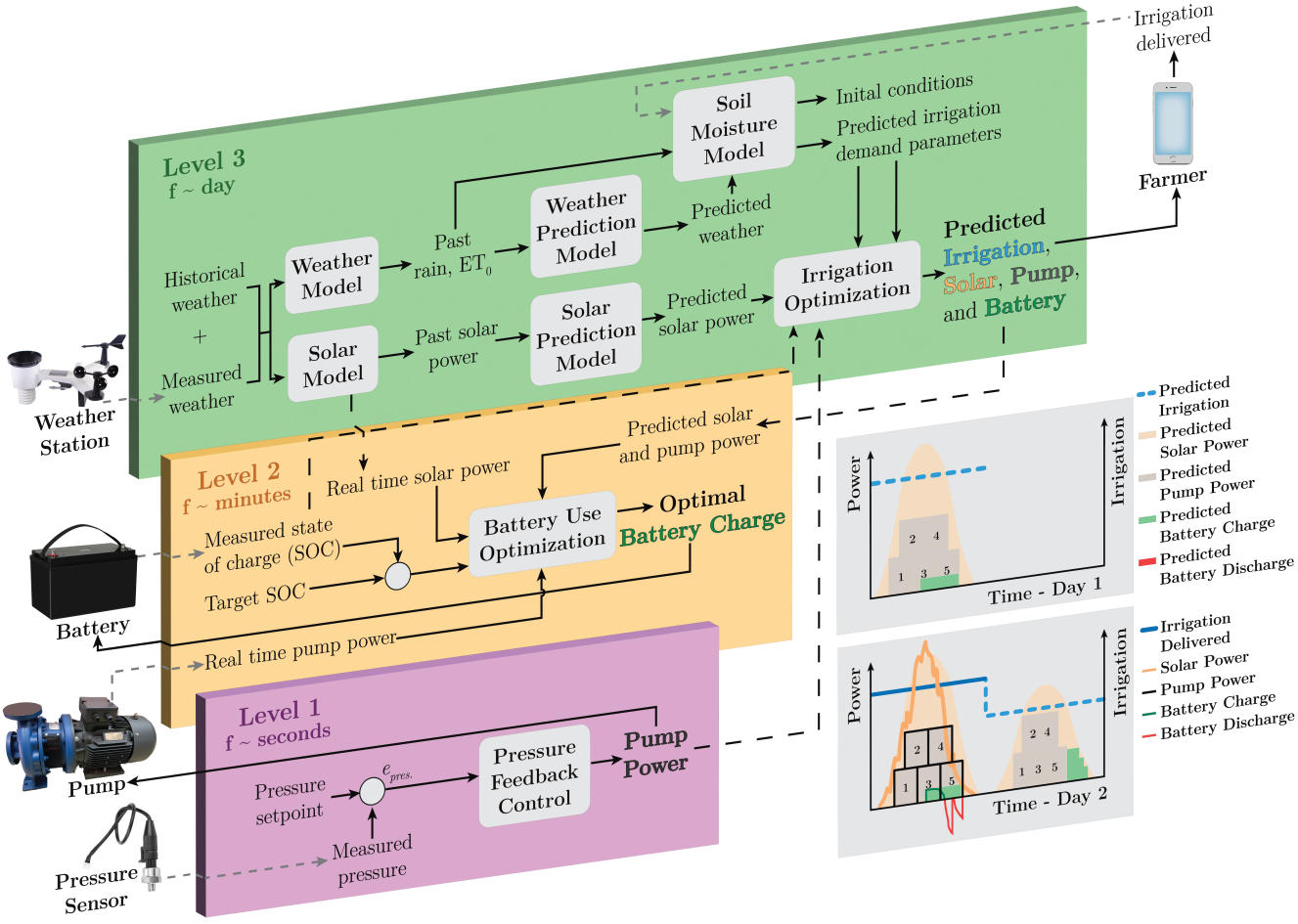

Figure 4.1: The updated, full Predictive Optimal Water and Energy Irrigation (POWEIr) controller architecture. At the start of the day Level 3 (green) predicts and optimizes an irrigation schedule based on measured and historical weather data. These data train solar and weather prediction models and initializes the soil moisture model. Prediction models forecast future solar power profiles and weather parameters, including reference evapotranspiration (ET_0) and rain. Rain and ET_0 inform the soil moisture model's calculations of crop water demand. The Level 3 optimized irrigation schedule is communicated to farmers through a smartphone app, and actual irrigation amounts are fed back to Level 3, keeping the farmer in the control loop. Throughout the day Level 2 (orange) optimizes battery charging based on Level 3 predictions and real-time measurements, while Level 1 (purple) maintains ideal pump operating powers using pressure feedback control. The ideal pump powers are calibrated once and used in the Level 3 irrigation optimization algorithm. The bottom right plots illustrate how Levels 2 and 1 adjust over the first day to meet Level 3 predictions despite uncertain solar power conditions.

Level 2

Level 2 implements MPC to govern the distribution of energy between the solar panels and the battery system on a sub-daily basis. Level 2 takes in measured inputs from the battery, solar power available, and pump power to make battery charging rate adjustments in real time. This strategy ensures adherence to the Level 3 irrigation schedule despite prediction error while simultaneously mitigating battery wear and extending its lifespan.

Level 1

Level 1 employs a pressure feedback control loop to ensure uniform flow, adapting to variations in hydraulic system pressure. This level supports the SPM schedule execution by dynamically modulating pump power in response to the number of open sections. Additionally, it aids in precisely characterizing pump operating powers for use in Level 3 and Level 2 calculations.

4.2.2 Daily Weather Model

The soil moisture model relies on an estimation of daily weather parameters, namely precipitation (Pr) and crop evapotranspiration [mm] (ET_c). The ET_c is approximated as

$$ET_c = K_c ET_0, \tag{4.1}$$

where ET_0 is the reference evapotranspiration [mm] and K_c is the crop coefficient. The POWEIr controller uses the Penman-Monteith equation, as described in Allen, Pereira, Raes, *et al.* [63], to calculate ET_0. The Penman-Monteith equation derives ET_0 under the assumption of a grass reference crop of 0.12 m height with complete shading of the ground and sufficient soil moisture. These assumptions mean that ET_0 depends solely on weather data inputs, specifically temperature, relative humidity, solar irradiance, and wind speed. These

weather inputs, along with Pr, can be measured with a local weather station and tabulated to get daily averages and totals.

4.2.3 Solar Power Model

The solar power model estimates the available solar power for the irrigation schedule optimization algorithm. The model utilizes hourly weather data to calculate the solar power available by approximating the solar panels using a single-diode model. The choice of a single-diode model was made due to its proven simplicity and accuracy in representing maximum power output under varying weather conditions, as demonstrated in Bishop [90]. To derive the maximum power output, the single-diode model relies on solar panel specifications typically found in the manufacturer's technical documentation, along with solar irradiance and temperature data. The additional parameters required for the single diode model are computed using the methodology outlined in De Soto, Klein, and Beckman [91].

4.2.4 Weather Prediction Model

Past daily Pr and ET_0 are fed into a weather prediction model to forecast future daily Pr and ET_0 used in the soil moisture model to calculate the crop water demand needed for the irrigation optimization algorithm. The POWEIr controller implements a locally installed low-cost weather station, described further in Section C.1, and machine learning methods to predict the necessary daily weather data. This implementation is particularly useful in resource-constrained settings where free, reliable weather forecasts are not readily available. The chosen forecasting algorithm for the weather prediction model is vector autoregression (VAR) [62]. The VAR algorithm makes multiple variable time-series predictions from related variables. This algorithm is well-suited for resource-constrained settings as it is not computationally expensive and does not require large amounts of training data [61]. Daily average, minimum, and maximum air temperature and relative humidity, average wind speed, total

solar radiation, total sun hours (calculated as the number of hours the hourly radiation was greater than 0.1 MJ/m^2), the reference evapotranspiration, ET_0 (calculated using Penman-Monteith equation), and total rain (Pr) are the weather data variables used in the VAR algorithm. The VAR model receives a defined time window of input data and forecasts a vector of the same data for the upcoming prediction period. The VAR algorithm is trained using a combination of one year of typical meteorological year (TMY) data obtained from the nearest weather station and historical observations from the locally connected weather station. To maintain accuracy, the VAR algorithm undergoes periodic retraining and reconstruction using both historical and incoming weather data at the beginning of each prediction cycle. This feedback and update process ensures that the algorithm captures and adapts to current trends in the data.

4.2.5 Solar Prediction Model

Past data of available solar power is needed for forecasting hourly solar power, which, in turn, is used to optimize the irrigation schedule. To predict the solar power available curve, the POWEIr controller employs a Long Short-Term Memory (LSTM) network [95]. An LSTM network is a type of recurrent neural network notable for its ability to retain past information, resistance to noise, and suitability for sequence data prediction. The choice of an LSTM network is informed by its aptitude for single-variable time series prediction over a full day's solar profile [92], [93].

The LSTM model takes as input the historical hourly solar power data and generates a 24-hour projection of the solar power available. The LSTM networks algorithm was developed using the Keras deep learning package [94]. The architecture of the LSTM model comprises a 100-cell LSTM layer with ReLU activation, a 50-cell LSTM layer with ReLU activation, and a dense layer [95]. The loss function employed is a mean square error, and the optimization algorithm used is Adam [96]. The LSTM algorithm is trained using one year of TMY data obtained from the nearest weather station, combined with measured historical data from

the locally connected weather station. Periodic retraining and reconstruction of the LSTM model occur at the start of each prediction cycle, ensuring that the algorithm incorporates all current data trends.

4.2.6 Soil Moisture Model

A soil moisture model is used to estimate the daily crop water requirement, which is subsequently fed into the irrigation schedule optimization algorithm. This model leverages a soil water balance framework, which tracks the inflow, outflow, and retention of water within the soil. These computations are conducted every day throughout the crop season, defined by the crop's planting and harvesting dates. The soil water balance, as delineated in Allen, Pereira, Raes, *et al.* [63], is defined as

$$D_{r,n} + (1 - k_{RO})Pr_n + \frac{1000 I_{del,n}}{A_s f_w} = D_{r,n-1} + K_{st} ET_{c,n}, \tag{4.2}$$

where $D_{r,n}$ and $D_{r,n-1}$ are the root zone depletion [mm] on day n and on the previous day, respectively, k_{RO} is the runoff coefficient estimated based on the soil texture, I_{del} is the delivered irrigation [m^3], A_s is the field's area [m^2], f_w is the soil wetted fraction, K_{st} is the water stress coefficient, and ET_c is the crop evapotranspiration [mm]. K_{st} is calculated as

$$K_{st} = \frac{TAW - D_r}{TAW(1 - f_d)}, \tag{4.3}$$

where f_d is depletion fraction calculated as

$$f_{d,n} = f_{d,const} + 0.04\,(5 - ET_{c,n}). \tag{4.4}$$

The $f_{d,const}$ is a crop-dependant constant defined in [63]. TAW is the total available water that the crop can extract from the soil [mm] which depends on the depth of the crop roots (Z_r) [m] and soil texture.

The soil moisture is equated to the volumetric soil water content (θ_v), which is defined as

$$\theta_v = \frac{V_{water}}{V_{soil}} \tag{4.5}$$

where V_{water} is the volume of water in the soil [m^3] and V_{soil} is the volume of soil [m^3]. The θ_v in the root zone can be related to D_r as

$$\theta_{v,n} = \theta_{v,fc} - \frac{D_{r,n}}{1000 Z_r}, \tag{4.6}$$

where $\theta_{v,fc}$ is the volumetric soil water content at field capacity, dependent on the soil texture. D_r is constrained to be less than TAW and greater than zero. If the D_r is greater than the readily available water (RAW), defined as

$$RAW_n = f_{d,n} TAW \tag{4.7}$$

then there is water stress and K_{st} is between zero and one. If D_r is less than or equal to the RAW then there is no water stress on the crop and K_{st} equals one.

The water stress affects the amount that crop evapotranspiration is adjusted ($ET_{c,adj}$) as

$$ET_{c,adj} = K_{st} ET_c. \tag{4.8}$$

If there is water stress on the crop, and K_{st} is between zero and one, then the reduction in evapotranspiration relates to a reduction in yield. The adjustment to the yield (Y_a) is accounted for as

$$1 - \frac{Y_a}{Y_{max}} = K_y \left(1 - \frac{ET_{c,adj}}{ET_c} \right), \tag{4.9}$$

where Y_{max} is the maximum yield [kg/m^2] calculated using the agro-ecological zone method defined in [66] and K_y is the crop yield response factor [67].

4.2.7 Irrigation Optimization

The primary goal of optimizing the irrigation schedule is to efficiently manage energy and water resources while ensuring crop yield remains unaffected. This optimization algorithm relies on forecasted available solar power and crop water demand parameters. The objective is to maximize revenue through enhanced crop yield, minimize operational costs associated with energy consumption and water usage, and maximize the reliability of irrigation by fully charging any battery capacity by the end of the prediction horizon. The objective function quantifies these goals in terms of cost, taking into account the unit capital costs associated with various components of the system. The objective is expressed as

$$\begin{aligned} min \Bigg[& \sum_{i=\delta t}^{N_{hor}} \frac{1}{N_{hor}} \Bigg(k_b u_{max}(u_{1,i} - u_{2,i}) + \sum_{s=1}^{N_{s,tot}} k_w q_s d_{s,i} \Bigg) \\ & - \sum_{n=1}^{N_{day}} \sum_{s=1}^{N_{s,tot}} \frac{1}{N_{day}} \big(k_c A_s \frac{dY_{a,s,n}}{dt} \big) \\ & + k_d (1 - SOC_{N_{hor}}) \Bigg], \end{aligned} \tag{4.10}$$

where N_{hor} and N_{day} are the prediction horizon in hours and days; i is the time step count; δt is the hourly time step; $N_{s,tot}$ is the total number of sections s the field is split into; k_b [\$/kWh] is the unit cost of the battery defined by the unit battery cost and its lifetime storage; u_1 and u_2 are the charging and discharging rate of the battery, normalized by u_{max} [kW], the maximum charging or discharging rate; k_w [\$/m^3] is the unit cost for water; q_s is the flow rate for section s [m^3/hr]; d_s is the binary variable for irrigating section s of the field; k_c [\$/kg] is the price weight on the crop; $\frac{dY_{a,s,n}}{dt}$ is the daily yield [kg/m^2/day], which is estimated by dividing Y_a in Equation 4.9 by the number of days in the crop growing season; k_d is the unit cost on the battery [\$/day] based on the cost of the system over its lifetime; and SOC is the state of charge of the battery.

This optimization problem operates within a single prediction horizon and involves con-

trol variables denoted as d_s and u_1. The control variables determine the daily predicted, optimal irrigation volume, battery power profile, and pump power profile. The control variables also have a direct impact on the state variables of the system, which include D_r and SOC.

The state variables are subject to specific constraints that govern the dynamics of the system. These constraints encompass energy and water flow dynamics, ensuring that the system operates within physical limits. Additionally, the moisture content of the soil is constrained according to Equation 4.2. The state of the battery is also controlled, allowing it to charge only when surplus solar power is available and discharge when the pump power exceeds the available solar power. The pump power is a function of the system's flow rate and is calibrated during the system installation. The optimization process is bound by constraints on its control and state variables, and these constraints are detailed in [25].

4.3 Methods for POWEIr Controller Technical Validation

An experiment was designed to validate the technical performance of the POWEIr controller in a variety of contexts. The objectives of the experiment were to:

1. check the performance of each level (only Level 3 is presented herein) of the POWEIr controller in multiple farm and agricultural contexts;

2. compare the performance of the POWEIr controller in terms of energy use, water use, and crop yield to similar reference farms' measured irrigation practices in multiple contexts;

4.3.1 POWEIr Controller Customization and Implementation in Multiple Contexts

According to Dongyu *et al.* [83], for a precision agriculture technology to achieve widespread adoption it must be adaptable to the local given context. In the MENA region, where water scarcity is severe and agriculture relies heavily on irrigation rather than rain-fed methods [4], [109], precision agriculture is crucial. Despite the scarcity of water, farmers in MENA tend to over-irrigate [16], [18], emphasizing the need for adaptable precision agriculture technologies in MENA, such as the POWEIr controller.

Van de Zande, Sheline, Amrose, *et al.* [22] investigated the market potential for a tool such as the POWEIr controller in Jordan and Morocco and specified modifications that could prove beneficial in these various contexts. Specifically, it was found that farmers had different levels of experience with irrigation systems and scheduling as well as the amount of automation they preferred in their systems. Therefore it was identified that customization of the POWEIr controller was needed to integrate water and energy management along with different levels of automation in MENA. Notably, there was a preference for automation and the inclusion of automatic valves among the farmers interviewed in Morocco. Whereas the farmers interviewed in Jordan had a preference for manual valves that were inexpensive and familiar [22].

The POWEIr controller, as described in this chapter, was intentionally designed to be adaptable to the local context of MENA. Customized versions of the POWEIr controller were implemented in Jordan and Morocco, addressing the specific needs and challenges faced by farmers in each location. Both versions calculated the irrigation schedules automatically using the theory presented in Section 4.2. The version implemented in Jordan relied on manual valves and farm labor to open the sections at specified times. The version tested in Morocco used automatic valves to open the sections according to the calculated schedule.

The two versions of the POWEIr controller were designed, built, and tested to achieve the objectives of the experiment. Figure 4.2 and Table C.1 show the experimental setup and

details, including the sensors used, hydraulic layout, valve operation, irrigation scheduling method, electricity type, crop type, and soil texture. The implementation and testing strategies for both versions of the controller were customized to meet the needs of the farmers in Jordan and Morocco. This adaptability makes the POWEIr controller a promising technology for promoting sustainable and efficient agricultural practices in the water-scarce MENA region.

Jordan

In Jordan, the POWEIr controller was installed on a research farm that grew intercropped young grape vines and okra from May to December 2023. Half of the research farm used the POWEIr controller to irrigate and the other half irrigated based on a local farmer's recommendations as a reference. The farmer had over 20 years of experience growing okra and grapes in Jordan. The POWEIr controller side had a SPDI system with six sections where the grapes and okra could be irrigated separately with manual valves and the controller communicated the irrigation schedule over a phone application [23]. The reference side used grid power and drip irrigation with six sections where the grapes and okra could be irrigated separately with manual valves.

Morocco

In Morocco, the POWEIr controller was installed on a research farm that grew potatoes from January to June 2023 and carrots from July to November 2023. The research farm with the POWEIr controller was split into six sections and had automated valves (Netafim Aquative Plus Actuator Valve) that routinely carried out the optimal irrigation schedule. A small farm that sells to the local market was chosen as a reference for measuring typical irrigation practices. The reference farmer had over 20 years of experience growing potatoes and carrots in Morocco. The reference farmer's field had a SPDI system and four sections with manual valves and grew the same crops at the same time as the research farm with the

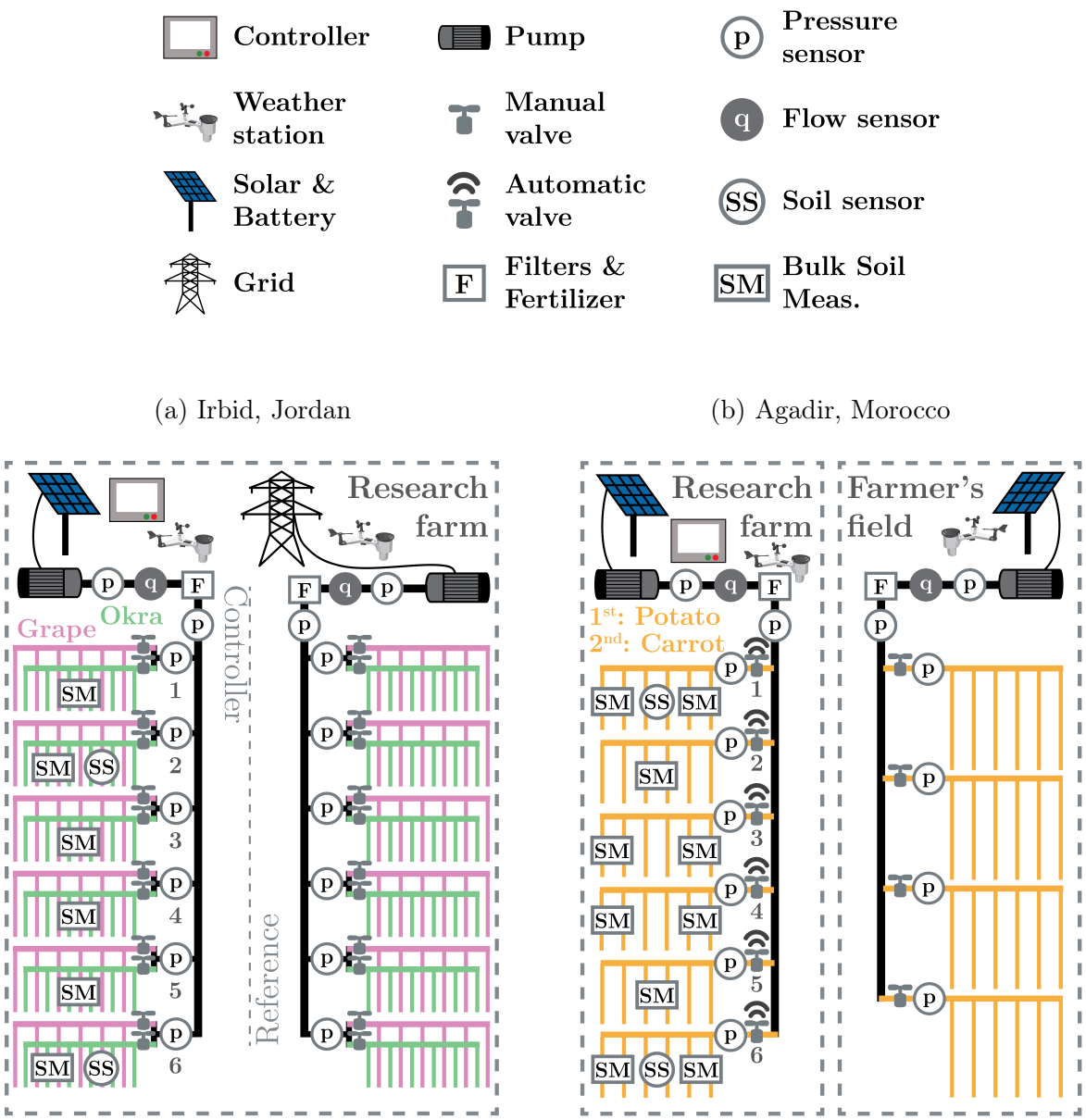

Figure 4.2: The experimental setups in Irbid, Jordan, and Agadir, Morocco. In Jordan, **a**, a one ha research farm irrigated inter-cropped grapes and okra, with half of the farm using the POWEIr controller and solar power on six sections, and the other half irrigating based on local farmer's recommendations with grid power as a reference. In Morocco, **b**, 0.6 ha research farm irrigated potatoes in the first season and carrots in the second season using the POWEIr controller and automatic valves on six sections compared to a neighboring farmer's 0.6 ha field with manual valves that irrigated the same crops in the same seasons based on the farmer's experience. Both of the experiments used drip irrigation and had weather stations, pressure sensors at the start of each section, a flow meter in the main pipe, pump power measurements and pressure sensors after the pump, and the filters and fertilizer injectors.

POWEIr controller.

Experimental Systems' Setup and Procedure

In Figure 4.2, both experimental setups used the same wired pressure sensors (ProSense SPT25-20-0060A), flow meter (ProSense FMM200-1002), and weather station (Ambient Weather WS-2902C). Also, the same type of soil sensor was used (Sentek Drill & Drop Probe). Each soil sensor took soil moisture measurements at one point in the field at multiple depths. In Jordan, the soil sensor in section two measured at 10 cm increments from 0 to 41 cm. The soil sensor in section six measured at 10 cm increments from 0 to 33 cm. In Morocco, both soil sensors took measurements at 10 cm increments from 0 to 60 cm. These are capacitance-based sensors and estimate θ_v directly. Bulk soil measurements were also taken on the fields with the controller in both Jordan and Morocco.

The bulk soil measurement conducted in Jordan used the gravimetric method where the soil water content (θ_g), was calculated as

$$\theta_g = \frac{m_{water}}{m_{soil}}, \tag{4.11}$$

with m_{water} as the mass of water in the soil [kg] and m_{soil} as the dry mass of the soil [kg]. The m_{water} was measured by taking the difference between the weight of wet soil sampled from multiple locations in the field and the weight of the same sample once it was dried in an oven (m_{soil}). The soil samples in Jordan were collected at a depth of 10 cm over the entire season, and additional 30 cm depth samples were collected towards the end of the season.

The bulk soil measurement taken in Morocco was from ten lysimeters spread evenly across the field with the controller. The soil water content from the lysimeter was calculated using Equation 4.11. The measurements taken were the weight of wet soil in the lysimeter buckets and the weight of the same lysimeter buckets from the start of the experiment when the soil was dry (m_{soil}). The difference of these measurements was m_{water}. For the potato crop, the

lysimeters were 60 cm deep and for the carrot crop the lysimeters were 20 cm deep.

Both the soil sample and lysimeter methods are common agronomic research methods for measuring bulk θ_g. The bulk soil measurements were used as a baseline to compare to the soil sensor measurements and POWEIr controller estimations of θ_v. To compare the bulk measurements, θ_g was converted to θ_v defined as

$$\theta_v = \theta_g \frac{\rho_{soil}}{\rho_{water}}, \tag{4.12}$$

where ρ_{soil} is the dry bulk density of the soil [g/cm^3] and ρ_{water} is the density of water [g/cm^3]. The ρ_{water} is assumed to be 1 g/cm^3. The ρ_{soil} values are reported in Table C.2. The ρ_{soil} for Morocco was measured and the ρ_{soil} for Jordan used default values based on the soil texture [112].

The pump and power systems used in Jordan were sized to be appropriate for the farm with additional battery capacity to allow for irrigation during non-sunlight hours and mitigate risk to the crops in the experiment. The batteries were oversized as there was uncertainty about how much additional irrigation would be needed during non-sunlight hours.

In Jordan, both the controller and reference side of the research farm used a 2.2 kW pump (Pedrollo pump F32/160B) and a locally sourced disk filter, sand filter, and fertilizer injector. The controller side was powered by six 540 Wp panels (Tiger Pro JKM535M-72HL4-V). The controller side also had a 10.2 kWh lithium iron phosphate (LFP) battery (DGRID DG-B-WM-48200). The reference side's pump was powered by the grid, measured using a grid meter (Carlo Gavazzi EM24); the reference side's data acquisition (DAQ) unit was powered by two 300 Wp solar panels (Jain Irrigation JJ-M672) and two 1200 Wh GEL batteries (NPP NPG12-100Ah–12V, 100Ah).

In Morocco, both the controller and reference side of the research farm used a 2.2 kW pump (Sealand CN 32-160B) and had a disk filter. The research farm and farmer's field were powered by eight 330 Wp panels (Eagle JKM330PP-72-V) each. The research farm also had

two 3.6 kWh lithium iron phosphate (LFP) batteries (Maribat MLFP 48V 3600Wh) to power the irrigation system at times of low solar irradiance and the DAQ unit at the farmer's field had two 1200 Wh GEL batteries (EcoGreen 6-GFJ-100–12V, 100Ah) to transmit data at times of low solar irradiance.

The POWEIr controller hardware in each country consisted of a solar and system monitoring controller (Victron Cerbo GX), a maximum power point tracker (Victron Smart Solar MPPT 250V 60A), an inverter (Victron Multiplus 48/5000/70), a battery monitor (Victron Smart Shunt 500A/50mV), a DC-DC Converter (Victron Energy Orion-Tr 48/24-12), a variable frequency drive or VFD (DURApulse G S11N-23P0), a programmable logic controller or PLC (CLICK PLUS PLC), and an LTE router, modem, and antenna (MikroTik RBSXTR&R11e-LTE and RBD52G-5HacD2HnD-TC). The DAQ unit hardware in each country consisted of a solar and system monitoring controller (Victron Cerbo GX), a maximum power point tracker (Victron Smart Solar MPPT 150V 35A), a battery monitor (Victron Smart Shunt 500A/50mV), a programmable logic controller or PLC (CLICK PLUS PLC), and an LTE router, modem, and antenna (MikroTik RBSXTR&R11e-LTE and RBD52G-5HacD2HnD-TC). The DAQ unit in Morocco also included a VFD (Delta VFD MS300 2.2kW) to power the pump directly using solar.

The POWEIr controller was programmed in Python. The Level 3 code ran once per day in each country starting March 28th, 2023. On-site researchers used the FAO 56 soil water balance method to calculate the crop water needs, similar to the method described in Section 4.2.6, during times when Level 3 wasn't active. A phone application (app) was used to communicate the Level 3 optimal irrigation schedule at the start of each day. In Jordan, users would look at the schedule on the app at the start of the day and use the app to communicate back to the controller when they opened and closed sections. The users of the app in Jordan were farmhands and on-site researchers. In Morocco, the automatic valves would record when they were opened and closed. Node-RED was used to program the sensors and hardware. An MQTT protocol was used to communicate the necessary input

and output data between the different POWEIr controller levels, hardware, sensors, and the app. Data were stored in an Influx database and could be monitored remotely.

Table C.2 shows the inputs used for the POWEIr controller calculations. Default agronomy parameters defined in Allen, Pereira, Raes, *et al.* [63] were used where applicable. The default parameters were adjusted with different calibration techniques in the various seasons that were tested. For the Morocco potato season, conducted from January to June 2023, local Z_r and K_c values were used. The Z_r and K_c values were obtained from the Ministry of Agriculture near Agadir, the Souss-Massa Regional Authority for Agricultural Development (Office Regional de Mise en Valeur Agricole du Souss-Massa or ORMVA-SM) [113]. The Level 3 calculated D_r value was updated at times when the on-site researchers detected that the potato crop was undergoing stress. For the Jordan okra and grape season, conducted from May to December 2023, the f_d, K_y, Z_r, and K_c values were sourced from literature [114]–[117]. The Z_r, and K_c values were updated periodically based on on-site researchers' measurements and observations. On July 21, 2023, the POWEIr controller's D_r and K_c values were updated when it was noted that the okra crop coefficient had been 30% too high. The f_w was calculated based on field measurements of the hydraulic layout and crops. For the Morocco carrot season, conducted from July to November 2023, local Z_r and K_c values were obtained from ORMVA-SM. The f_w was calculated based on field measurements of the hydraulic layout and crops. On-site research experts in both Jordan and Morocco added additional irrigation beyond what the controller calculated if they perceived the crops to be undergoing stress.

4.3.2 POWEIr Controller Performance Hypotheses and Methods

Hypotheses, metrics, and experimental methods were developed for Level 3 of the POWEIr controller to validate its performance.

The main hypothesis for the Level 3 optimal irrigation schedule is that it reduces water use and energy use compared to typical farmer practices without harming or putting the crops

at risk as a result. The method used for testing this hypothesis was to measure the water and pump energy use on fields with the POWEIr controller and compare this to similar fields irrigated based on local farmers' practices or recommendations as a reference. The total cumulative pump energy and irrigation amount (I_{total}) [m^3/ha] used by the POWEIr controller as well as the total crop yield (Y_{total}) [tonne/ha] were compared to the reference as indicators of performance. A further performance metric used was the water use efficiency (WUE) [kg/ha], defined herein as

$$WUE = \frac{Y_{total}}{I_{total}} 1000. \tag{4.13}$$

Another hypothesis for Level 3 is that its soil moisture model, described in Section 4.2.6, can track the actual soil moisture with sufficient accuracy to ensure crop health. The method used for testing this hypothesis was to compare the Level 3 soil moisture estimates to soil moisture sensors and in-field bulk soil moisture measurements. A final hypothesis for Level 3 is that the error associated with the solar power predictions would not significantly affect the irrigation schedule or crops. The method for testing this hypothesis was to compare the solar power predictions to calculated values from the measured weather.

4.4 Technical Validation of the POWEIr Controller Results

The experimental results show the performance of each level of the POWEIr controller and the benefit of the POWEIr controller compared to reference farms in each country in terms of energy use, water use, crop yield, and WUE.

4.4.1 Level 3 Validation

The Level 3 performance was evaluated based on the error in its predictions, namely the solar energy prediction error and the error associated with its soil moisture, or θ_v, estimates. The daily solar energy was calculated as the solar power multiplied by its time duration summed over the day. The predicted solar power curve consisted of 24-hour predictions linearly interpolated into 10-minute increments. The measured solar curve consisted of solar power calculated using the theory in Section 4.2.3 and 5-minute aggregated weather data. To get the solar error, the daily predicted solar energy was compared to the solar energy calculated from the measured weather data. The daily percent error between the predicted solar energy and the calculated solar energy from the weather data is shown in Figure 4.3.

The solar prediction error was calculated for the duration of the experiment. For Morocco (Figure 4.3a) the mean solar energy prediction error was 32%, with a standard deviation of 93% (SD = 93%). For Jordan (Figure 4.3b) the mean solar energy prediction error was 31% (SD = 68%). The mean solar prediction error was around 30% for both countries; although there was a large SD, meaning there were many days when the solar prediction error was much higher. The histograms are shown to be skewed positive, signifying the POWEIr controller often over-predicted the daily solar energy it had available. Additionally, because the POWEIr controller's solar predictions were based on a linear interpolation of hourly data they did not capture fluctuations, such as those due to clouds, which added to the error.

The average θ_v in the root zone was calculated by the POWEIr controller using Equation 4.6 and the soil moisture model described in Section 4.2.6. Also, soil moisture sensors with measurements at multiple depths and bulk θ_v measurements based on soil weight were taken at the Morocco and Jordan research farms. Figures 4.4–4.6 show the θ_v that the POWEIr controller estimated compared to the soil sensors and bulk soil measurements for the various Morocco and Jordan crop seasons at the sections where the soil sensors were located.

Figure 4.4 shows the θ_v results for the Morocco potato season. Only one soil moisture sensor was used in this season and it was placed in the middle of the last section of the re-

(a) Morocco

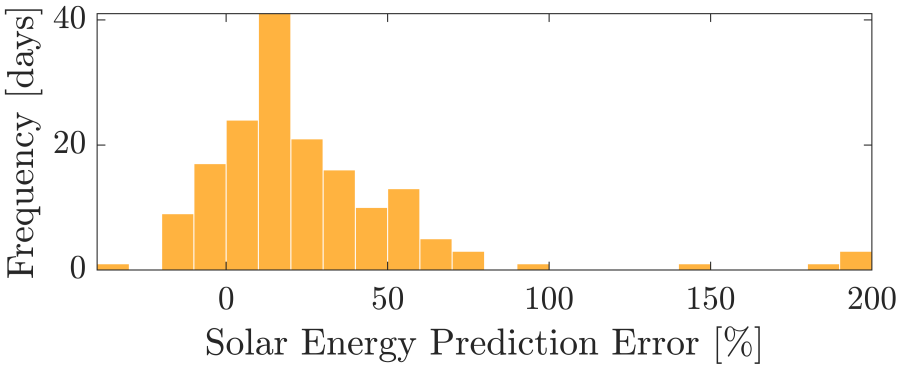

(b) Jordan

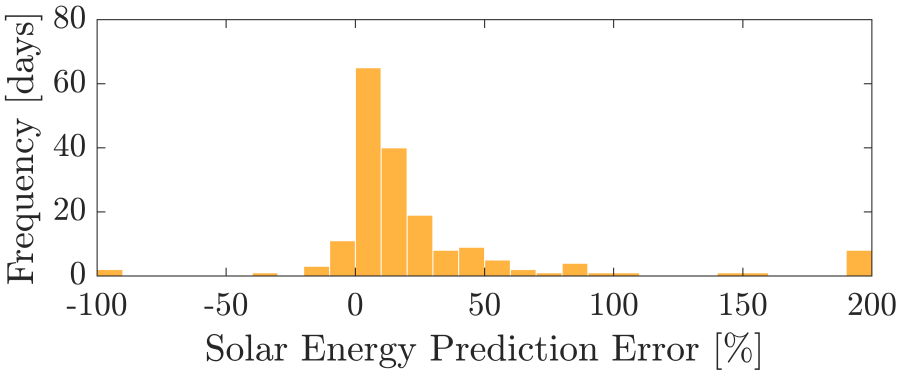

Figure 4.3: Daily solar energy prediction error for Morocco and Jordan. The error is the difference between the energy under the predicted solar power curve and the energy under the solar power curve calculated from the measured weather data. The energy error was calculated daily and made into a histogram for **a**, both potato and carrot seasons in Morocco, and for **b**, the okra and grape season in Jordan.

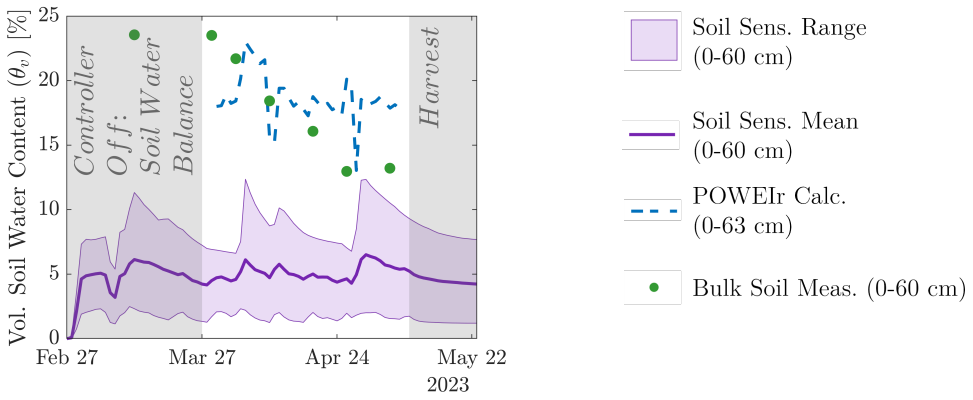

Figure 4.4: Volumetric soil water content (θ_v) comparison for the Morocco farm during the potato season for section 6. Estimates from the POWEIr controller (blue dashed line) compared to the full range and average soil sensor readings (purple area and line) and in-field bulk measurements (green dot). The legend summarizes the depth(s) that each measurement was taken at. Lysimeters were used to take the bulk θ_v measurements up to 60 cm. The grey boxes show times that the controller wasn't running during crop germination, harvest, or when the controller wasn't fully set up and researchers implemented a soil water balance to irrigate.

search farm, section six. The bulk soil measurements taken in the field were from lysimeters that calculated the average θ_v from 0–60 cm. The POWEIr controller bulk θ_v calculations were on average 2% (SD = 5%) higher than the lysimeter bulk measurements. The POWEIr controller calculated D_r was reset based on the lysimeter measurements when on-site researchers detected crop stress. The D_r values were reset on March 30, April 10, and April 27, 2023. This could have helped the POWEIr controller estimations of θ_v more closely match the bulk soil measurements. The soil moisture sensor reported 13% (SD = 5%) lower θ_v averaged over all depths compared to the bulk soil measurements. The inaccuracy in the soil sensor was most likely due to a placement issue, either it was not placed close enough to where the water from the emitter was or it was placed in a patch of soil that was dry due to emitter malfunction or variability in the soil. Soil moisture sensors are prone to placement issues and, to get an understanding of what is happening in the bulk of the soil, multiple sensors are necessary [118], [119].

Figure 4.5 shows the θ_v results for the Jordan okra and grape season. Soil moisture sensors were placed in the middle of section two and section six of the controller side of the

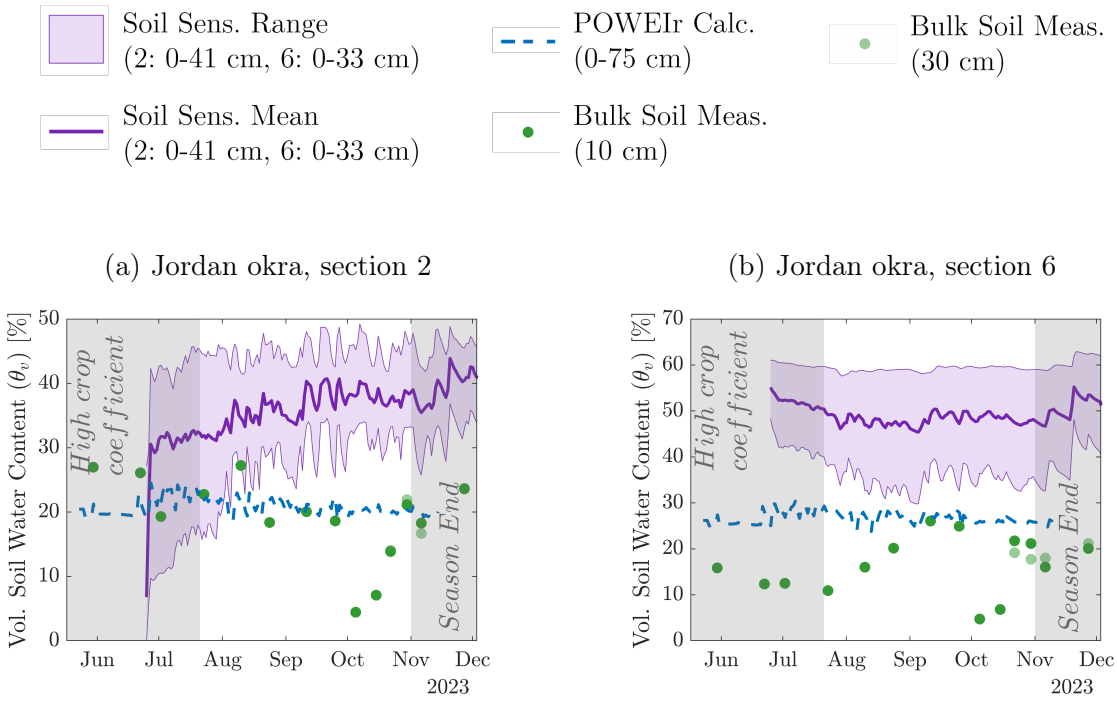

Figure 4.5: Volumetric soil water content (θ_v) comparison for the Jordan farm on sections 2 and 6 growing the okra crop. Estimates from the POWEIr controller (blue dashed line) compared to the full range and average soil sensor readings (purple area and line) and in-field bulk measurements (green dot). The legend summarizes the depth(s) that each measurement was taken at. The θ_v soil sensor measurements for section 2 (**a**) and section 6 (**b**) were taken over different depths, 0–41 cm and 0–33 cm, respectively. The bulk θ_v was measured using the gravimetric method with oven drying from soil samples taken at 10 cm. Four bulk soil samples were also taken at 30 cm (light green dots) at the end of the season in both sections. The grey boxes show when the crop coefficient and the controller's irrigation amounts were high and the end of the season when the controller was off.

farm near an emitter and the okra crop. Section two had loam soil of a consistent texture and low salt content while section six had sandy clay soil with an inconsistent texture and higher salt content. Even with the difference in soil texture, the POWEIr controller calculations are shown to match well with the bulk measurements. The controller θ_v calculations are on average 2% (SD = 6%) and 11% (SD = 6%) higher than the bulk soil measurements for sections two and six, respectively. It should be noted that the bulk soil measurement θ_v values were calculated based on default ρ_{soil} values in Jordan, which could have added error to these measurements. Future publications on this work will incorporate measured ρ_{soil} values to mitigate this error. Additionally, the bulk measurements were taken at 10 cm depth whereas the controller calculated the θ_v up to the root zone depth, which went up to 75 cm for the okra. The large difference in depths implies using the bulk soil measurements may not be a direct comparison. However, a small amount of bulk soil measurements were taken at 30 cm and shown to be 0.2% (SD = 1%) and 0.7% (SD = 3%) lower compared to the 10 cm measurements for sections two and six, respectively. The small difference in θ_v between depths demonstrates that the 10 cm measurements may have been a good indicator of the θ_v at higher depths. The soil moisture sensors reported 19% (SD = 8%) and 32% (SD = 7%) higher θ_v averaged over all depths compared to the bulk θ_v measurements for sections two and six, respectively. The larger difference in the θ_v of the soil sensor suggests that it under-performed compared to the POWEIr controller estimates.

Figure 4.6 shows the θ_v results for the Morocco carrot season. Similar measurements were taken in this season as in the previous Morocco potato season, except there were two soil moisture sensors, one in section one and one in section six. Additionally, the lysimeters measured the bulk θ_v at a shallower depth, from 0–20 cm. The shallower depth made the lysimeters smaller which facilitated the measurement process and allowed data to be collected more frequently. The controller-calculated D_r was not re-calibrated at all during this season; this more closely represents the desired design of the POWEIr controller to have minimal calibration. The POWEIr controller θ_v calculations were on average 2% (SD

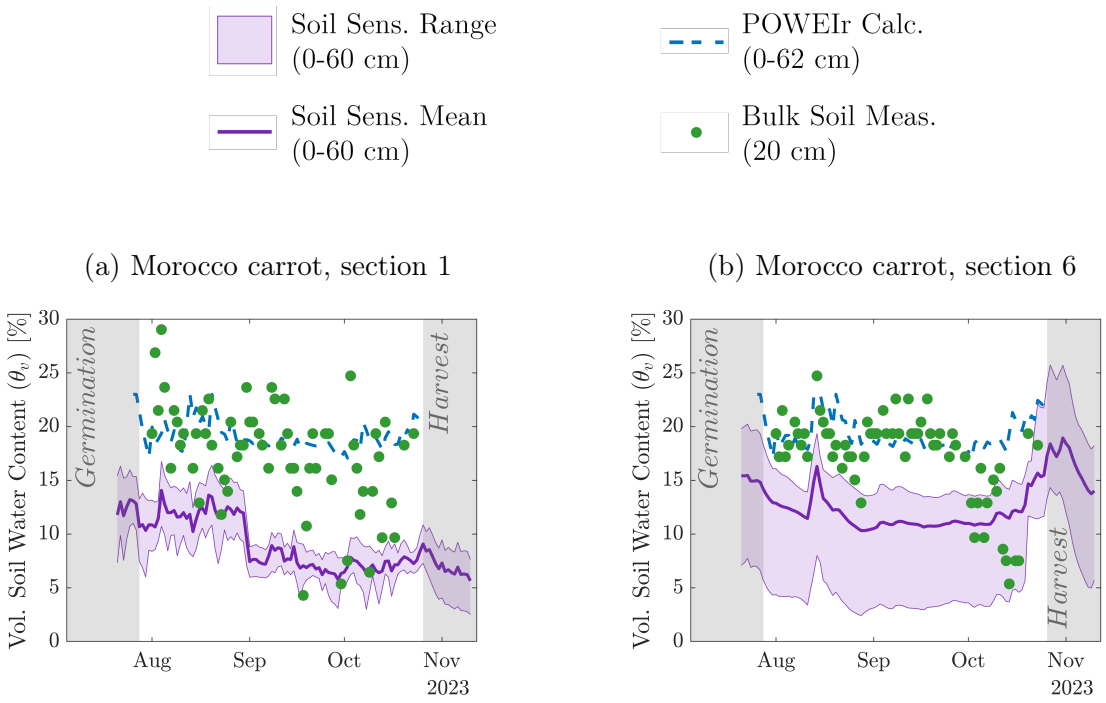

Figure 4.6: Volumetric soil water content (θ_v) comparison for the Morocco farm during the carrot season for sections 1 and 6. Estimates from the POWEIr controller (blue dashed line) compared to the full range and average soil sensor readings (purple area and line) and in-field bulk measurements (green dot). The legend summarizes the depth(s) that each measurement was taken at. All the θ_v measurements for section 1 (**a**) and section 6 (**b**) were taken over the same depths, 0–60 cm. Lysimeters were used to take the bulk θ_v measurements up to 20 cm. The grey boxes show times that the controller wasn't running during crop germination or harvest.

= 5%) and 2% (SD = 4%) higher than the lysimeter bulk measurements for sections one and six, respectively. This small difference indicates good agreement between the POWEIr controller calculations and lysimeter measurements, although it should be noted that they were taken at different depths. The θ_v for depths up to 20 cm may differ compared to depths up to 62 cm due to climate conditions and soil stratification. Yet, the soil moisture sensor reported 8% (SD = 4%) and 6% (SD = 4%) lower θ_v averaged over all depths compared to the bulk soil measurements for sections one and six, respectively. The closely matching data for the θ_v between the 60 cm soil sensors and the 20 cm lysimeters indicate that the shallower measurements may have been close to the θ_v at higher depths. Therefore the POWEIr controller calculations may have been accurate even to higher depths.

4.4.2 POWEIr Controller Energy, Water, and Crop Yield

The cumulative irrigation volume applied and the pump energy consumed at the research farms equipped with the POWEIr controller were compared to the corresponding resources used at the reference fields over each season. The cumulative irrigation water applied was calculated by summing the measured water from the flow meter over each season. The cumulative pump energy used was calculated by summing the measured pump power from either the inverter, VFD, or grid meter on each farm over each season. Also, the crops were harvested and their yields were weighed for both the farms with the controller and the reference farms.

Morocco Potato Season – January to June 2023

Figure 4.7 shows the cumulative volume of irrigation water applied to and pump energy used by both the research farm with the POWEIr controller and the reference farmer's field during the Morocco potato season from January to June 2023. The controller pump power was measured from the output of the inverter, going into the VFD, and the reference pump power

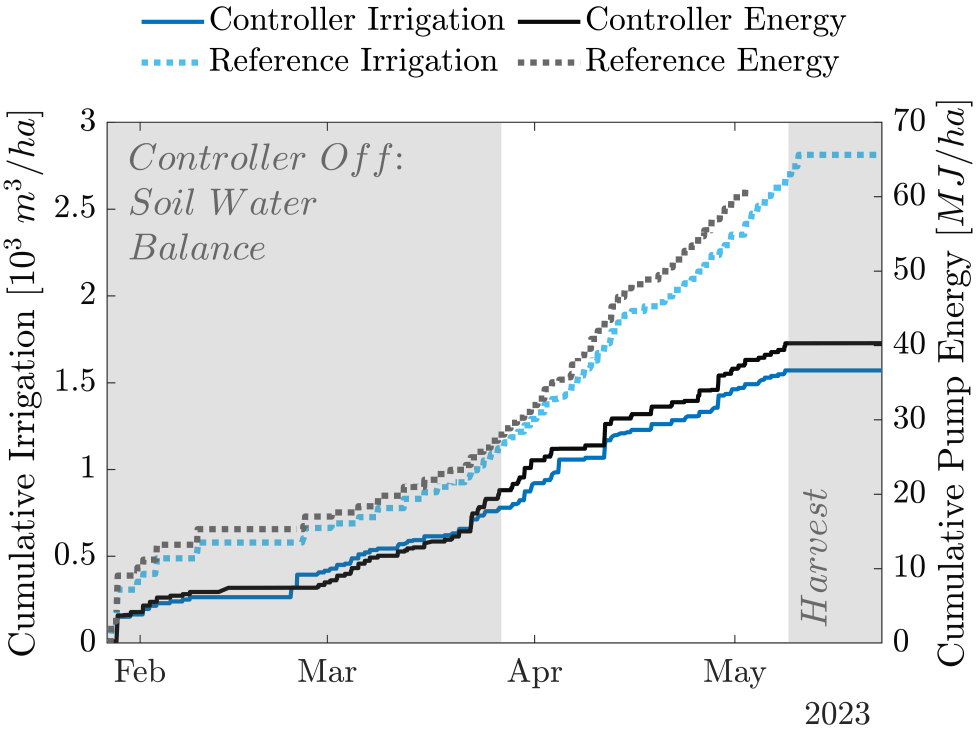

Figure 4.7: Cumulative irrigation volume and pump energy comparison between the farm with the POWEIr controller and the reference farm for the Morocco potato season. The POWEIr controller optimal irrigation scheduling did not start until March 28, 2023. Prior to this (grey box), the farm with the POWEIr controller was irrigated based on the soil water balance, similar to the theory is Section 4.2.6. The POWEIr controller also did not run during the potato harvest (grey box).

was measured from the output of the VFD. This means the pump power measurement for the farm with the POWEIr controller included the VFD inefficiency while the reference pump power did not include the VFD inefficiency. The reference farm's pump power measurement stopped recording on May 3, 2023, so results for the pump energy were compared on this date. The results show the POWEIr controller saved 38% in total pumping energy compared to the reference farm. Additionally, the POWEIr controller saved 44% in water compared to the reference of a local farmer irrigating according to their typical practice.

The controller and reference potato yields were 23.7 tonne/ha and 26.2 tonne/ha, respectively, with a 9% difference. This difference could be attributed to the respective quality of the water used on each farm. Electrical conductivity (EC) of the water on the research farm was measured to be 2.4 mS/m during this season, which represents a level of salts in the water that could have contributed to up to a 25% reduction in potato yield [120, Chapter 2]. The EC of the water on the reference field was measured to be 1.4 mS/m have contributed to minimal reduction in potato yield [120, Chapter 2]. Therefore the 9% reduction in yield on the farm with the controller could be accounted for due to the lower water quality. The WUE was 15.1 kg/m^3 for the farm with the controller and 9.3 kg/m^3 for the reference farm. This means the controller saved a considerable amount of pumping energy and irrigation water compared to measured typical SPDI practice for similar crop yield and made a 62% improvement to the WUE.

Jordan Okra and Grape Season – May to December 2023

Figure 4.8a shows the cumulative volume of irrigation water applied to and pump energy used by both the research field with the POWEIr controller and the reference field which was irrigated based on well-practiced farmer's recommendations during the Jordan okra and grape season from May to December 2023. The controller pump power was measured from the output of the inverter and the reference pump power was measured from the output of the grid meter. From May 28 to July 21, 2023, the crop coefficient for the okra was set 30%

(a) Cumulative irrigation volume and pump energy for okra and grape

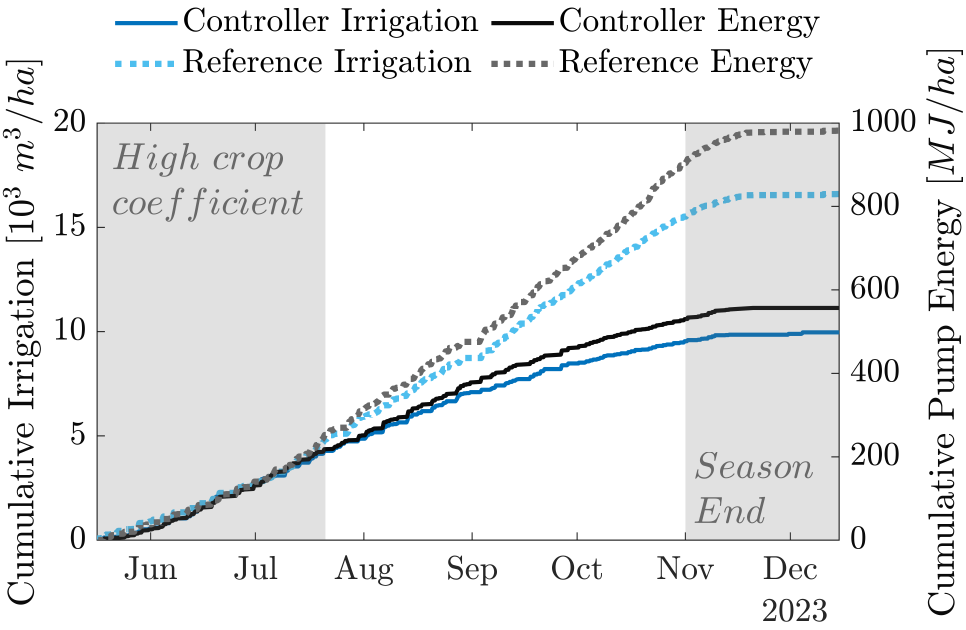

(b) Cumulative yield for okra

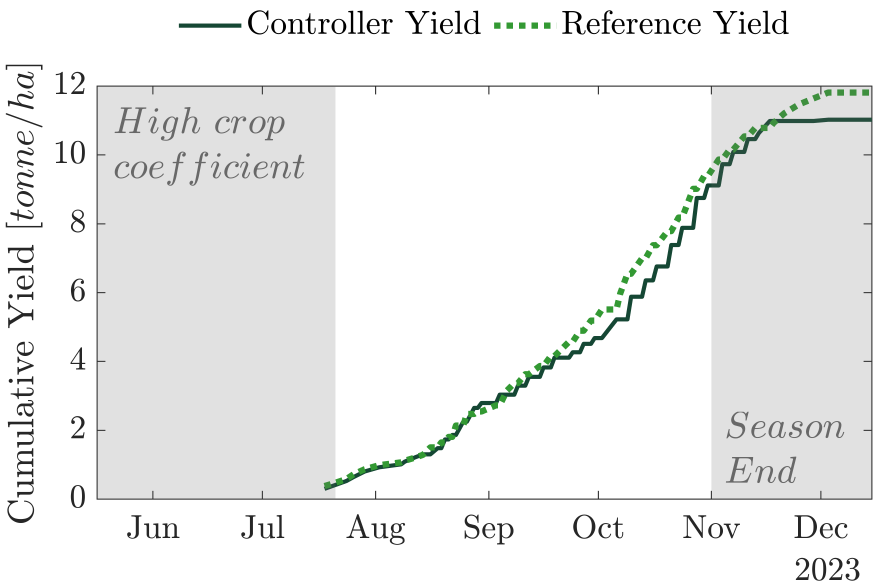

Figure 4.8: Cumulative irrigation volume, pump energy, and okra yield comparison between the farm with the POWEIr controller and the reference field for the Jordan season. The crop coefficients for the okra crop were set 30% too high and later adjusted on July 21st, 2023 (grey box). Harvesting of the okra began on July 18th, 2023, and continued until the end of the season. The end of the okra season (grey box) could have happened anytime from November 1 to December 15, 2023.

higher than required; during this time the irrigation amounts and pumping energy between the fields were similar. The controller assumed the okra and grape irrigation seasons ended on November 15, 2023. Additionally, the rainy season started on November 15, 2023, after which little irrigation was required. November 1 to December 15, 2023 was a window of time when okra farmers in the region would end harvesting okra. The end of the okra season could have happened at any point during this window depending on the farm. The results vary depending on when it is assumed that the okra season ended. Therefore, instead of assuming a single end-of-season date, results are presented for two end-of-season dates. The first date is November 15, 2023, when the controller stopped calculating an irrigation schedule. The second date is December 3, 2023, the last date that okra was harvested on both sides of the farm. The results show that if the end of the okra season is assumed to be November 15, 2023, the controller saved 42% in energy and 40% in water compared to the reference field. If the end of the season is assumed to be December 3, 2023, the controller's energy saving increased to 43% with no change in the water saving.

The grapes were young grape vines and did not produce any yield on both fields. Figure 4.8b shows the okra started producing yield on July 18, 2023 until December 3, 2023. The field with the POWEIr controller and the reference field had okra yields on November 15, 2023 of 11.0 tonne/ha and 10.8 tonne/ha, respectively. At this assumed end of the season, the okra yield for the controller field was 2% greater than the reference field's yield. Assuming the end of the okra season was December 3, 2023, the yields for the controller and reference fields were 11.0 tonne/ha and 11.8 tonne/ha, respectively, or 7% less for the controller field. The field with the controller stopped producing okra by November 17, 2023 whereas the reference field produced an extra tonne of okra through December 3, 2023. The extension of the okra season for the reference field could be because more irrigation was applied during the season. Even though the reference field had a slightly higher okra yield its WUE ranged from 0.65 to 0.71 kg/m^3 over the end of the okra season, whereas the WUE stayed at 1.11 kg/m^3 for the controller field. The 55–72% higher WUE means the POWEIr controller saved significantly

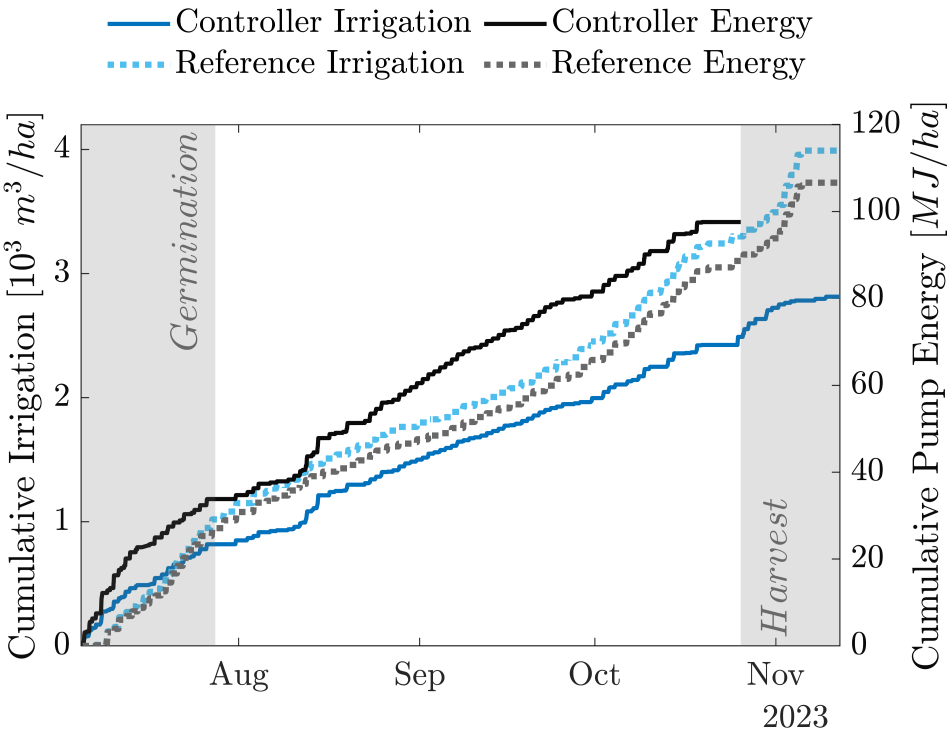

Figure 4.9: Cumulative irrigation volume and pump energy comparison between the farm with the POWEIr controller and the reference farm for the Morocco carrot season. Morocco experienced an extreme heat wave during this season and additional irrigation was added to the farm with the POWEIr controller by on-site researchers on August 12th, August 14th, and August 19th, 2023. The controller did not determine irrigation amounts during carrot germination or harvest (grey boxes).

in pumping energy and water compared to measured typical drip irrigation practice for comparable okra yields.

Morocco Carrot Season – July to November 2023

Figure 4.9 shows the cumulative volume of irrigation water applied to and pump energy used by both the research farm with the POWEIr controller and the reference farmer's field during the Morocco carrot season from July to November 2023. At the start of the carrot harvest, on October 26, 2023, the controller had a 10% increase in energy and 25% decrease in irrigation amounts compared to the reference of a farmer irrigating according to their typical practice. The increase in energy is because of the difference in the operating flow

rate, and the related difference in pump efficiency, for the farm with the POWEIr controller and the reference farm. The pump at the controller farm was operated at lower flow rates and had an average pump efficiency of 49% (SD = 8%) compared to the pump at the reference farm, which had a pump efficiency of 57% (SD = 5%). Furthermore, the pump power measurement on the reference farm comes from the output of the VFD and the pump power measurement for the farm with the POWEIr controller comes from the input to the VFD. This means VFD efficiency losses are included in the controller energy calculation, but not in the reference energy calculation. Figures C.1 and C.2 in Appendix C show the cumulative pump energy broken down into hydraulic pump output energy, calculated input pump power, and measured input power to the pump as well as a histogram of the pump efficiency for the farm with the controller and the reference farm.

The spikes in the POWEIr controller's cumulative irrigation amounts shown in Figure 4.9 are due to additional irrigation applications. The crops were temperature stressed due to extreme temperatures (over 50°C) starting on August 11th; because of this additional irrigation was applied on August 12th, August 14th, and August 19th, 2023. Also, on-site researchers applied additional irrigation on October 9th and October 18th, 2023. The POWEIr controller stopped calculating the daily irrigation schedules on October 26th, 2023, after which on-site researchers irrigated the carrots to facilitate harvesting and keep the carrots fresh to sell in the local market. The water savings increased to 29% by the end of the carrot harvest but the controller stopped recording pump data on October 26th, 2023 so no additional change in energy was recorded.

The reference and controller yields were 24.4 tonne/ha and 13.8 tonne/ha, respectively, which was a 44% decrease in the controller yield. The deficit in yield on the controller farm was due to a root-knot nematode infestation. At the end of the season, a soil sample was taken which indicated a severe parasitic nematode infestation of 253 Meloidogyne species per 100 g of soil at the controller field. It has been shown that root-knot nematode infestations can cause between 25–45% reduction in carrot yield, with a potential for total yield loss

[121]–[125]. Additional yield reduction could have been caused by a difference in water quality between the farm with the controller and the reference farm. EC of the water at the controller field could have contributed to a 15% greater reduction in carrot yield compared to the EC of the water at the reference field [120, Chapter 2]. Due to the decrease in yield, the controller WUE was less than the reference WUE, which were 4.89 and 6.12 kg/m^3, respectively. Although a large loss in yield occurred on the controller field, a sample of the best carrots from each farm showed that similar yields were possible. A sample of 50 carrots per section was taken from each field and the best samples from the controller field and reference farm both had weights of 0.2 kg. The similarities in the best carrot sample weight indicate that without the pest and water quality issues, the total yield of the field with the controller and the reference field could have been similar. If the yield of the field with the controller was the same as the reference farm's yield, the controller field's WUE would have been 8.68 kg/m^3.

Water, Energy, and Yield Comparison in Multiple Contexts

The POWEIr controller exhibited significant savings of 29–44% in total irrigation water use and up to 43% in pumping energy compared to typical drip irrigation practices across diverse settings. Notably, consistent savings were observed across multiple contexts, crop types, soil textures, and levels of automation. The incorporation of an irrigation amount feedback loop enabled the controller to achieve water savings when additional irrigation was applied due to user error, extreme temperatures, or to address observed crop stress.

Water savings were achieved even with manual irrigation in Jordan where the irrigation schedule was not perfectly executed. In fact, Van de Zande [23] showed that the schedule was only followed correctly 49% of the time in Jordan, mostly due to users not being on-site on weekends and holidays. This means that the users in Jordan did not open and close the valves according to the POWEIr controller's schedule over 50% of the time. Yet, the users reported when they opened and closed the valves with 97% accuracy. This indicates that there was a

large amount of user scheduling error in Jordan, but also users reliably reported the irrigation delivered that was fed back into the POWEIr controller. This accurate data feedback allowed the controller to update its calculations and deliver precise irrigation amounts to the crops over the season. Even with the large user scheduling error the POWEIr controller was able to save water and energy compared to typical practice without compromising crop yield.

The POWEIr controller exhibited comparable water and energy savings in Morocco, where automated valves eliminated user scheduling errors. Furthermore, the controller demonstrated robustness in the face of user scheduling errors in Jordan, reinforcing its reliability and versatility across different irrigation management scenarios. The controller's consistent results over various contexts and users with different levels of expertise underscore its adaptability and scalability, proving it to be effective with a potential for widespread adoption.

4.5 Discussion

This chapter met its aims of implementing the POWEIr controller in multiple contexts, validating each level, and assessing overall performance in terms of water usage, energy consumption, and crop yields. The findings demonstrate that the POWEIr controller enhances the benefits of smart and sustainable agriculture technology in resource-constrained settings. With further enhancements, the POWEIr controller holds the potential to broaden access to water- and energy-efficient irrigation technology.

4.5.1 Design for Multiple Contexts

The first aim of the chapter was to describe modifications, customization, and implementation strategies for the POWEIr controller in multiple contexts. Section 4.3.1 identifies necessary design changes for different contexts, which were then implemented on SPDI systems in Morocco and Jordan. Each design was tailored to meet the specific requirements

of the country; for instance, manual valves were used in Jordan, while Morocco utilized automatic valves. Users in Jordan were shown to follow the irrigation schedule correctly only 49% of the time, yet they had 97% accuracy in reporting irrigation delivered [23]. The controller's design to feedback the reported irrigation delivered allowed it to be robust to the high amount of user scheduling error. The POWEIr controller was designed to be adaptable to these various contexts to enable widespread adoption in LMICs. The POWEIr controller provided benefits in terms of water and energy savings for comparable yields in all of these contexts. This means that the POWEIr controller is not only adaptable, but its performance is also repeatable across variations in design and context.

4.5.2 POWEIr Controller's Level 3 Validation

The second aim of the chapter was to validate the POWEIr controller in relevant environments, showing that Level 3 performed as expected. The study verified the Level 3 hypotheses that the solar power prediction error and soil moisture model accuracy would not adversely affect the crops. The mean daily solar energy prediction error was between 31–32%, which did not impact irrigation delivery due to sufficient battery capacity. The soil moisture model was shown to be effective as the controller's θ_v calculations had similar accuracy compared to soil moisture sensors when both were compared to bulk in-field measurements. The controller calculated θ_v had much better accuracy than the soil moisture sensors when the sensors were improperly placed. This indicates that the POWEIr controller's method of calculating soil moisture without sensors could be as good or better than placing a few soil moisture sensors in a field. Adjustments to important crop parameters during experiments, based on field observations, contributed to the POWEIr controller's θ_v accuracy. Additionally, in-field researchers could apply extra irrigation if crop stress was detected. Future work should take into consideration that this level of adjustment may not be intuitive to all farmers who would use the POWEIr controller. Additionally, the study validated the main hypothesis that the POWEIr controller would reduce water and energy

use for comparable yields to typical drip irrigation practice. The subsequent subsection expands on the validation of this performance metric.

4.5.3 POWEIr Controller Performance

The third aim quantified controller performance in terms of water and energy savings without compromising crop yields compared to typical drip irrigation. The POWEIr controller demonstrated savings of 29–44% in total irrigation water volume and up to 43% in pump energy use while maintaining comparable yields. This highlights the controller's potential to enable farmers to achieve adequate crop yields with significantly fewer resources across different crops, climates, and soil textures.

4.5.4 Limitations and Future Work

The experiment presented in this chapter used hardware and techniques that are potentially inaccessible in LMICs. Higher-cost, research-quality controller hardware, including the power and battery monitoring and control, inverter, and MPPT, was implemented to allow for the collection of validation data. Future work will aim to reduce the cost of the POWEIr controller hardware and confirm that similar results to those presented herein can be achieved with affordable hardware. Additionally, the crop parameter inputs used in the experiment were tuned based on local irrigation engineers' and agronomists' advice. Farmers will not have access to expert advice so future iterations of the POWEIr controller must not rely on on-site crop parameter tuning by agronomists. Future work could explore the incorporation of crop image-based feedback with the phone application for easier parameter tuning.

Additional future design considerations were noted during the experiment. Irrigation amounts and fertilizer requirements are closely tied, but fertilizer calculations have not yet been included in the POWEIr controller. Future work should look into the best way to incorporate fertilizer scheduling with the POWEIr controller. This study tested the POWEIr

controller in the MENA region. It has been shown that a tool such as the POWEIr controller could be beneficial not only in MENA but also in East Africa [22]. Future work should explore the implementation of the POWEIr controller in East Africa and if the POWEIr controller would be valuable in any additional markets.

4.5.5 Impact of Results

This chapter demonstrates that the POWEIr controller, with its physics-based models, minimal sensor reliance, and machine learning algorithms, can accurately calculate crop water needs and manage variable energy without compromising crop yields. This presents a promising option for resource-constrained farmers who often over-irrigate due to risk aversion. The POWEIr controller is an affordable and user-friendly solution, increasing accessibility for cost-constrained farmers in the realm of sustainable irrigation. Implementing these findings in addition to progressing the POWEIr controller with planned future work can contribute to making precise irrigation technology even more accessible and beneficial for farmers facing financial constraints.

4.6 Conclusions

To meet the second SDG by 2030, particularly in LMICs, it is imperative to enhance crop production sustainably. Existing sustainable agriculture technologies are cost-prohibitive to farmers in LMICs. Even when these technologies are adopted, they can still be operated unsustainably – unknowingly on the part of the user – to mitigate perceived risks to crop yield. The insights presented in this chapter propose that the POWEIr controller holds promise in assisting farmers in LMICs to curtail their water and energy consumption, fostering sustainable irrigation practices without compromising crop health. The POWEIr controller aims to bolster sustainable operation and increase the adoption of SPDI and precision agriculture technologies in LMICs.

This chapter describes an experimental validation of the POWEIr controller's performance and unveils this controller's potential for water and energy conservation as well as its impact on crop yield on farms in Jordan and Morocco. The results underscore that the POWEIr controller's energy predictions and soil moisture estimates – derived from physics-based models, machine learning algorithms, and measurements by a cost-effective weather station – maintained a level of accuracy that did not adversely affect crop yields while reducing water and energy use. The implementations of the POWEIr controller demonstrated reductions in water usage by up to 44% and up to 43% decline in pump energy consumption compared to conventional drip irrigation practices on similar farms.

The POWEIr controller was validated on small-scale farms over four crop seasons in various LMIC contexts, encompassing diverse crop and soil types, to ensure its performance is generalizable and repeatable. This validation, coupled with ongoing efforts to test economical iterations of the controller, is poised to establish the POWEIr controller's consistent performance. Disseminating news of the controller's benefits holds the potential to catalyze increased adoption among farmers in LMICs. By enhancing the accessibility of this economical, sustainable, and precise irrigation technology, the POWEIr controller could empower farmers in LMICs to grow more food while utilizing fewer water and energy resources. Ultimately, the POWEIr controller's aims align with meeting the second SDG, to end hunger.

Chapter 5

Conclusions

5.1 Concluding Insights and Impact of the Current Research

This thesis introduces and evaluates the Predictive Optimal Water and Energy Irrigation (POWEIr) controller, a cost-effective and precise irrigation controller that effectively lowers the barrier to sustainable water and energy technology. The key research contributions can be summarized as follows:

- In Section 2.2, a comprehensive cost analysis revealed a potential 18–74% reduction in the lifetime cost of SPDI pump and power systems. This resulted in irrigation delivery improvements ranging from 31–66%, surpassing the performance of existing commercial sizing tools through innovative modeling and operational adjustments.
- Sections 2.3 and 2.4 outlined the theoretical foundation of the POWEIr controller and presented an initial prototype. The prototype demonstrated a 46% increase in solar irrigation reliability compared to simulated typical operations. Furthermore, it delivered the required irrigation while using six times less battery capacity.
- Chapter 3 explored the sensitivity of POWEIr's optimized irrigation schedules to errors

in agronomy inputs and weather data. The findings suggested an 83% reduction in weather sensor costs with negligible simulated effects on multiple crop yields, underscoring the system's adaptability and cost efficiency.

- Chapter 4 validated the POWEIr controller's performance in real-world settings in Jordan and Morocco. The results showcased notable resource reductions—up to 43% in pumping energy and 44% in water usage—for comparable crop yields when compared to local farmer practices.

Publications based on these contributions are in preparation [25], [75], [108]. The POWEIr controller emerges as a promising solution, not only in terms of economic viability but also in delivering enhanced efficiency and sustainability in irrigation practices.

5.2 Recommended Future Work

The next steps for the POWEIr controller are instrumental in paving the path for commercialization. In order for the POWEIr controller to be a commercial product some design changes are necessary, informed by lessons learned from prototypes and implementation on real farms. Specifically:

1. The experimental prototype of the POWEIr controller used high-cost hardware and relied on some expert advice that would be inaccessible to more farmers in LMICs. Future iterations of the POWEIr controller should use lower-cost controller hardware, including the power and battery monitoring and control, inverter, and MPPT. Future work should aim to reduce the cost of the POWEIr controller hardware and confirm that similar results to those presented herein can be achieved.

2. The current POWEIr controller objective for optimizing irrigation schedules does not include farm labor costs. Future versions of the POWEIr controller should include

farm labor costs to minimize the total time that the user spends each day enacting the irrigation schedules.

3. Irrigation scheduling and application of fertilizers are closely linked. Future versions of the POWEIr controller should include fertilizer recommendations as part of the irrigation scheduling, meaning a fertilizer model should be incorporated into the POWEIr controller. This could also help inexperienced farmers and help reduce fertilizer pollution due to mismanagement.

4. Currently the POWEIr controller's reference evapotranspiration is calculated on a daily basis, based on daily average, minimum, and maximum weather conditions. A single crop coefficient is used for calculating crop evapotranspiration. This is then used in the soil water balance, which is also calculated daily. There are models to calculate reference evapotranspiration on a sub-daily basis. Also, the use of a dual crop coefficient is stated to be more accurate than the single crop coefficient, especially for micro-irrigation. It could be worthwhile to explore using the hourly reference evapotranspiration calculations and dual crop coefficient to explore the trade-off between the added input complexity and the benefit to model accuracy.

5. Methods to reduce the prediction errors should be considered. This could mean incorporating other machine learning algorithms to make the predictions. Additionally, for versions of the controller that use automated valves, it could be possible to do profile matching in real-time instead of sending a schedule in advance.

6. This work showed that local calibration of the crop coefficient could be needed for some farms using the POWEIr controller. Future work should explore creating an easy-to-use tool that will allow farmers to do these calibrations themselves. One direction that could be explored is tracking crop growth and any crop stress with image processing techniques. Then farmers could take images of their crops periodically and the agronomy inputs, including the crop coefficient, could be updated based on the information

in these images.

7. The POWEIr controller has been designed for use in farming practices in arid, LMICs, but affordable, precise irrigation could be used in other markets. For example, there could be a need for the POWEIr controller in smart building water and energy management, landscaping, and home gardens. The use of the POWEIr controller in these additional markets should be explored.

Appendix A

Chapter 2 Supplemental Information

A.1 SDrOP Cost Data

Table A.1 shows the SDrOP model's cost inputs that were used in the cost analysis in Section 2.2. These numbers were obtained while working with the local research partners and contractors.

Table A.1: SDrOP Local Economic Parameters.

Parameter	**Definition**	**Unit**	**Value**
k_{cp}	Crop price coefficient	-	0.605
k_i	Installation coefficient	-	0.11
IR	Interest rate	-	0.035 [126]
FR	Inflation rate	-	0.02 [126]
k_m	Maintenance coefficient	-	0.009
UC_{pump}	Pump unit cost	$\left[\frac{\text{USD}}{\text{kW}}\right]$	450
UC_{pv}	Panel unit cost	$\left[\frac{\text{USD}}{\text{m}^2}\right]$	152
UC_{batt}	Battery unit cost	$\left[\frac{\text{USD}}{\text{kWh}}\right]$	350
UC_{tank}	Tank unit cost	$\left[\frac{\text{USD}}{\text{m}^3}\right]$	170
m_{inv}	Inverter Linear Coefficient	$\left[\frac{\$}{\text{W}}\right]$	0.28 [51]
b_{inv}	Inverter Linear Constant	[$]	0 [51]
m_{MPPT}	MPPT Linear Coefficient	$\left[\frac{\$}{\text{W}}\right]$	0.0632 [52]
b_{MPPT}	MPPT Linear Constant	[$]	10 [52]
m_{VFD}	VFD Linear Coefficient	$\left[\frac{\$}{\text{W}}\right]$	43.1 [53]
b_{VFD}	VFD Linear Constant	[$]	142 [53]

A.2 Solar-Powered Drip Irrigation Optimal Performance Model (SDrOP) Operation Simulation

This section is copied from Grant, Sheline, Sokol, *et al.* [36] to provide context on how the SDrOP model's operation simulation works.

The operation simulation is a logic loop that calculates where energy and water will flow for each time step of the irrigation season. Every time step is simulated with historical weather. This allows for the performance of a design to be evaluated in terms of how much of the crop water demand it can deliver. There are four different energy paths that can be taken to deliver water to the crops and two paths to store energy. These six paths are illustrated in Fig. A.1a.

Within the logic loop the irrigation demand, or the amount of water the irrigation system must deliver to meet the crop water demand, is calculated at the start of each day in m^3 by rearranging the soil water balance defined in the FAO Irrigation and Drainage Paper No. 56 [63] as

$$I_{dem,n} = f_w \, A_{field}(D_{r,n-1} - Pr_n + RO_n - RAW_n + ET_{c,n})/1000. \tag{A.1}$$

Here, the soil water level is set to the minimum needed to not stress the crop ($D_{r,n} = RAW_n$), n is the day of the irrigation season, D_r is the water lost to the root zone of the crop, or the root zone depletion [mm], Pr is precipitation [mm], RO is runoff [mm], f_w is the soil wetted fraction (which is set to 0.3 for drip irrigation [63]), and A_{field} is the field area [m^2]. RAW is the readily available water [mm], or the amount of water in the root zone that the plant can uptake most efficiently. This soil water balance assumes a deep groundwater table, so there is no capillary rise, it neglects deep percolation, and $I_{dem,n}$ is calculated such that the $D_{r,n}$ is at RAW_n and $D_{r,n-1}$ is at the $D_{r,n}$ of the previous day. RAW_n is defined as

$$RAW_n = d_n \, TAW, \tag{A.2}$$

(a) Energy and water flow diagram

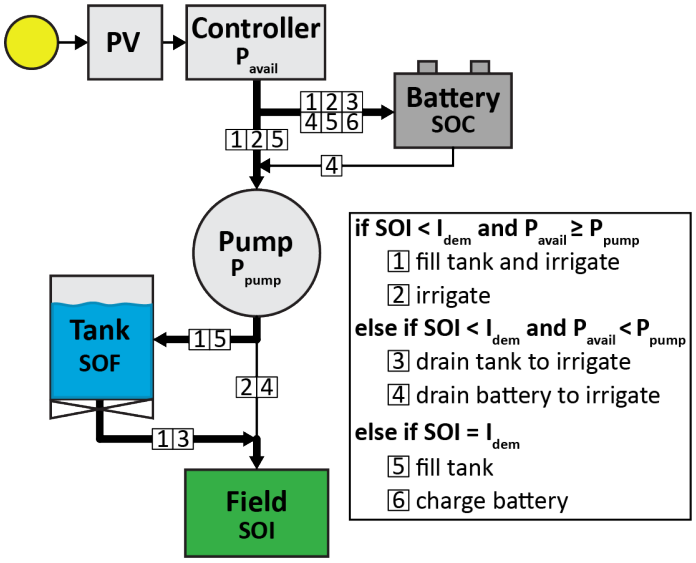

(b) Power and state variables for two days of operation

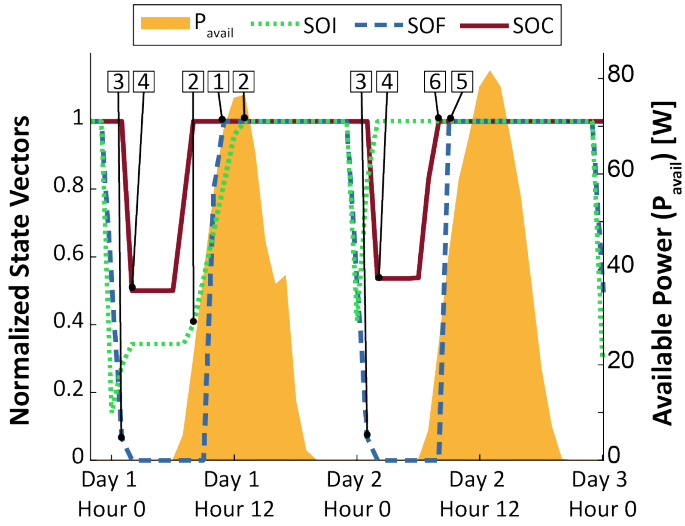

Figure A.1: An illustration of the logic flow loop and representation of the simulated system operation. In **a** the energy and water flow diagram is shown. There are six flow paths of energy connecting the photovoltaic (PV) system (power, P_{PV}), controller (power, P_{avail}), battery, pump (power, P_{pump}), water storage tank, and field. The arrowed connections corresponding to each of the energy paths are designated by numbers 1-6 (e.g., the first path is made up of all the connections labeled with a 1 and path 1 is bolded as an example). As described in the boxed conditional statement, flow paths are checked in numbered order at each time step and activated based on the weather-dependent available power (P_{avail}) and the state of the battery, tank, and irrigation of the field, designated as the state of charge (SOC), state of fill (SOF), state of irrigation (SOI), and irrigation demand (I_{dem}). In **b** the power values and normalized SOC, SOF, and SOI for two days of operation on a representative small field illustrate the conditions under which each flow path might be activated.

where TAW is the total available water that the crop can extract from the soil [mm], a constant that depends on the depth of the crop roots and soil properties defined in the Case Definition. The depletion fraction on day n, d_n, is calculated as

$$d_n = d_{const} + 0.04\,(5 - ET_{c,n}), \tag{A.3}$$

where d_{const} is the constant crop dependant depletion fraction assuming $ET_c = 5mm/day$.

The available power is calculated throughout the day as

$$P_{avail,i} = P_{PV,i}\,\eta_{MPPT}\,\eta_{conv}\,A_{PV}, \tag{A.4}$$

where i is the sub-daily time interval indices (dependent on the resolution of the input weather data), $\eta_{MPPT} = 98\%$ and $\eta_{conv} = 95\%$ are the assumed efficiencies for the MPPT unit and the electrical converter, and A_{PV} is the solar panel area for the system design [m^2].

$P_{avail,i}$ can go towards charging the battery or powering the pump (P_{pump}), and water from the pump can go towards filling the tank or irrigating the crops on the field. State vectors, namely the state of charge (SOC) of the battery [Wh], state of fill (SOF) of the tank [m^3], and state of irrigation (SOI) of the field [m^3], are calculated in the operation logic loop to keep track of where energy and water are used or stored at each time interval.

Before the irrigation demand is met, the time remaining to irrigate [s], t_{ri}, is calculated as

$$t_{ri,i} = min\left(\frac{I_{dem,n} - SOI_{i-1}}{Q_{sys}}, \Delta t\right), \tag{A.5}$$

where Δt is the time interval. The calculation of t_{ri}, and other time variables, allows for other paths to be used during the same time step once a state vector is filled. Note that SOI is initialized at zero and is set to zero at the start of each day.

The conditions required to select each flow path are checked in order, following a fixed operation priority as depicted in the boxed conditional statement in Fig. A.1a. If the

irrigation demand has not been met, the first check is if there is enough $P_{avail,i}$ to deliver water through path 1. Path 1 fills the tank and irrigates at the same time. During this path, the time to fill the tank, t_{tf} [s], is calculated as

$$t_{tf,i} = \min\left(\frac{C_{tank} - SOF_{i-1}}{Q_{tank,i} - Q_{sys}}, t_{ri,i}\right), \tag{A.6}$$

where C_{tank} is the tank capacity [m^3] and Q_{tank} is the flow rate from the pump going into the tank [m^3/s] (details of the tank flow rate calculation are provided in the SI section 3). The state equations for path 1 are

$$SOI_i = SOI_{i-1} + Q_{sys}\, t_{ri,i}, \tag{A.7}$$

$$SOF_i = SOF_{i-1} + (Q_{tank,i} - Q_{sys})\, t_{tf,i}, \tag{A.8}$$

and

$$SOC_i = SOC_{i-1} + (P_{avail,i} - P_{pump,i})\, t_{tf,i}. \tag{A.9}$$

Figure A.1b illustrates the relative state of $P_{avail,i}$, SOC, SOF, and SOI corresponding to each of the flow paths over a period of two days. For example, path 1 is selected mid-way through day one when there is sufficient $P_{avail,i}$, $SOF < 1$, and $SOI < 1$.

If there is not enough $P_{avail,i}$ to complete path 1, the next check is if there is enough $P_{avail,i}$ to irrigate the field directly through path 2. The state equations for path 2 are Eq.A.7, as well as

$$SOF_i = SOF_{t-1} \tag{A.10}$$

and

$$SOC_i = SOC_{i-1} + (P_{avail,i} - P_{pump})\, t_{ri,i}. \tag{A.11}$$

If there is not enough P_{avail} for path 1 or 2, there is not enough power from the panels

to directly deliver water to the field. If the irrigation demand is still not met, the tank and the battery storage are checked. The time to drain the tank, t_{tdt} [s], and the time to drain battery, t_{tdb} [s], are calculated as

$$t_{tdt,i} = min\left(\frac{0 - SOF_{i-1}}{Q_{tank,i} - Q_{sys}}, t_{ri,i}\right) \tag{A.12}$$

and

$$t_{tdb,i} = min\left(\frac{0.5C_{batt} - SOC_{i-1}}{P_{avail,i} - P_{pump,i}/\eta_{batt}}, t_{ri,i}\right), \tag{A.13}$$

where C_{batt} is the battery capacity [J], $\eta_{batt} = 85\%$ is the assumed battery efficiency, and the maximum depth of discharge for the battery is set to 50%. If the tank or battery are already at their minimum capacities then t_{tdt} and t_{tdb} are zero and pathways $\boxed{3}$ and $\boxed{4}$ are not used.

If there is enough water stored in the tank, path $\boxed{3}$ is used with the state equations

$$SOI_i = SOI_{i-1} + Q_{sys}\, t_{tdt,i}, \tag{A.14}$$

$$SOF_i = SOF_{i-1} - Q_{sys}\, t_{tdt,i}, \tag{A.15}$$

and

$$SOC_i = SOC_{i-1} + P_{avail,i}\, t_{tdt,i}. \tag{A.16}$$

If there is enough energy stored in the battery, path $\boxed{4}$ is used with state equations including Eq. A.10, as well as

$$SOI_i = SOI_{i-1} + Q_{sys}\, t_{tdb} \tag{A.17}$$

and

$$SOC_i = SOC_{i-1} + (P_{avail,i} - P_{pump}/\eta_{batt})\, t_{tdb}. \tag{A.18}$$

If there is not enough power or energy storage to run the other paths, or the irrigation

demand for the day has already been met, the SOI_i is set to SOI_{i-1}. The loop checks if the tank and battery are full, and if not, it tries to fill them using paths [5] and [6], respectively. For path [5], the t_{tf} is updated as

$$t_{tf} = min\left(\frac{C_{tank} - SOF_{i-1}}{Q_{tank,i}}, \Delta t\right). \tag{A.19}$$

The state equations to fill the tank for path [5] are

$$SOF_i = SOF_{i-1} + Q_{tank,i}\, t_{tf} \tag{A.20}$$

and

$$SOC_i = SOC_{i-1} + (P_{avail,i} - P_{tank,i})\, t_{tf}. \tag{A.21}$$

The system uses any remaining power to charge the battery through path [6]. The state equations are Eq. A.10 and

$$SOC_i = SOC_{i-1} + P_{avail,i}\, \Delta t. \tag{A.22}$$

For all the paths, any extra power is used to charge the battery until the battery is fully charged. If there is any extra power after path [6] and the battery is fully charged, the power is unused.

The operation is defined such that any energy storage is drained to irrigate at the start of each day and later filled when there is enough solar energy available. For example, in Fig. A.1b at the start of both days the irrigation demand has not been met but there is no solar power available yet, so paths [3] and [4] are used to irrigate, draining the energy storage. Towards the middle of each day, once there is enough P_{avail}, the simulation uses paths [1] and [2] to irrigate and fill the energy storage if the irrigation demand has not yet been met (day one) or it uses paths [5] and [6] to fill the energy storage if the irrigation demand has already been met (day two).

At the end of each day, the daily amount of irrigation that has been delivered [m^3] by the system, I_{del}, is determined as

$$I_{del,n} = SOI_{i,end}, \tag{A.23}$$

where i, end is the last time interval of the day. The adjusted crop evapotranspiration, ET_a, in mm and D_r are calculated at the end of the day as

$$ET_{a,n} = K_{s,n}\, ET_{c,n} \tag{A.24}$$

and

$$D_{r,n} = D_{r,n-1} - Pr_n + RO_n - I_{del,n} + ET_{a,n}, \tag{A.25}$$

where D_r is constrained such that $0 \leq D_{r,n} \leq TAW$ and K_s is the water stress coefficient which accounts for the water stress felt by the crop. If D_r is less than or equal to RAW, then $K_s = 1$. If the D_r is greater than RAW, then K_s is calculated as

$$K_{s,n} = \frac{TAW - D_{r,n}}{(1 - d_n)\, TAW}. \tag{A.26}$$

The operation simulation defines the relationship between the crop irrigation demand and the irrigation that can be delivered by the specified system design. The system performance affects crop water stress through ET_a, and in turn the crop growth and yield, as well as the system reliability.

A.3 Additional Experimental Prototype Results

Figures A.2 to A.6 show the power profiles for the five test days not shown in Section 2.4.2. The figures show the state of charge (SOC) of the battery (blue) as well as the power used by other system components: solar (orange), pump (grey), battery charge (green), battery discharge (red). The figure also shows the Level 3 (L3) predictions (solid), Level 2 (L2) optimal points (asterisks), measured data from the POWEIr controller (lines), and single section operation (SSO) reference data (dashed line). The SSO reference data was simulated to represent how a farm with PVDI but without the POWEIr controller would have traditionally been operated, irrigating a single section at a time.

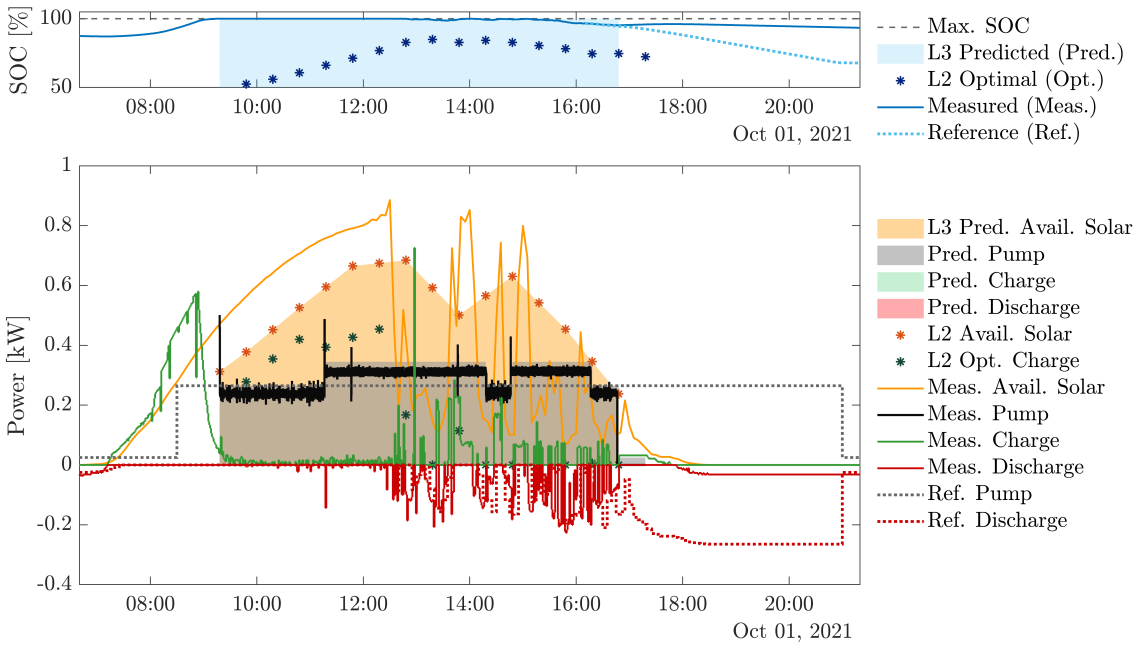

Figure A.2: The power profiles for October 1, 2021.

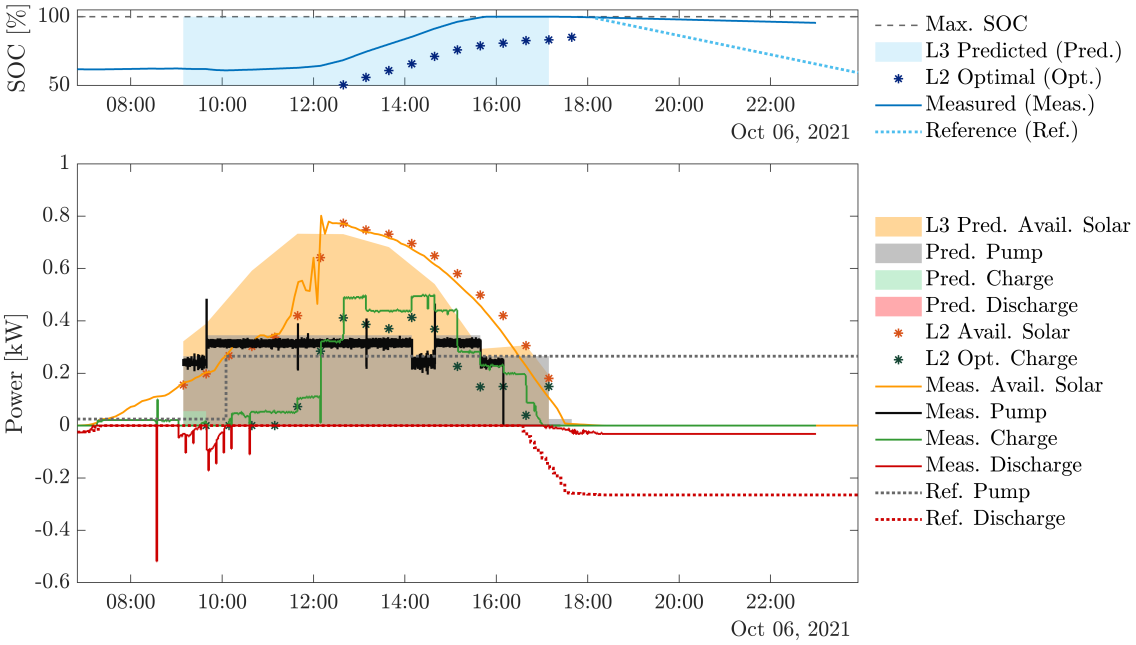

Figure A.3: The power profiles for October 6, 2021.

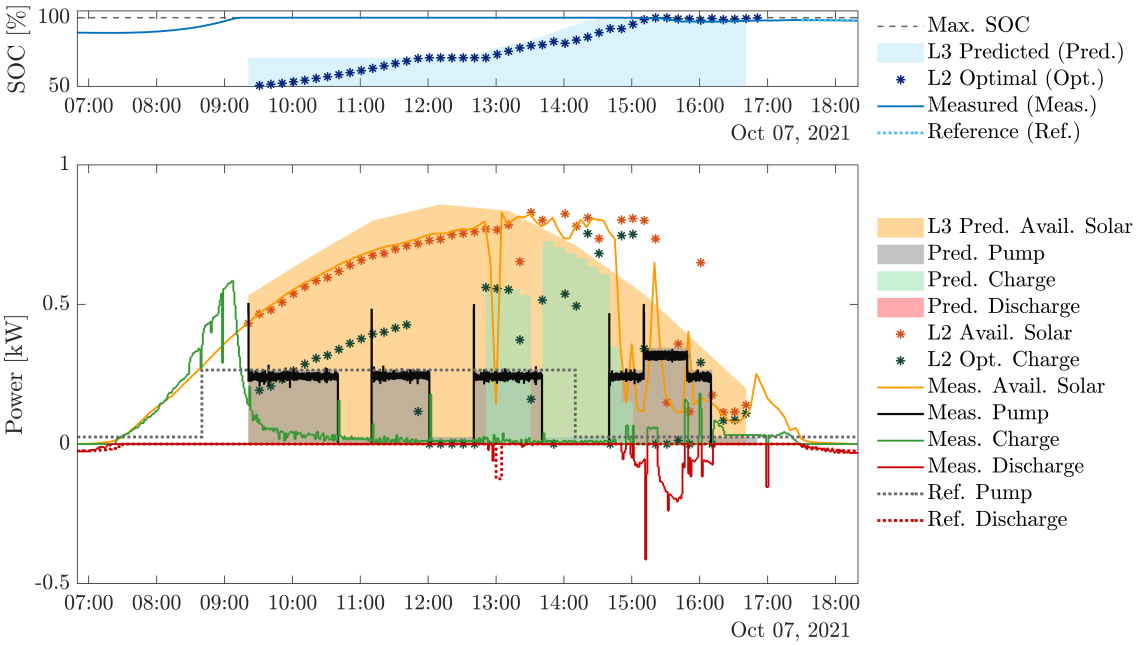

Figure A.4: The power profiles for October 7, 2021.

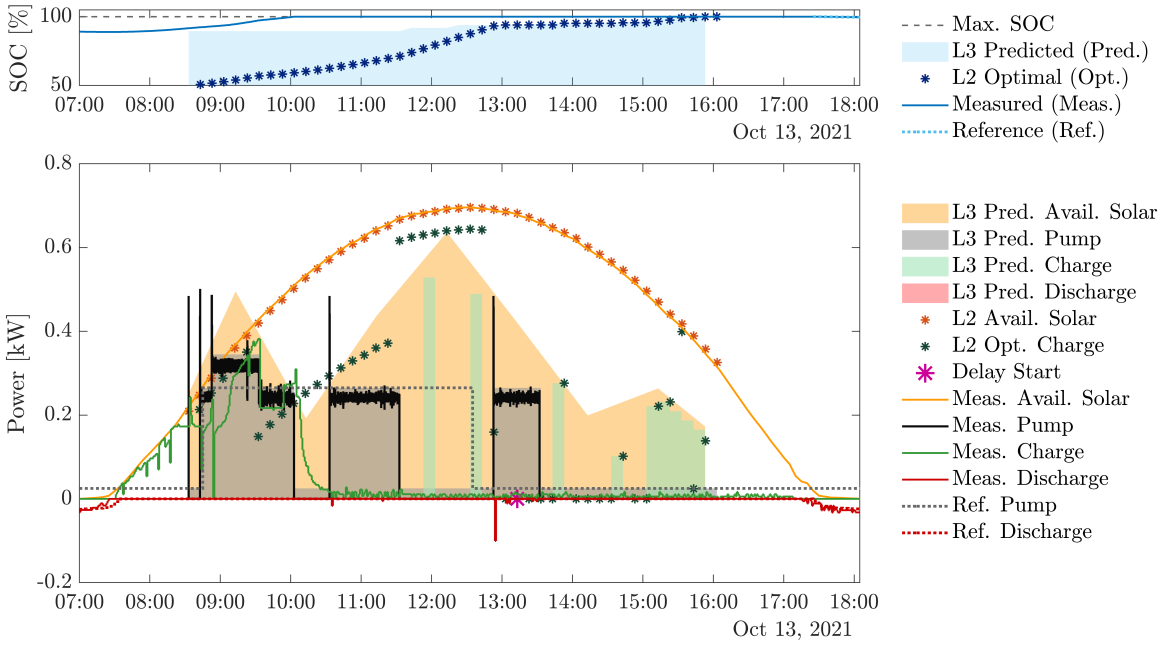

Figure A.5: The power profiles for October 13, 2021.

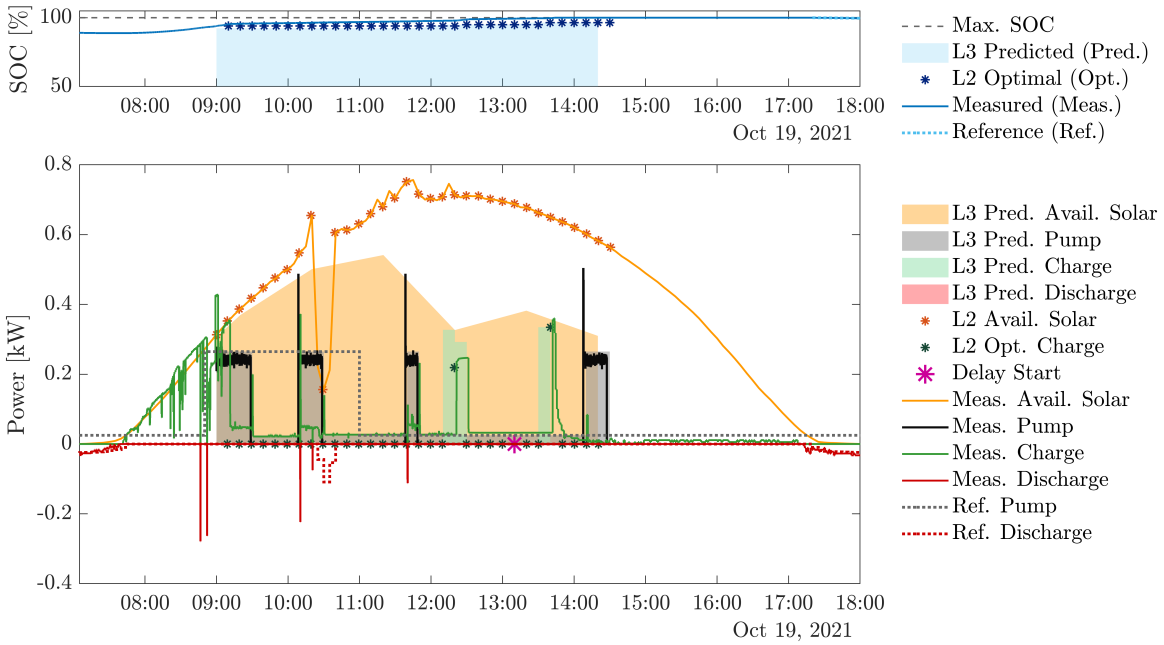

Figure A.6: The power profiles for October 19, 2021.

Appendix B

Chapter 3 Supplemental Information

B.1 Kenya and Morocco Soil Texture

The soil texture for Kenya and Morocco was determined using Python and ArcGIS. First, raster maps were created for Kenya and Morocco of the percentage of sand, silt, and clay in the subsoil (30 to 100 cm depth) for land area that was at least 50% cropland [127]. Then, code was developed to translate the percent sand, silt, and clay rasters to soil textures based on the commonly used USDA soil texture classification triangle equations [128]. Histograms of the soil texture were plotted for Kenya, Figure B.1, and Morocco, Figure B.2.

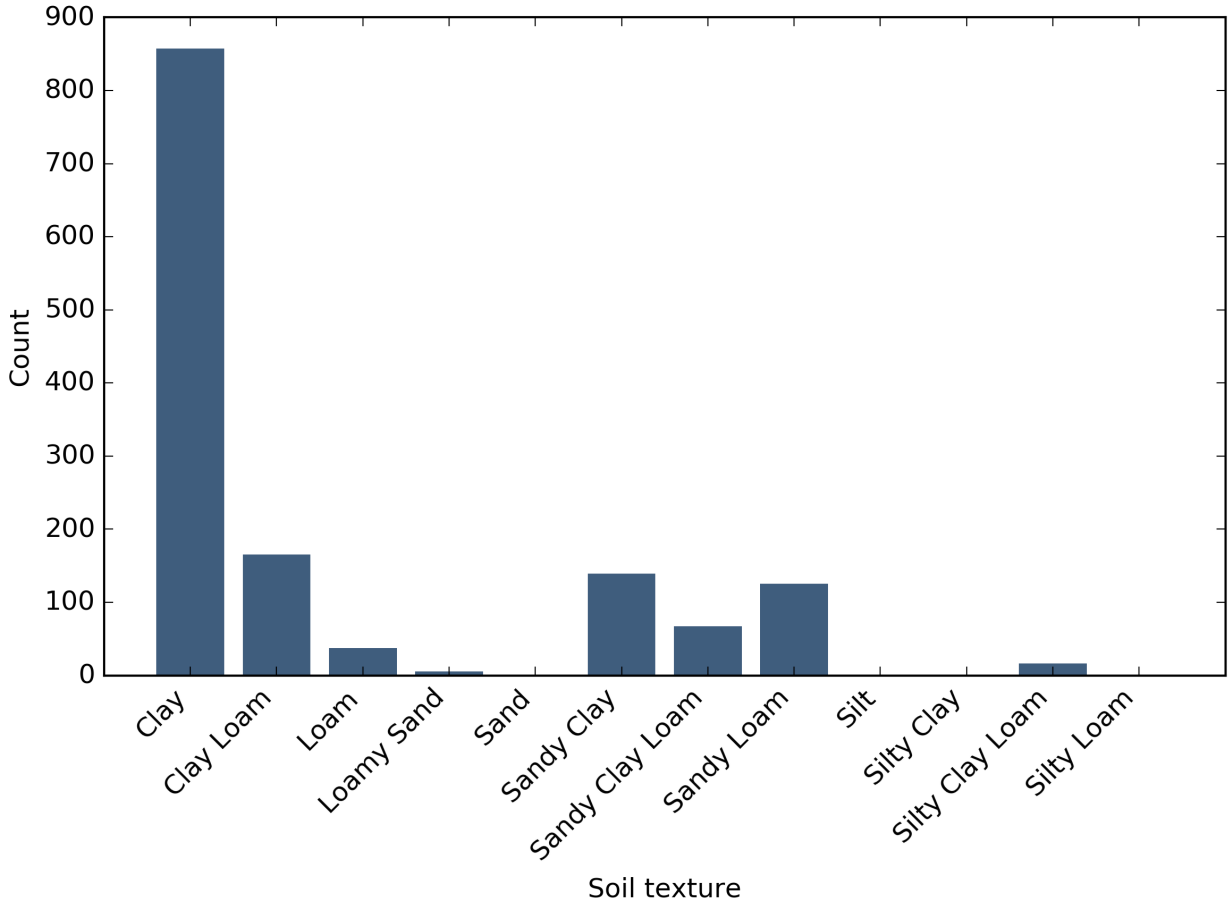

Figure B.1: Kenya soil texture histogram.

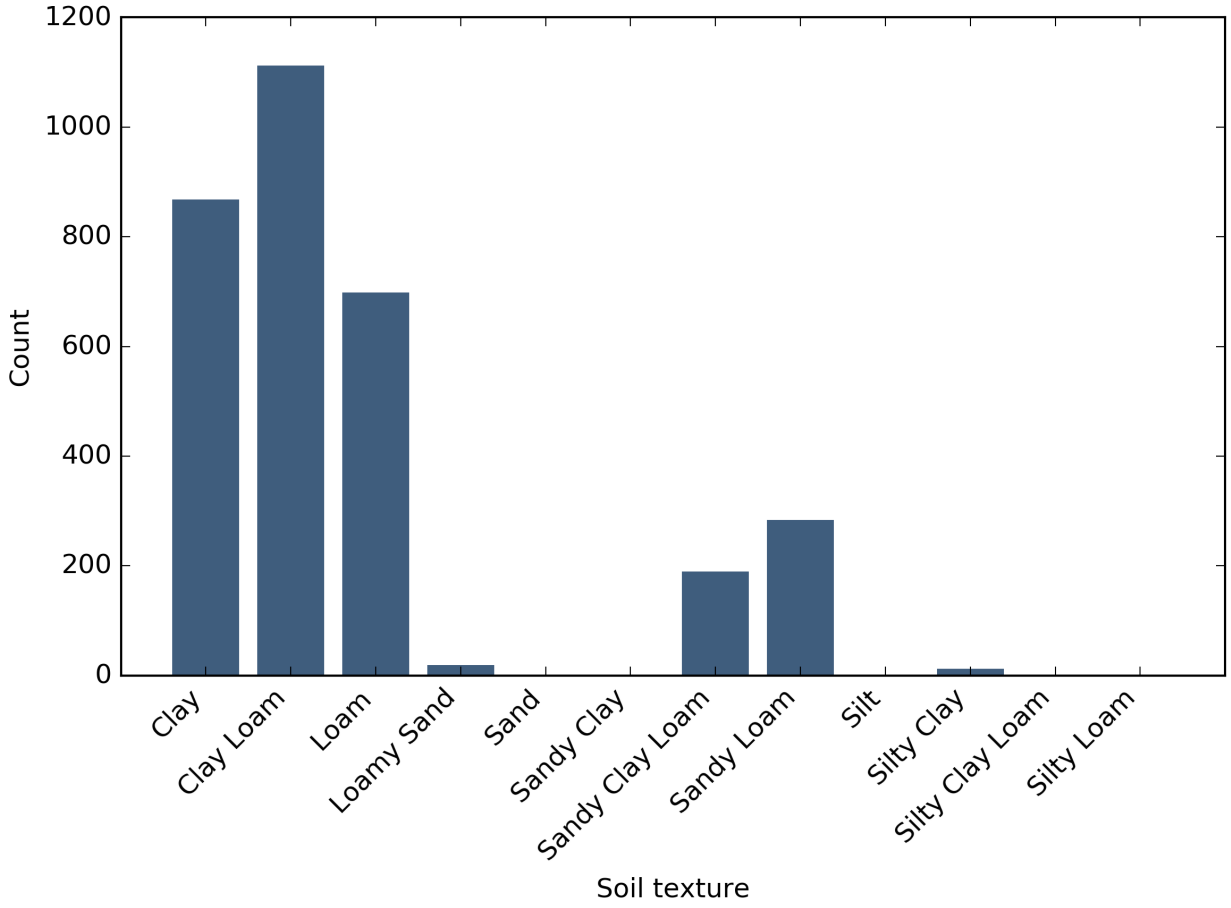

Figure B.2: Morocco soil texture histogram.

B.2 Measured Weather Data and Predictions

The measured and predicted weather parameters used in the weather prediction model are shown in Figures B.3 to B.5. The daily parameters are the average, minimum, and maximum air temperatures, average wind speed, average, minimum, and maximum relative humidity, total rain, total solar radiation, number of sunlight hours, and total reference evapotranspiration. The 'Measured' parameters were calculated using weather data from the high-cost weather station (HCWS) and low-cost weather station (LCWS). The 'Predicted' parameters came from the machine learning models trained using the HCWS or LCWS data. The normalized root mean square error (NRMSE) for all of the weather parameters are shown in Figure B.6.

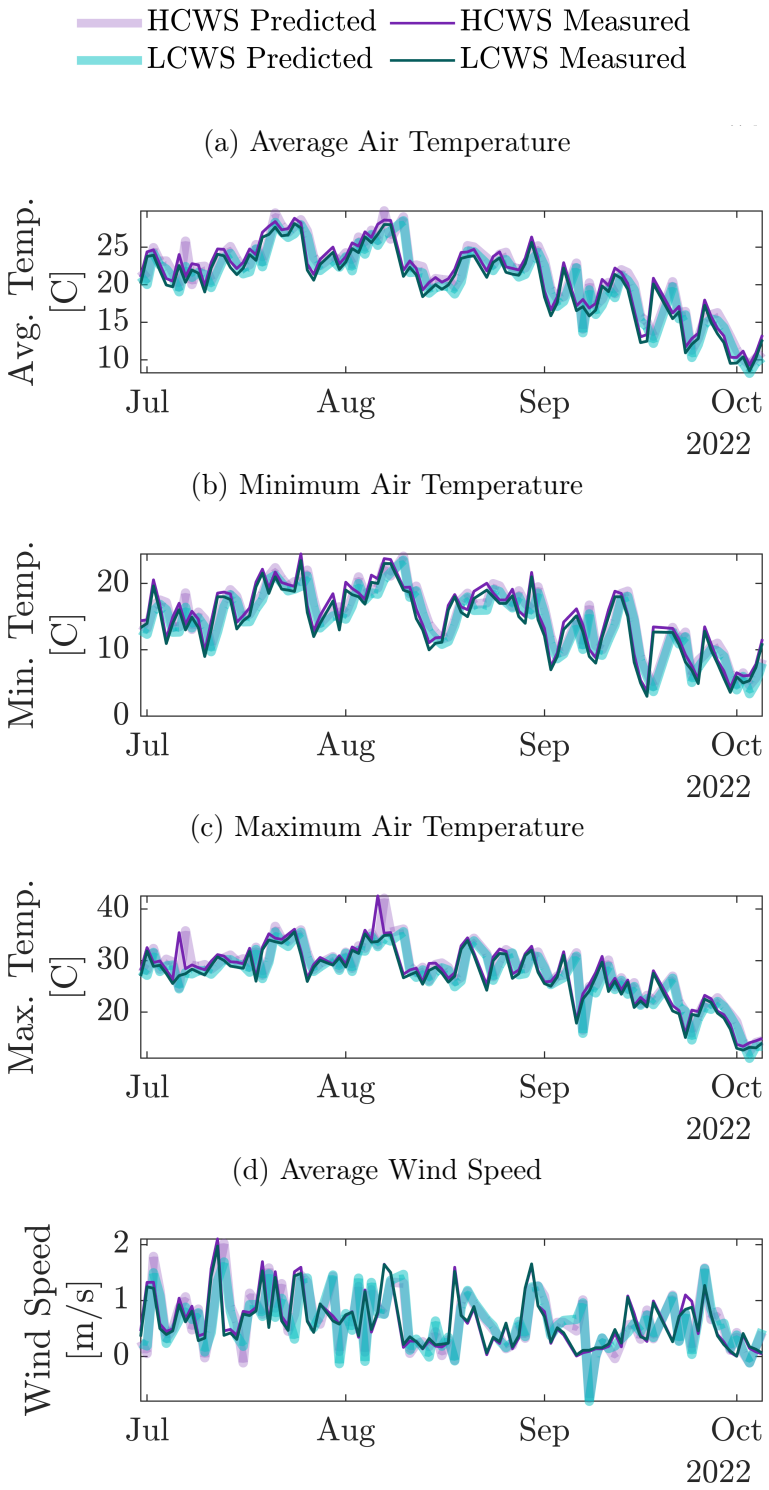

(a) Average Air Temperature

(b) Minimum Air Temperature

(c) Maximum Air Temperature

(d) Average Wind Speed

Figure B.3: Measured and predicted weather parameters used in the daily weather prediction model.

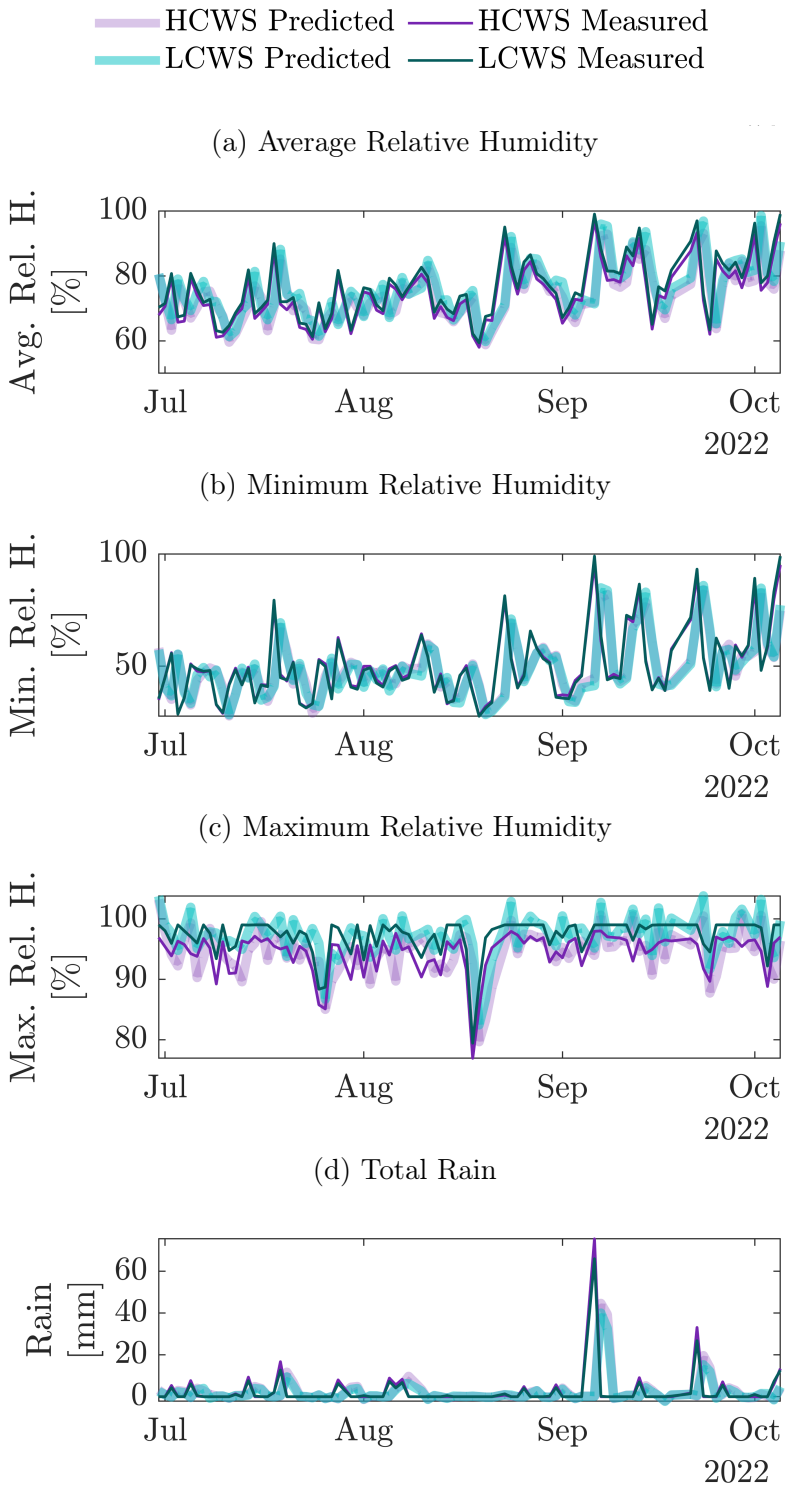

(a) Average Relative Humidity

(b) Minimum Relative Humidity

(c) Maximum Relative Humidity

(d) Total Rain

Figure B.4: Measured and predicted weather parameters used in the daily weather prediction model.

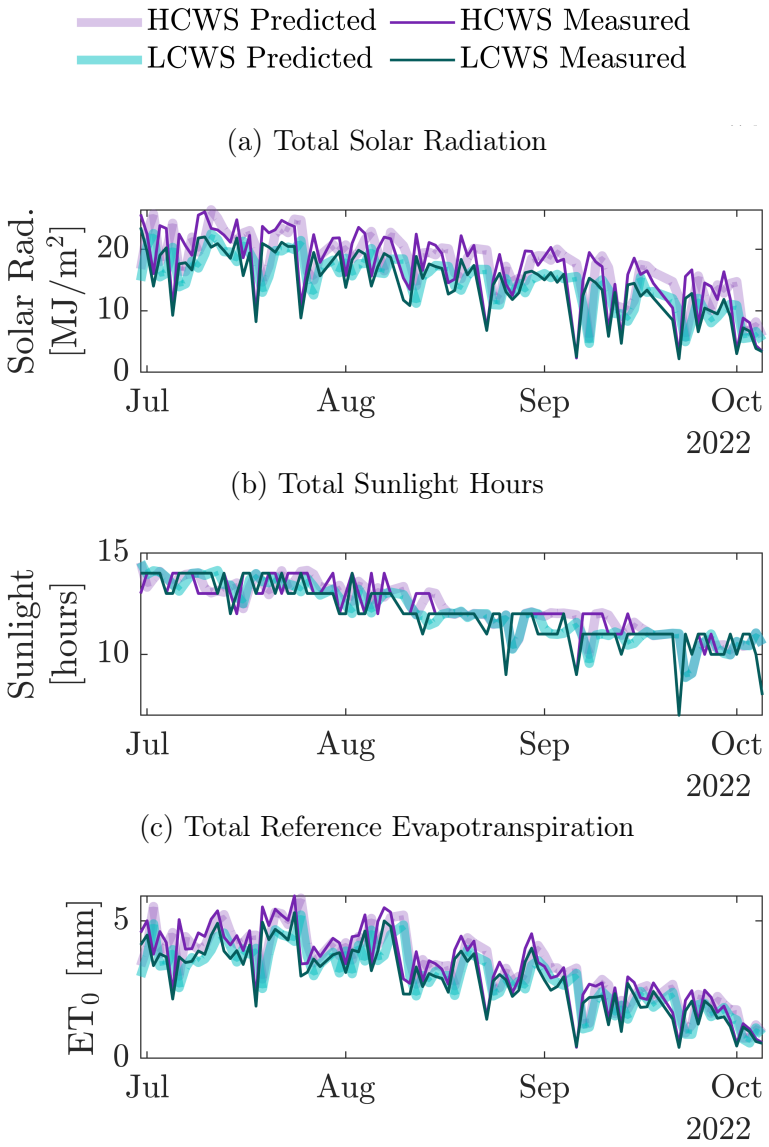

Figure B.5: Measured and predicted weather parameters used in the daily weather prediction model.

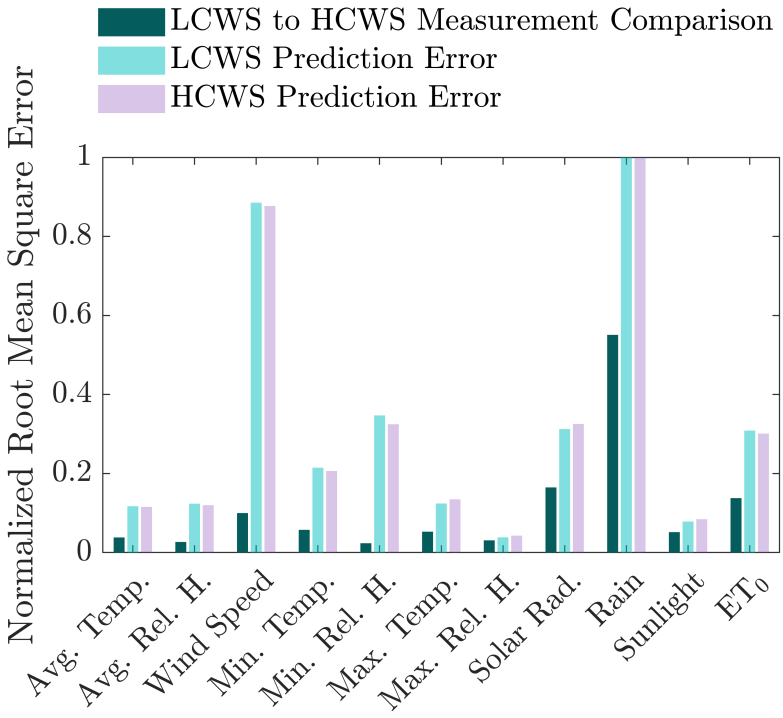

Figure B.6: Normalized root mean square error (NRMSE) in measured and predicted weather parameters.

B.3 Histograms of Weather Error

Histograms of the RMSE for the daily reference evapotranspiration and rain and the hourly solar power are shown in Figures B.7, B.8, and B.7, respectively. The RMSE histograms are shown comparing the LCWS to the HCWS measurements (dark aqua), the LCWS predicted to the LCWS measured (light aqua), and the HCWS predicted to the HCWS measured (purple).

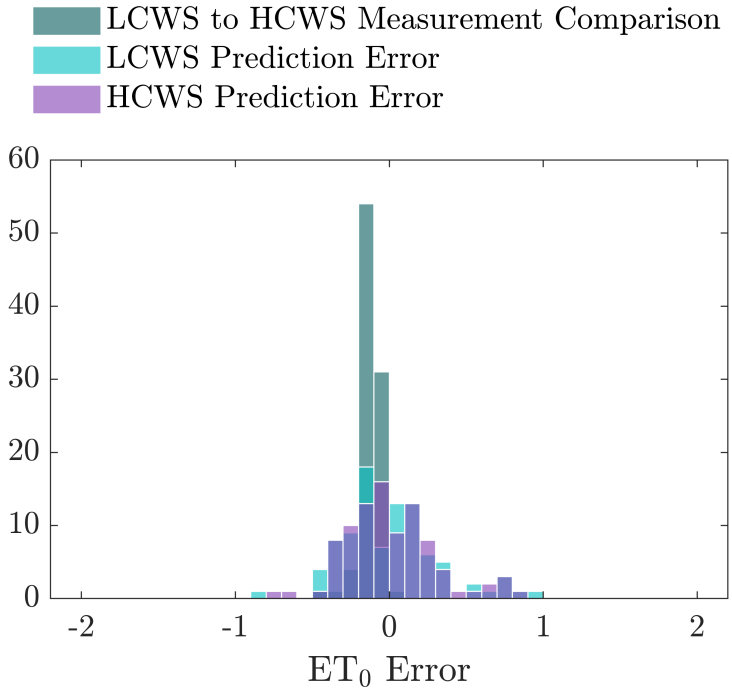

Figure B.7: Reference evapotranspiration error histogram.

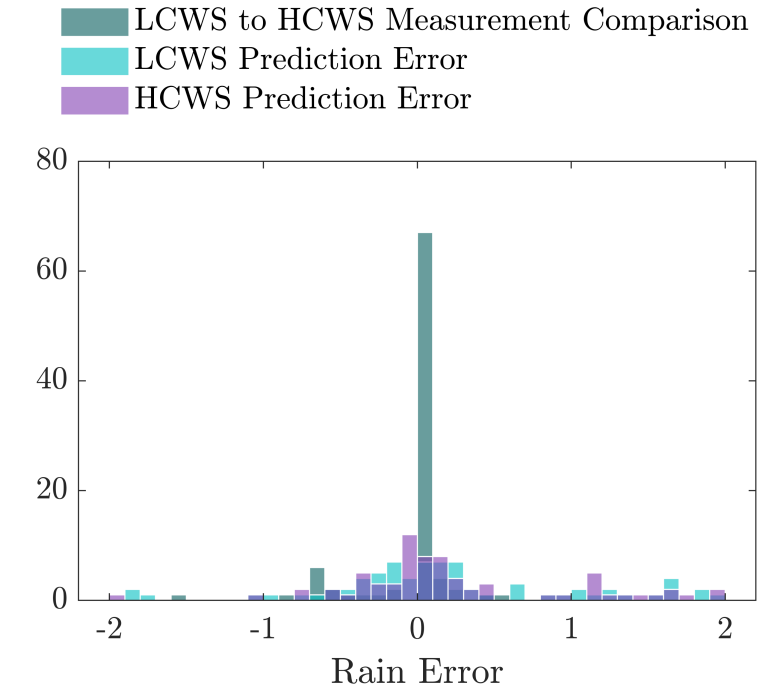

Figure B.8: Rain error histogram.

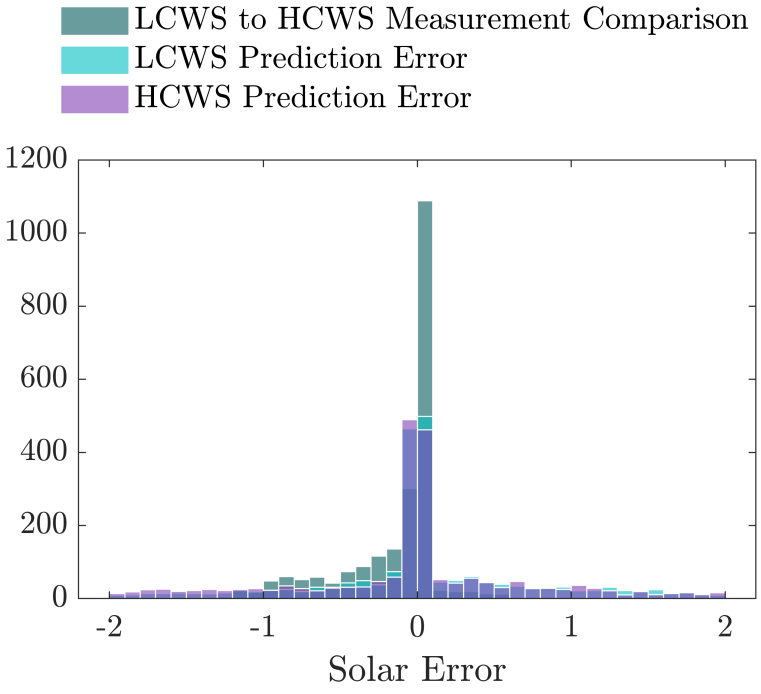

Figure B.9: Solar power error histogram.

B.4 Input Curves of Crop Parameter Sensitivity Study

The scaled input curves used to create Figure 3.6 are shown in Figure B.10. The scaled input curves are based on the tomato crop default curves. Default curves for tomato, potato, and maize that were used to create Figure 3.5 are also shown.

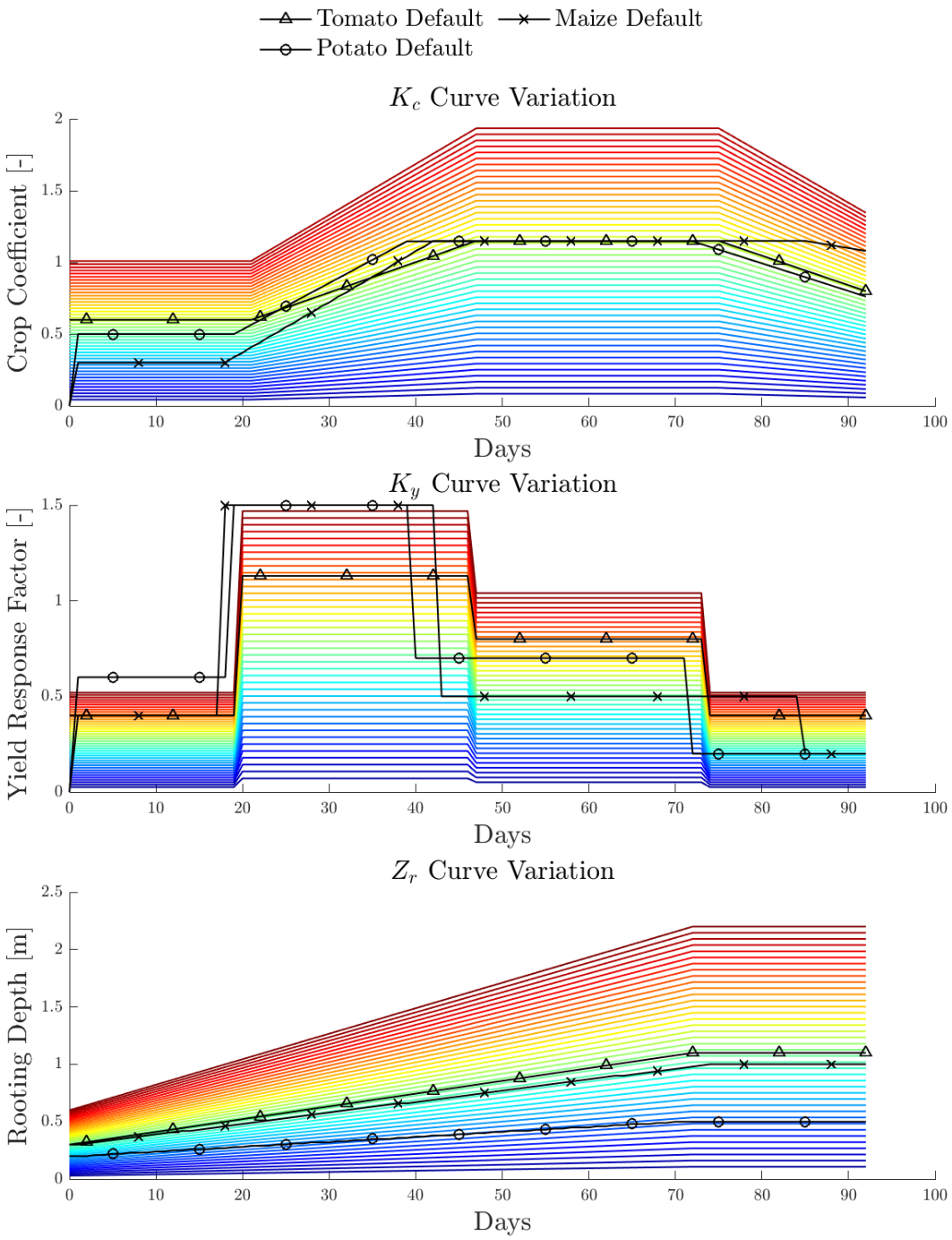

Figure B.10: Input curves for testing sensitivity to irrigation and yield to crop parameters. The black line shows the default (un-scaled) curve for tomato, potato, and maize. The scaled curves (rainbow lines) are based on the tomato default.

Appendix C

Chapter 4 Supplemental Information

C.1 Experimental Setup and Inputs

The experimental setup details are shown in Table C.1. The inputs to the POWEIr controller used in the experiment are shown in Table C.2. The methods for how these values were obtained are described in Section .

Table C.1: Experimental Setup Details.

	Irbid, Jordan		**Agadir, Morocco**	
	Controller	**Reference**	**Controller**	**Reference**
Valve Operation	Manual	Manual	Automatic	Manual
Irrigation Schedule	POWEIr optimization	Local farmer rec.	POWEIr optimization	Farmer observation/ experience
Elec. Input	Solar	Grid	Solar	Solar
Farm Type	Half of research station	Half of research station	Research station	Medium-to-small farm, sell at local market
Crops	Okra + grape	Okra + grape	Potato; carrot	Potato; carrot
Time Frame	May-Dec 2023	May-Dec 2023	Jan-June 2023; July-Nov 2023	Jan-June 2023; July-Nov 2023
Soil Texture	Loam, Sandy Clay	Loam, Sandy Clay	Sandy Loam	Sandy Loam
Field Size	0.5 ha	0.5 ha	0.6 ha	0.6 ha
Number Sections	6	6	6	4

Table C.2: Experimental Inputs for the POWEIr controller.

Input	**Jordan, grape**	**Jordan, okra**	**Morocco, potato**	**Morocco, carrot**
soil texture	Loam and Sandy Clay	Loam and Sandy Clay	Sandy Loam	Sandy Loam
$K_{c[ini,mid,late]}$	[0.3, 0.7, 0.54]	[0.46, 1.03, 0.7]	[0.4, 0.96, 0.68]	[0.6, 1, 0.9]
$Z_{r[min,max]}$	[0.4, 1.1]	[0.2, 0.9]	[0.2, 0.63]	[0.1, 0.65]
$K_{y[ini,dev,mid,late]}$	[0.2, 0.7, 0.85, 0.4]	1.25	[0.6, 1.5, 0.7, 0.2]	[0.2, 0.95, 0.45, 0.6]
k_{RO}	[0.5, 0.375]	[0.5, 0.375]	0.25	0.25
A_s per section $[m^2]$	[1980, 1764, 1665, 1512, 1728, 1296]	[1980, 1764, 1665, 1512, 3024]	920	920
f_w	0.1	0.36	0.3	0.51
$TAW_{[min,max]}$ $[mm]$	[52, 145]	[26, 119]	[24, 76]	[12, 78]
$f_{d,const}$	0.35	0.3	0.35	0.35
Y_{max} $[kg/ha]$	7196	13559	5948	6305
k_b $[\$/kWh]$	303	303	711	711
u_{max}	13.8	13.8	12.4	12.4
k_w $[\$/m^3]$	0.001	0.001	0.001	0.001
q_s per section $[m^3/hr]$	[5.1, 5.4, 4.5, 4.5, 4.98, 4.98]	[8.4, 8.4, 7.2, 8.4, 15.6]	8.7	8.7
k_c $[\$/kg]$	0.866	1.726	0.244	0.228
k_d $[\$/day]$	0.847	0.847	0.929	0.929
ρ_{soil} $[g/cm^3]$	[1.4, 1.1]	[1.4, 1.1]	1.29	1.29

C.2 Pump Energy and Efficiency

The cumulative pump energy broken down into hydraulic pump output energy, calculated input pump power, and measured input power to the pump for the farm with the controller and the reference farm are shown in Figure C.1 for the Morocco carrot season. Figure C.2 shows the pump efficiency at the farm with the controller and the reference farm for the Morocco carrot season.

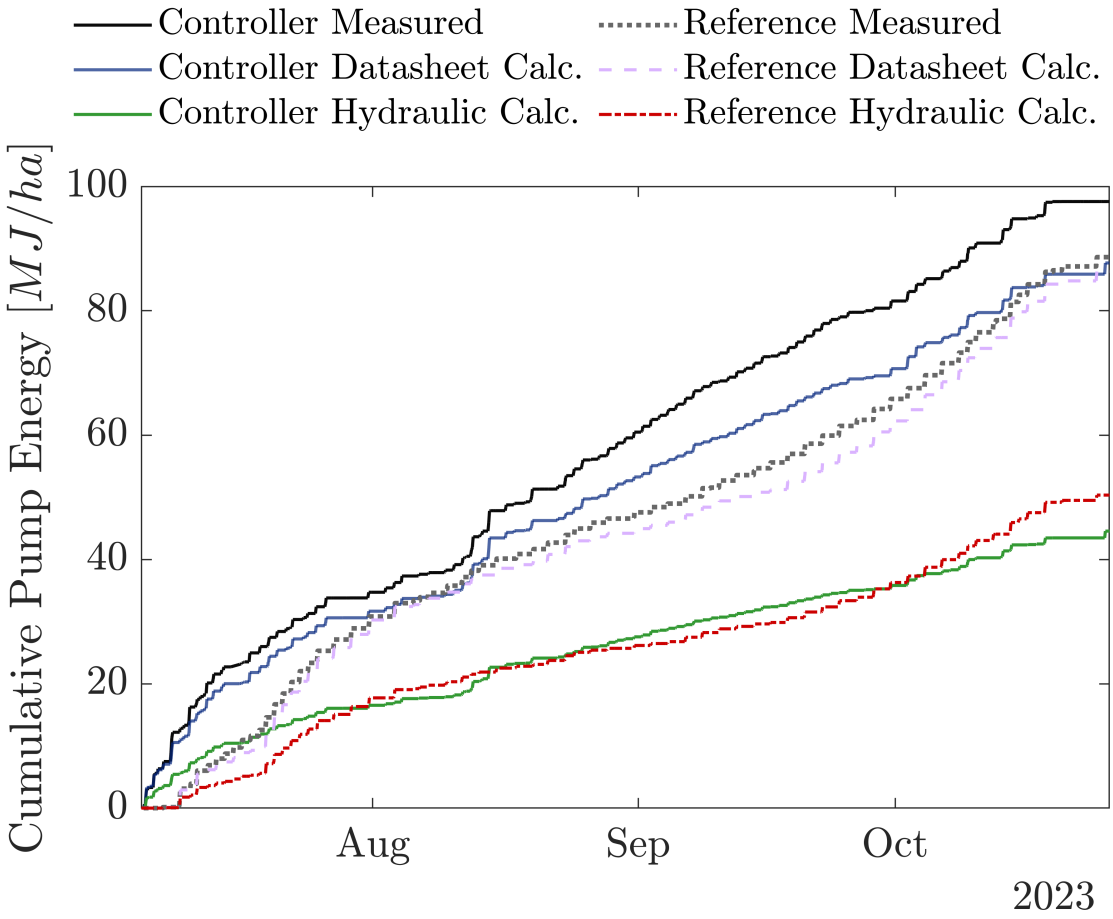

Figure C.1: Cumulative pumping energy breakdown comparison between the farm with the POWEIr controller and the reference farm for the Morocco carrot season. The 'Hydraulic Pump' energy was calculated from the flow and pressure at the pump. The 'Pump Datasheet' energy was calculated by dividing the 'Hydraulic Pump' by the pump efficiency, with pump efficiency calculated from the measured flow rate according to the pump's efficiency curve reported by the manufacturer.

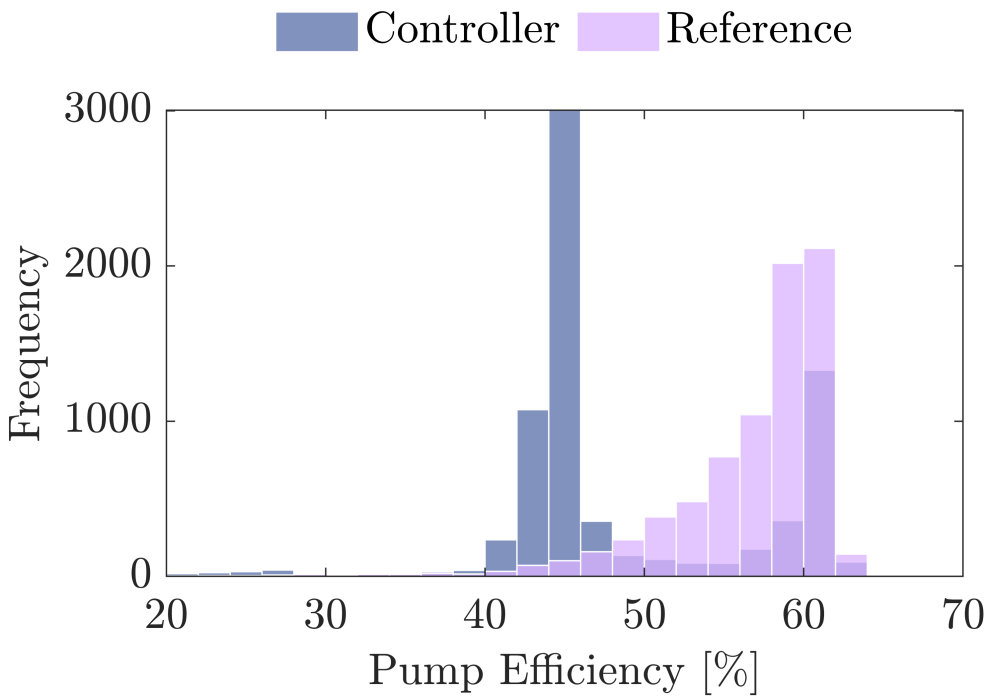

Figure C.2: Histogram of the pump efficiency for the farm with the POWEIr controller and reference farm for the Morocco carrot season. The pump efficiency was calculated at all irrigation times from the measured flow rate according to the pump's efficiency curve reported by the manufacturer.

References

[1] UN, *The Sustainable Development Goals Report 2023: Special Edition*. United Nations Department of Economic and Social Affairs, 2023.

[2] U. Khanal, C. Wilson, S. Rahman, B. L. Lee, and V.-N. Hoang, "Smallholder farmers' adaptation to climate change and its potential contribution to un's sustainable development goals of zero hunger and no poverty," *Journal of Cleaner Production*, vol. 281, p. 124 999, 2021.

[3] J. D. Sachs, G. Schmidt-Traub, M. Mazzucato, D. Messner, N. Nakicenovic, and J. Rockström, "Six transformations to achieve the sustainable development goals," *Nature sustainability*, vol. 2, no. 9, pp. 805–814, 2019.

[4] W. Bank, *Beyond Scarcity: Water Security in the Middle East and North Africa*. The World Bank, 2017.

[5] A. Flammini, X. Pan, F. N. Tubiello, S. Y. Qiu, L. Rocha Souza, R. Quadrelli, S. Bracco, P. Benoit, and R. Sims, "Emissions of greenhouse gases from energy use in agriculture, forestry and fisheries: 1970–2019," *Earth System Science Data*, vol. 14, no. 2, pp. 811–821, 2022.

[6] M. Crippa, E. Solazzo, D. Guizzardi, F. Monforti-Ferrario, F. N. Tubiello, and A. Leip, "Food systems are responsible for a third of global anthropogenic ghg emissions," *Nature Food*, vol. 2, no. 3, pp. 198–209, 2021.

[7] B. Paris, F. Vandorou, A. T. Balafoutis, K. Vaiopoulos, G. Kyriakarakos, D. Manolakos, and G. Papadakis, "Energy use in open-field agriculture in the eu: A critical review recommending energy efficiency measures and renewable energy sources adoption," *Renewable and Sustainable Energy Reviews*, vol. 158, p. 112 098, 2022.

[8] G. Todde, M. Caria, A. Pazzona, L. Ledda, and L. Narvarte, "Does Precision Photovoltaic Irrigation Represent a Sustainable Alternative to Traditional Systems?" en, in *Innovative Biosystems Engineering for Sustainable Agriculture, Forestry and Food Production*, A. Coppola, G. C. Di Renzo, G. Altieri, and P. D'Antonio, Eds., vol. 67, Series Title: Lecture Notes in Civil Engineering, Cham: Springer International Publishing, 2020, pp. 585–593, ISBN: 978-3-030-39298-7 978-3-030-39299-4. DOI: 10.1007/978-3-030-39299-4_64. [Online]. Available: http://link.springer.com/10.1007/978-3-030-39299-4_64 (visited on 08/04/2023).

[9] O. Adeyemi, I. Grove, S. Peets, and T. Norton, "Advanced Monitoring and Management Systems for Improving Sustainability in Precision Irrigation," en, *Sustainability*, vol. 9, no. 3, p. 353, Feb. 2017, ISSN: 2071-1050. DOI: 10.3390/su9030353. [Online]. Available: http://www.mdpi.com/2071-1050/9/3/353 (visited on 03/01/2023).

[10] A. Mérida García, I. Fernández García, E. Camacho Poyato, P. Montesinos Barrios, and J. Rodríguez Díaz, "Coupling irrigation scheduling with solar energy production in a smart irrigation management system," en, *Journal of Cleaner Production*, vol. 175, pp. 670–682, Feb. 2018, ISSN: 09596526. DOI: 10.1016/j.jclepro.2017.12.093. [Online]. Available: https://linkinghub.elsevier.com/retrieve/pii/S0959652617330433 (visited on 08/04/2023).

[11] F. IRENA, "Renewable energy and agri-food systems: Advancing energy and food security towards sustainable development goals," 2021.

[12] J. Jägermeyr, D. Gerten, J. Heinke, S. Schaphoff, M. Kummu, and W. Lucht, "Water savings potentials of irrigation systems: Global simulation of processes and linkages," *Hydrology and Earth System Sciences*, vol. 19, no. 7, pp. 3073–3091, 2015.

[13] L. Friedlander, A. Tal, and N. Lazarovitch, "Technical considerations affecting adoption of drip irrigation in Sub-Saharan Africa," *Agricultural Water Management*, vol. 126, pp. 125–132, Aug. 2013. DOI: 10.1016/j.agwat.2013.04.014.

[14] U. IFAD, "Smallholders, food security and the environment," *Rome: International Fund for Agricultural Development*, vol. 29, 2013.

[15] V. Nangia, R. Moussadek, and G. Montanaro, "Ultra-low energy drip irrigation for MENA countries: Drip Irrigation in Morocco," *International Center for Agricultural Research in the Dry Areas (ICARDA)*, 2017.

[16] G. Jobbins, J. Kalpakian, A. Chriyaa, A. Legrouri, and E. H. El Mzouri, "To what end? Drip irrigation and the water-energy-food nexus in Morocco," en, *International Journal of Water Resources Development*, vol. 31, no. 3, pp. 393–406, Jul. 2015, ISSN: 0790-0627, 1360-0648. DOI: 10.1080/07900627.2015.1020146. [Online]. Available: https://www.tandfonline.com/doi/full/10.1080/07900627.2015.1020146 (visited on 02/02/2019).

[17] F. A. Ward and M. Pulido-Velazquez, "Water conservation in irrigation can increase water use," en, *Proceedings of the National Academy of Sciences*, vol. 105, no. 47, pp. 18 215–18 220, Nov. 2008, ISSN: 0027-8424, 1091-6490. DOI: 10.1073/pnas.0805554105. [Online]. Available: http://www.pnas.org/cgi/doi/10.1073/pnas.0805554105 (visited on 03/20/2019).

[18] M. Benouniche, M. Kuper, A. Hammani, and H. Boesveld, "Making the user visible: Analysing irrigation practices and farmers' logic to explain actual drip irrigation performance," *Irrigation Science*, vol. 32, pp. 405–420, 2014.

[19] Food and A. O. of the United Nations (FAO), *The state of food and agriculture 2022. leveraging automation in agriculture for transforming agrifood systems*, 2022.

[20] G. D. Van de Zande, C. Sheline, and A. G. Winter, "Evaluating the Potential for a Novel Irrigation System Controller to Be Adopted by Medium-Scale Contract Farmers in East Africa," en, in *Volume 6: 34th International Conference on Design Theory and Methodology (DTM)*, St. Louis, Missouri, USA: American Society of Mechanical Engineers, Aug. 2022, V006T06A037, ISBN: 978-0-7918-8626-7. DOI: 10.1115/DETC2022-88328. [Online]. Available: https://asmedigitalcollection.asme.org/IDETC-CIE/proceedings/IDETC-CIE2022/86267/V006T06A037/1150535 (visited on 12/21/2022).

[21] G. D. Van de Zande, S. Amrose, E. Donlon, P. Shamshery, and A. G. Winter V, "Identifying opportunities for irrigation systems to meet the specific needs of farmers in east africa," *Water*, vol. 16, no. 1, p. 75, 2023.

[22] G. D. Van de Zande, C. Sheline, S. Amrose, J. Costello, A. Ghodgaonkar, F. Grant, and A. G. Winter V., "Design and evaluation of an automatic scheduling-manual operation (as-mo) tool to bring precision irrigation to resource-constrained farmers," *In Preparation*, 2024.

[23] G. D. Van de Zande, "Bringing the water-efficiency benefits of precision irrigation to resource-constrained farms through an automatic scheduling-manual operation irrigation tool," Ph.D. dissertation, Massachusetts Institute of Technology, 2023.

[24] F. Grant, S. Amrose, S. Talozi, and A. G. Winter V, "Evaluating the potential for the sustainable, user-centered implementation of PV-powered drip irrigation (PVDI) in the Middle East and North Africa," *In Preparation*, 2024.

[25] C. Sheline, F. Grant, S. Gelmini, and A. G. Winter, "Designing a predictive optimal water and energy irrigation (poweir) controller for pv-powered drip irrigation systems in resource-constrained contexts," *In Preparation*, 2024.

[26] *The State of Food and Agriculture 2020*, en. FAO, 2020, ISBN: 978-92-5-133441-6. DOI: 10.4060/cb1447en. [Online]. Available: http://www.fao.org/documents/card/en/c/cb1447en (visited on 08/04/2023).

[27] T. Searchinger, C. Hanson, J. Ranganathan, B. Lipinski, R. Waite, R. Winterbottom, A. Dinshaw, and R. Heimlich, "The great balancing act," 2013.

[28] T. Khokhar, "Chart: Globally, 70% of freshwater is used for agriculture," *World Bank Data Blog*, 2017.

[29] C. Klobucista and K. Robinson, "Water stress: A global problem that's getting worse," *Council on Foreign Relations, August*, vol. 2, 2022.

[30] World Resources Institute, *Aqueduct: Using cutting-edge data to identify and evaluate water risks around the world*, https://www.wri.org/aqueduct, 2023.

[31] Energy Sector Management Assistance Program administered by the World Bank, *Global Solar Atlas*, https://globalsolaratlas.info/map, 2023.

[32] P. Yang, L. Wu, M. Cheng, J. Fan, S. Li, H. Wang, and L. Qian, "Review on drip irrigation: Impact on crop yield, quality, and water productivity in china," *Water*, vol. 15, no. 9, p. 1733, 2023.

[33] M. Benouniche, M. Kuper, A. Hammani, and H. Boesveld, "Making the user visible: Analysing irrigation practices and farmers' logic to explain actual drip irrigation performance," en, *Irrigation Science*, vol. 32, no. 6, pp. 405–420, Nov. 2014, ISSN: 0342-7188, 1432-1319. DOI: 10.1007/s00271-014-0438-0. [Online]. Available: http://link.springer.com/10.1007/s00271-014-0438-0 (visited on 08/04/2023).

[34] E. Bwambale, F. K. Abagale, and G. K. Anornu, "Smart irrigation monitoring and control strategies for improving water use efficiency in precision agriculture: A review," en, *Agricultural Water Management*, vol. 260, p. 107 324, Feb. 2022, ISSN: 03783774. DOI: 10.1016/j.agwat.2021.107324. [Online]. Available: https://linkinghub.elsevier.com/retrieve/pii/S0378377421006016 (visited on 08/04/2023).

[35] L. García, L. Parra, J. M. Jimenez, J. Lloret, and P. Lorenz, "IoT-Based Smart Irrigation Systems: An Overview on the Recent Trends on Sensors and IoT Systems for Irrigation in Precision Agriculture," en, *Sensors*, vol. 20, no. 4, p. 1042, Feb. 2020, ISSN: 1424-8220. DOI: 10.3390/s20041042. [Online]. Available: https://www.mdpi.com/1424-8220/20/4/1042 (visited on 08/04/2023).

[36] F. Grant, C. Sheline, J. Sokol, S. Amrose, E. Brownell, V. Nangia, and A. G. Winter, "Creating a solar-powered drip irrigation optimal performance model (sdrop) to lower the cost of drip irrigation systems for smallholder farmers," *Applied Energy*, vol. 323, p. 119 563, 2022, ISSN: 0306-2619. DOI: https://doi.org/10.1016/j.apenergy.2022.119563. [Online]. Available: https://www.sciencedirect.com/science/article/pii/S0306261922008741.

[37] M. Carrillo Cobo, E. Camacho Poyato, P. Montesinos, and J. Rodríguez Díaz, "New model for sustainable management of pressurized irrigation networks. Application to Bembézar MD irrigation district (Spain)," en, *Science of The Total Environment*, vol. 473-474, pp. 1–8, Mar. 2014, ISSN: 00489697. DOI: 10.1016/j.scitotenv.2013.11.093. [Online]. Available: https://linkinghub.elsevier.com/retrieve/pii/S0048969713013764 (visited on 08/04/2023).

[38] V. Zavala, "Optimal management of a multisector standalone direct pumping photovoltaic irrigation system," en, *Applied Energy*, 2020.

[39] *The State of Food and Agriculture 2022*, en. FAO, Nov. 2022, ISBN: 978-92-5-136043-9. DOI: 10.4060/cb9479en. [Online]. Available: http://www.fao.org/documents/card/en/c/cb9479en (visited on 08/04/2023).

[40] E. A. Abioye, M. S. Z. Abidin, M. S. A. Mahmud, S. Buyamin, M. H. I. Ishak, M. K. I. A. Rahman, A. O. Otuoze, P. Onotu, and M. S. A. Ramli, "A review on monitoring and advanced control strategies for precision irrigation," en, *Computers and Electronics in Agriculture*, vol. 173, p. 105 441, Jun. 2020, ISSN: 01681699. DOI: 10.1016/j.compag.2020.105441. [Online]. Available: https://linkinghub.elsevier.com/retrieve/pii/S0168169919314826 (visited on 08/04/2023).

[41] C. Lozoya, C. Mendoza, A. Aguilar, A. Román, and R. Castelló, "Sensor-Based Model Driven Control Strategy for Precision Irrigation," en, *Journal of Sensors*, vol. 2016, pp. 1–12, 2016, ISSN: 1687-725X, 1687-7268. DOI: 10.1155/2016/9784071. [Online]. Available: https://www.hindawi.com/journals/js/2016/9784071/ (visited on 08/04/2023).

[42] S. K. Lowder, J. Skoet, and T. Raney, "The Number, Size, and Distribution of Farms, Smallholder Farms, and Family Farms Worldwide," en, *World Development*, vol. 87, pp. 16–29, Nov. 2016, ISSN: 0305750X. DOI: 10.1016/j.worlddev.2015.10.041. [Online]. Available: https://linkinghub.elsevier.com/retrieve/pii/S0305750X15002703 (visited on 08/04/2023).

[43] I. Fernández García, J. A. Rodríguez Díaz, E. Camacho Poyato, and P. Montesinos, "Optimal Operation of Pressurized Irrigation Networks with Several Supply Sources," en, *Water Resources Management*, vol. 27, no. 8, pp. 2855–2869, Jun. 2013, ISSN: 0920-4741, 1573-1650. DOI: 10.1007/s11269-013-0319-y. [Online]. Available: http://link.springer.com/10.1007/s11269-013-0319-y (visited on 08/04/2023).

[44] Y. Ding, L. Wang, Y. Li, and D. Li, "Model predictive control and its application in agriculture: A review," en, *Computers and Electronics in Agriculture*, vol. 151, pp. 104–117, Aug. 2018, ISSN: 01681699. DOI: 10.1016/j.compag.2018.06.004. [Online]. Available: https://linkinghub.elsevier.com/retrieve/pii/S0168169917315296 (visited on 08/04/2023).

[45] D. Delgoda, H. Malano, S. K. Saleem, and M. N. Halgamuge, "Irrigation control based on model predictive control (MPC): Formulation of theory and validation using weather forecast data and AQUACROP model," en, *Environmental Modelling & Software*, vol. 78, pp. 40–53, Apr. 2016, ISSN: 13648152. DOI: 10.1016/j.envsoft.2015.12.012. [Online]. Available: https://linkinghub.elsevier.com/retrieve/pii/S1364815215301262 (visited on 08/04/2023).

[46] E. A. Abioye, M. S. Z. Abidin, M. N. Aman, M. S. A. Mahmud, and S. Buyamin, "A model predictive controller for precision irrigation using discrete lagurre networks," en, *Computers and Electronics in Agriculture*, vol. 181, p. 105 953, Feb. 2021, ISSN: 01681699. DOI: 10.1016/j.compag.2020.105953. [Online]. Available: https://linkinghub.elsevier.com/retrieve/pii/S0168169920331586 (visited on 08/04/2023).

[47] T. Roje, D. Sáez, C. Muñoz, and L. Daniele, "Energy–water management system based on predictive control applied to the water–food–energy nexus in rural communities," *Applied Sciences*, vol. 10, no. 21, p. 7723, Oct. 31, 2020, ISSN: 2076-3417. DOI: 10.3390/app10217723. [Online]. Available: https://www.mdpi.com/2076-3417/10/21/7723 (visited on 09/04/2023).

[48] J. Navarro Navajas, P. Montesinos, E. C. Poyato, and J. Rodríguez Díaz, "Impacts of irrigation network sectoring as an energy saving measure on olive grove production," en, *Journal of Environmental Management*, vol. 111, pp. 1–9, Nov.

2012, ISSN: 03014797. DOI: 10.1016/j.jenvman.2012.06.034. [Online]. Available: https://linkinghub.elsevier.com/retrieve/pii/S0301479712003490 (visited on 08/04/2023).

[49] *Grundfos size page for drip, micro spray soaker hose irrigation*, https://product-selection.grundfos.com/us/size-page?qcid=2153423512, Accessed: 2021-01-14.

[50] *Grundfos sp submersible borehole pumps*, https://product-selection.grundfos.com/us/products/sp-sp-g?tab=products, Accessed: 2021-01-14.

[51] *How much do solar inverters cost*, https://luxpowertek.com/blog/solar-inverters-cost, Accessed: 2023-7-18.

[52] *Mppt solar charge controllers explained*, https://www.cleanenergyreviews.info/blog/mppt-solar-charge-controllers, Accessed: 2023-7-18.

[53] *Variable frequency drives price list*, http://www.vfds.org/price-list.html, Accessed: 2023-7-18.

[54] R. Alley, K. Emanuel, and F. Zhang, "Advances in weather prediction," *Science*, vol. 363, 2019.

[55] E. Nkiaka, A. Taylor, and A. Dougill, "Identifying user needs for weather and climate services to enhance resilience to climate shocks in sub-Saharan Africa," *Environmental Research Letters*, 2019.

[56] J. Woetzel, D. Pinner, H. Samandari, H. Engel, M. Krishnan, R. McCullough, T. Melzer, and S. Boettiger, *How will African farmers adjust to changing patterns of precipitation?* https://www.mckinsey.com/capabilities/sustainability/our-insights/how-will-african-farmers-adjust-to-changing-patterns-of-precipitation, Accessed: 2023-01-10, 2020.

[57] H. Feleke, "Assessing weather forecasting needs of smallholder farmers for climate change adaptation in the central rift valley of ethiopia," *Journal of Earth Science and Climate Change*, 2015.

[58] G. Brunet, D. B. Parsons, D. Ivanov, B. Lee, P. Bauer, N. B. Bernier, V. Bouchet, A. Brown, A. Busalacchi, G. C. Flatter, *et al.*, "Advancing weather and climate forecasting for our changing world," *Bulletin of the American Meteorological Society*, vol. 104, no. 4, E909–E927, 2023.

[59] D. P. Rogers, V. V. Tsirkunov, H. Kootval, A. Soares, D. Kull, A.-M. Bogdanova, and M. Suwa, *Weathering the change: how to improve hydromet services in developing countries?* World Bank, 2019.

[60] J. Lofstead, "Weather forecasting limitations in the developing world," in *International Conference on Human-Computer Interaction*, Springer, 2023, pp. 86–96.

[61] C. Sheline and V. Winter Amos, "Machine learning method for forecasting weather needed for crop water demand estimations in low-resource settings using a case study in morocco," vol. 3B: 47th Design Automation Conference (DAC), American Society of Mechanical Engineers, 2021. DOI: 10.1115/DETC2021-70571. [Online]. Available: https://doi.org/10.1115/DETC2021-70571.

[62] *Vector autoregression (var) comprehensive guide with examples in python*, https://www.machinelearningplus.com/time-series/vector-autoregression-examples-python/, Accessed: 2020-11-30.

[63] R. G. Allen, L. S. Pereira, D. Raes, and M. Smith, "Crop evapotranspiration: Guidlines for computing crop water requirements," *FAO Irrigation and Drainage Paper No. 56*, 1998.

[64] S. Seabold and J. Perktold, "Statsmodels: Econometric and statistical modeling with python," in *Proceedings of the 9th Python in Science Conference*, Austin, TX, vol. 57, 2010, pp. 10–25 080.

[65] M. G. Villalva, J. R. Gazoli, and E. R. Filho, "Comprehensive approach to modeling and simulation of photovoltaic arrays," *IEEE Transactions on Power Electronics*, vol. 24, no. 5, pp. 1198–1208, 2009.

[66] J. Doorenbos and A. H. Kassam, "Yield response to water," *FAO Irrigation and Drainage Paper No. 33*, 1979.

[67] P. Steduto, T. C. Hsiao, E. Fereres, and D. Raes, "Crop yield response to water," *FAO Irrigation and Drainage Paper No. 66*, 2012.

[68] H. Hesse, M. Schimpe, D. Kucevic, and A. Jossen, "Lithium-Ion Battery Storage for the Grid—A Review of Stationary Battery Storage System Design Tailored for Applications in Modern Power Grids," en, *Energies*, vol. 10, no. 12, p. 2107, Dec. 2017, ISSN: 1996-1073. DOI: 10.3390/en10122107. [Online]. Available: https://www.mdpi.com/1996-1073/10/12/2107 (visited on 08/08/2023).

[69] J. Sokol, J. Narain, J. Costello, T. McLaurin, D. Kumar, and A. G. Winter, "Analytical model for predicting activation pressure and flow rate of pressure-compensating inline drip emitters and its use in low-pressure emitter design," *Irrigation Science*, vol. 40, no. 2, pp. 217–237, Feb. 2022. DOI: 10.1007/s00271-022-00771-5. [Online]. Available: https://doi.org/10.1007/s00271-022-00771-5.

[70] R. Folea, *Click PLC: Temperature Pid Tuning Resource Page*, Jan. 2021. [Online]. Available: https://library.automationdirect.com/click-plc-temperature-pid-tuning-resource-page/.

[71] *System Identification: Identify models of dynamic systems from measured data - MATLAB*. [Online]. Available: https://www.mathworks.com/help/ident/ref/systemidentification-app.html?s_tid=srchtitle_site_search_1_systemidentification.

[72] G. F. Franklin, J. D. Powell, and A. Emami-Naeini, *Feedback control of dynamic systems*, 7th ed. Upper Saddle River, NJ: Pearson, Apr. 2014.

[73] F. Grant, C. Sheline, S. Amrose, E. Brownell, V. Nangia, S. Talozi, and A. Winter, "Validation of an analytical model to lower the cost of solar-powered drip irrigation systems for smallholder farmers in the MENA region," in *Volume 11B: 46th Design Automation Conference (DAC)*, American Society of Mechanical Engineers, Aug. 2020. DOI: 10.1115/detc2020-22610.

[74] ASHRAE, *International Weather Files for Energy Calculations 2.0 (IWEC2)*, https://www.ashrae.org/technical-resources/bookstore/ashrae-international-weather-files-for-energy-calculations-2-0-iwec2.

[75] C. Sheline, S. Ingersoll, S. Irmak, and A. G. Winter, "Sensitivity study of the predictive optimal water and energy irrigation (poweir) controller's irrigation schedules for pv-powered drip irrigation systems in resource-constrained contexts," *In Preparation*, 2024.

[76] T. Searchinger, R. Waite, C. Hanson, J. Ranganathan, P. Dumas, E. Matthews, *et al.*, "World resources report: Creating a sustainable food future," *World Resources Institute*, 2019.

[77] M. Van Dijk, T. Morley, M. L. Rau, and Y. Saghai, "A meta-analysis of projected global food demand and population at risk of hunger for the period 2010–2050," *Nature Food*, vol. 2, no. 7, pp. 494–501, 2021.

[78] N. Alexandratos and J. Bruinsma, "World agriculture towards 2030/2050: The 2012 revision," 2012.

[79] J. Bruinsma, *World agriculture: towards 2015/2030: an FAO study*. Routledge, 2017.

[80] WFP and FAO, *Hunger hotspots. fao-wfp early warnings on acute food insecurity: June to september 2022 outlook*, 2022.

[81] M. M. Maja and S. F. Ayano, "The impact of population growth on natural resources and farmers' capacity to adapt to climate change in low-income countries," *Earth Systems and Environment*, vol. 5, pp. 271–283, 2021.

[82] A. del Pozo, N. Brunel-Saldias, A. Engler, S. Ortega-Farias, C. Acevedo-Opazo, G. A. Lobos, R. Jara-Rojas, and M. A. Molina-Montenegro, "Climate change impacts and adaptation strategies of agriculture in mediterranean-climate regions (mcrs)," *Sustainability*, vol. 11, no. 10, p. 2769, 2019.

[83] Q. Dongyu *et al.*, *The state of the world's land and water resources for food and agriculture: systems at breaking point*. FAO, 2022.

[84] M. A. Hasan and S. K. Parida, "An overview of solar photovoltaic panel modeling based on analytical and experimental viewpoint," *Renewable and Sustainable Energy Reviews*, vol. 60, pp. 75–83, 2016.

[85] R. Kumar, S. Singh, *et al.*, "Solar photovoltaic modeling and simulation: As a renewable energy solution," *Energy Reports*, vol. 4, pp. 701–712, 2018.

[86] A. R. Jordehi, "Parameter estimation of solar photovoltaic (pv) cells: A review," *Renewable and Sustainable Energy Reviews*, vol. 61, pp. 354–371, 2016.

[87] A. M. Humada, S. Y. Darweesh, K. G. Mohammed, M. Kamil, S. F. Mohammed, N. K. Kasim, T. A. Tahseen, O. I. Awad, and S. Mekhilef, "Modeling of pv system and parameter extraction based on experimental data: Review and investigation," *Solar Energy*, vol. 199, pp. 742–760, 2020.

[88] S. Shongwe and M. Hanif, "Comparative analysis of different single-diode pv modeling methods," *IEEE Journal of photovoltaics*, vol. 5, no. 3, pp. 938–946, 2015.

[89] V. J. Chin, Z. Salam, and K. Ishaque, "Cell modelling and model parameters estimation techniques for photovoltaic simulator application: A review," *Applied Energy*, vol. 154, pp. 500–519, 2015.

[90] J. Bishop, "Computer simulation of the effects of electrical mismatches in photovoltaic cell interconnection circuits," *Solar Cells*, vol. 25, 1988. DOI: https://doi.org/10.1016/0379-6787(88)90059-2. [Online]. Available: https://www.sciencedirect.com/science/article/pii/0379678788900592.

[91] W. De Soto, S. A. Klein, and W. A. Beckman, "Improvement and validation of a model for photovoltaic array performance," *Solar energy*, vol. 80, no. 1, pp. 78–88, 2006.

[92] M. Gao, J. Li, F. Hong, and D. Long, "Day-ahead power forecasting in a large-scale photovoltaic plant based on weather classification using lstm," *Energy*, vol. 187, p. 115 838, 2019.

[93] X. Qing and Y. Niu, "Hourly day-ahead solar irradiance prediction using weather forecasts by lstm," *Energy*, vol. 148, pp. 461–468, 2018.

[94] *Keras*, https://keras.io/, Accessed: 2021-11-30.

[95] S. Gautam, *Time series forecasting of solar radiation*, https://towardsdatascience.com/time-series-forecasting-of-solar-radiation-294b2a0c94e5, Accessed: 2021-12-01.

[96] D. P. Kingma and J. Ba, "Adam: A method for stochastic optimization," *arXiv preprint arXiv:1412.6980*, 2014.

[97] S. Tenzin, S. Siyang, T. Pobkrut, and T. Kerdcharoen, "Low cost weather station for climate-smart agriculture," in *2017 9th international conference on knowledge and smart technology (KST)*, IEEE, 2017, pp. 172–177.

[98] E. A. Abioye, M. S. Z. Abidin, M. S. A. Mahmud, S. Buyamin, M. K. I. AbdRahman, A. O. Otuoze, M. S. A. Ramli, and O. D. Ijike, "Iot-based monitoring and data-driven modelling of drip irrigation system for mustard leaf cultivation experiment," *Information Processing in Agriculture*, vol. 8, no. 2, pp. 270–283, 2021.

[99] K. Keary, J. Stoochnoff, T. Graham, and M. Dixon, "Irrigation scheduling for container grown spiraea japonica based on cumulative vapor pressure deficit," in *International Symposium on Advanced Technologies and Management for Innovative Greenhouses: GreenSys2019 1296*, 2019, pp. 815–822.

[100] I. Dunaieva, V. Vecherkov, Y. Filina, V. Popovych, E. Barbotkina, V. Pashtetsky, V. Terleev, W. Mirschel, and L. Akimov, "Review of automatized meteorological stations use for agricultural purposes," in *IOP Conference Series: Earth and Environmental Science*, IOP Publishing, vol. 937, 2021, p. 032 097.

[101] *Food and agriculture organization of the united nations data platform*, https://www.fao.org/faostat, Accessed: 2010-09-30.

[102] A. Parmar, K. Mistree, and M. Sompura, "Machine learning techniques for rainfall prediction: A review," in *International conference on innovations in information embedded and communication systems*, vol. 3, 2017.

[103] Z. Popova, S. Eneva, and L. S. Pereira, "Model validation, crop coefficients and yield response factors for maize irrigation scheduling based on long-term experiments," *Biosystems engineering*, vol. 95, no. 1, pp. 139–149, 2006.

[104] H. Jayanthi, C. M. Neale, and J. L. Wright, "Development and validation of canopy reflectance-based crop coefficient for potato," *Agricultural water management*, vol. 88, no. 1-3, pp. 235–246, 2007.

[105] N. Yarami, A. Kamgar-Haghighi, A. Sepaskhah, and S. Zand-Parsa, "Determination of the potential evapotranspiration and crop coefficient for saffron using a water-balance lysimeter," *Archives of Agronomy and Soil Science*, vol. 57, no. 7, pp. 727–740, 2011.

[106] S. S. Anapalli, L. R. Ahuja, P. H. Gowda, L. Ma, G. Marek, S. R. Evett, and T. A. Howell, "Simulation of crop evapotranspiration and crop coefficients with data in weighing lysimeters," *Agricultural Water Management*, vol. 177, pp. 274–283, 2016.

[107] O. Raphael, K. Ogedengbe, J. Fasinmirin, D. Okunade, I. Akande, and A. Gbadamosi, "Growth-stage-specific crop coefficient and consumptive use of capsicum chinense using hydraulic weighing lysimeter," *Agricultural water management*, vol. 203, pp. 179–185, 2018.

[108] C. Sheline, F. Grant, G. D. Van de Zande, *et al.*, "Technical validation of the predictive optimal water and energy irrigation (poweir) controller for solar-powered drip irrigation systems in the middle east and north africa," *In Preparation*, 2024.

[109] *United nations global sustainable development goal (sdg) indicators data platform*, https://unstats.un.org/sdgs/dataportal, Accessed: 2023-09-30.

[110] *National Water Strategy 2023-2040*. The Ministry of Water and Irrigation, Jordan, 2023.

[111] *Generation Green 2020-2030*. Ministry of Agriculture, Fisheries, Rural Development, Water, and Forests: Department of Agriculture, Morocco, 2020.

[112] G. Nilo and M. J. Tao, "Standard operating procedure for soil bulk density, cylinder method," FAO, Tech. Rep., 2023.

[113] *The souss-massa regional authority for agricultural development (office regional de mise en valeur agricole du souss-massa or ormva-sm)*, https://ormvasm.m.

[114] *Grape information*, https://www.fao.org/land-water/databases-and-software/crop-information/grape/en/, Accessed: 2023-04-09.

[115] C. S. Patil, "Crop coefficient and water requirement of okra (abelmoschus esculentus l. moench)," *MAUSAM*, vol. 61, no. 1, pp. 121–124, 2010.

[116] S. Ayas, "Response of okra (abelmoschus esculentus l. yalova akköy-41) to different irrigation and fertigation levels," *Turkish Journal of Agriculture-Food Science and Technology*, vol. 8, no. 10, pp. 2225–2235, 2020.

[117] A. UNLUKARA and B. Cemek, "Response of okra to water stress," *Mustafa Kemal Üniversitesi Tarım Bilimleri Dergisi*, vol. 24, pp. 313–319, 2019.

[118] K. X. Soulis, S. Elmaloglou, and N. Dercas, "Investigating the effects of soil moisture sensors positioning and accuracy on soil moisture based drip irrigation scheduling systems," *Agricultural Water Management*, vol. 148, pp. 258–268, 2015.

[119] L. Zotarelli, M. D. Dukes, and M. Paranhos, "Minimum number of soil moisture sensors for monitoring and irrigation purposes: Hs1222, 7/2013," *Edis*, vol. 2013, no. 7, 2013.

[120] R. S. Ayers, D. W. Westcot, *et al.*, *Water quality for agriculture*. Food and Agriculture Organization of the United Nations Rome, 1985, vol. 29.

[121] B. Anita and N. Selvaraj, "Biology, yield loss and integrated management of root-knot nematode, meloidogyne hapla infecting carrot in nilgiris," *Indian Journal of Nematology*, vol. 41, no. 2, pp. 144–149, 2011.

[122] S. A. Anwar and M. McKenry, "Incidence and population density of plant-parasitic nematodes infecting vegetable crops and associated yield losses in punjab, pakistan," *Pakistan Journal of Zoology*, vol. 44, no. 2, 2012.

[123] R. M. Davis and J. Nu ez, "Integrated approaches for carrot pests and diseases management," in *General Concepts in Integrated Pest and Disease Management*, Springer, 2007, pp. 149–188.

[124] R. Singh and U. Kumar, "Assessment of nematode distribution and yield losses in vegetable crops of western uttar pradesh in india," *Int. J. Sci. Res*, vol. 4, no. 5, pp. 2812–2816, 2015.

[125] T. Widmer, J. Ludwig, and G. Abawi, "The northern root-knot nematode on carrot, lettuce, and onion in new york," New York State Agricultural Experiment Station, Tech. Rep., 1999.

[126] D. H. Muhsen, T. Khatib, and T. E. Abdulabbas, "Sizing of a standalone photovoltaic water pumping system using hybrid multi-criteria decision making methods," *Solar Energy*, vol. 159, pp. 1003–1015, 2017.

[127] W. Wieder, J. Boehnert, G. Bonan, and M. Langseth, "Regridded harmonized world soil database v1. 2," *ORNL DAAC*, 2014.

[128] USDA, *Soil texture calculator*, https://www.nrcs.usda.gov/resources/education-and-teaching-materials/soil-texture-calculator.